PHOTOCHEMISTRY OF BENZO[2,3-*g*]QUINOXALINE DERIVATIVES

by

Muriel Rakotomalala
B.Sc. in Chemistry with Honours, University of Bristol 2004

THESIS SUBMITTED IN PARTIAL FULFILLMENT OF
THE REQUIREMENTS FOR THE DEGREE OF

MASTER OF SCIENCE

In the
Department of Chemistry

SIMON FRASER UNIVERSITY

Spring 2008

Your file Votre référence
ISBN: 978-0-494-46903-3
Our file Notre référence
ISBN: 978-0-494-46903-3

APPROVAL

Name: Muriel Rakotomalala

Degree: Master of Science

Title of Thesis: Photochemistry of Benzo[2,3-g]quinoxaline Derivatives

Examining Committee:

Chair

Dr. David J. Vocadlo
Assistant Professor, Department of Chemistry

Dr. Vance E. Williams
Senior Supervisor
Associate Professor, Department of Chemistry

Dr. Neil R. Branda
Supervisor
Professor, Department of Chemistry

Dr. Steven Holdcroft
Supervisor
Professor, Department of Chemistry

Dr. Peter D. Wilson
Internal Examiner
Associate Professor, Department of Chemistry

Date Defended/Approved: March 25, 2008

ABSTRACT

Since its discovery in 1867, the photodimerisation of anthracene has been one of most exploited reactions for reversibly connecting materials at a molecular level. The cumbersome synthesis of many substituted anthracene derivatives combined with their tendency to form endoperodixes when irradiated in presence of oxygen and the short wavelengths needed to convert the dimer to its monomer prohibit their use in practical applications. In an attempt to circumvent some of these problems, we undertook the synthesis and the investigation of the photochemistry of benzo[2,3-*g*]quinoxalines, which are structurally similar to anthracenes. Surprisingly, the photochemical behaviour of these molecules has not been investigated.

Upon irradiation, 2,3-diphenylbenzo[2,3-*g*]quinoxaline (**DPBQ**) and 2,3-di(2-dipyridyl)benzo[2,3-*g*]quinoxaline (**DPyBQ**) both underwent photodimerisation to yield **di-DPBQ** and **di DPyBQ** respectively. The head-to-tail structure of **di-DPBQ** was confirmed by X-ray crystallography. Preliminary studies suggested that the presence of $ZnCl_2$ and $Zn(OAc)_2$ reduced the yield of dimerisation of **DPyBQ**.

DEDICATION

To my parents and brother.

"Ny hazo no vanon ko lakana, ny tany naniriany no tsara"

ACKNOWLEDGEMENTS

First I would like to thank my senior supervisor, Dr. Vance Williams, for giving me the opportunity to join his group and his support and guidance throughout my Master's studies. I would also like to show my appreciation to the members of my supervisory committee, Dr. Neil Branda and Dr. Steven Holdcroft, for their time and helpful suggestions.

I would also like to show my appreciation to the past and present members of the Williams' lab, Dr. David Bailey, Mr. Oliver Calderon, Dr. Johan Foster, Ms. Christine Lavigueur, Ms. Laura Stusiak and Maitre Emilie Voisin, for their help throughout the different aspects of my project and laughing to all my French jokes.

I am thankful to Dr. Daniel Spantulesku (Branda Lab) for the synthesis of 4,4'-dimethoxybenzil, Ms. Emilie Voisin for the crystallisation of the dimers, the DSC measurements and for the synthesis and characterisation of 2,3,6,7-tetrahexyloxybenzil and 2,3,6,7-tetraoctyloxybenzil, Dr. Cornelia Bohne and Tamara Pace (University of Victoria) for the lifetime measurements and Ms. Chirstine Lavigueur and Mr. Michael Katz for crystallographic data, and the Holdcroft group for the GPC measurements.

I would also like to express my gratitude to Mrs. Marcy Tracey (NMR), Mr Colin Zhang (NMR), Dr. Andrew Lewis (NMR), Mr. Simon Wong (MS and CHN

microanalysis), Mr. Mikki Yang (CHN microanalysis) for their technical assistance.

Last but not least, I would I am grateful to Simon Fraser University and the Natural Sciences and Engineering Research Council of Canada for their financial assistance.

TABLE OF CONTENTS

LIST OF FIGURES

LIST OF EQUATIONS

LIST OF SCHEMES

LIST OF ABBREVIATIONS

δ	Chemical shift
°C	Degree Celcius
A	Anthracene
BP	Benzophenazine
BQ	Benzo[2,3-*g*]quinoxaline
Br	Broad
Cm	Centimetre
D	Doublet
di-A	Di-anthracene
DMA	9,10-Dimethylanthracene
DMF	N,N'-Dimethylformamide
DMoBQ	2,3-Di(4-methoxyphenyl) benzo[2,3-*g*]quinoxaline
DMSO	Dimethylsulfoxide
DPBQ	2,3-Diphenylbenzo[2,3-*g*]quinoxaline
DPyBQ	2,3-Di(2-pyridyl)benzo[2,3-*g*]quinoxaline
DSC	Differential Scanning calorimetry
EtOH	Ethanol
FT-IR	Fourier Transform Infrared
g	Gram

GPC	Gas permeation chromatography
h	Hours
hh	Head-to-head
HOMO	Highest occupied molecular orbital
ht	Head-to tail
Hz	Hertz
hν	Irradiation with light
J	Coupling constant
LUMO	Lowest unoccupied molecular orbital
m	Multiplet
M	Mol per litre
m.p.	Metling point
m/z	Mass to charge ratio
MALDI-TOF	Matrix assisted laser desorption ionisation time of flight
MeOH	Methanol
mg	Milligram
MHz	Megahertz
min	Minutes
mL	Millilitre
mmol	Millimole
MoBQ	2-(4-Methoxyphenyl) benzo[2,3-*g*]quinoxaline
mol	Mole

MS	Mass spectroscopy
nm	Nanometre
NMR	Nuclear magnetic resonance
OAc	Acetate
P	Pyrazine
PBQ	2-phenylbenzo[2,3-*g*]quinoxaline
Ph	Phenyl
ppm	Parts per million
PQ	Pyrazo[2,3-*g*]quinoxaline
PS	Polystyrene
Q	Quinoxaline
S	Singlet
T	Triplet
TLC	Thin layer chromatography
TPA	2,3,6,7-tetraphenylanthracene
TPPQ	2,3,7,8-tetraphenylpyrazo[2,3-*g*]quinoxaline
UV-Vis	Ultraviolet-visible
λ	Wavelength
μL	Microlitre

CHAPTER 1: GENERAL INTRODUCTION

1.1 Introduction

The focus of this thesis was the investigation of the photochromic properties of benzo[2,3-*g*]quinoxaline derivatives, which we anticipated would undergo [4+4] photocycloaddition reactions. The present chapter will introduce photochromism in general and the photochemical properties of molecules that are structurally related to our target compounds.

1.2 Photochromism

Light represents an attractive stimulus for chemical reactions as it is a clean and easily tunable source of energy that can be focused on small areas without significant diffusion. The interaction of light with unsaturated organic molecules may induce photophysical and photochemical changes in the molecule in question. In the case of photochromic molecules, absorption of a photon of given energy $E = h\nu$ will induce a reversible change in the electronic properties of the chromophore resulting in a change of colour (Equation 1.1).[1] The colour can then be reverted either thermally or photochemically.

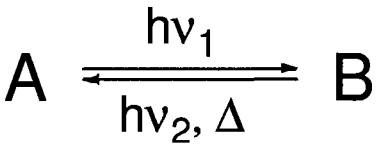

Equation 1.1: Light-stimulated reversible interconversion between state A and B.[1]

Several photochromic systems were investigated as a mean to introduce change of properties at the macroscopic level using a light as a stimulus. One of the most extensively studied systems is the azobenzene system (**1**). As shown in Scheme 1.1, azobenzenes undergo *cis-trans* isomerisation across the N=N double bond upon irradiation with UV-light. The change of geometry accompanying the isomerisation, has been used to photo-induce change in volume in polymers and liquid crystals.[2,3] However, such systems suffer from the high thermal instability of the *cis* form. The lack of thermal stability combined with the small difference UV-Vis absorption between the two isomers represent drawbacks for potential applications such as optical data storage.[3] Other systems based on electrocyclic photocyclisation such as spiropyrans (**2**) and diarylethenes (**3**) (Scheme 1.1) have also the subject to extensive research.[4,5] In these systems, the change of conjugation induced by the cyclisation is translated in large change in UV-Vis absorption that could potentially be used for protective lenses.[5-7] Spiropyrans (**2**) have been more extensively studied than diarylethenes (**3**), however they suffer from a lack of thermal stability accompanied by a low fatigue resistance which prevents their use in practical application requiring cycling.[8]

The focus of this thesis will be molecules that undergo intermolecular cycloaddition reactions to yield photodimers.[1] Similarly to the unimolecular systems shown in Scheme 1.1, irradiation of bimolecular systems leads to a change of UV-Vis absorption and other physical properties. However, such systems have the advantage of enabling the use of light to reversibly assemble materials at the molecular level. A non-exhaustive list of attempts to use such systems in materials will be described in Chapter 1.4.

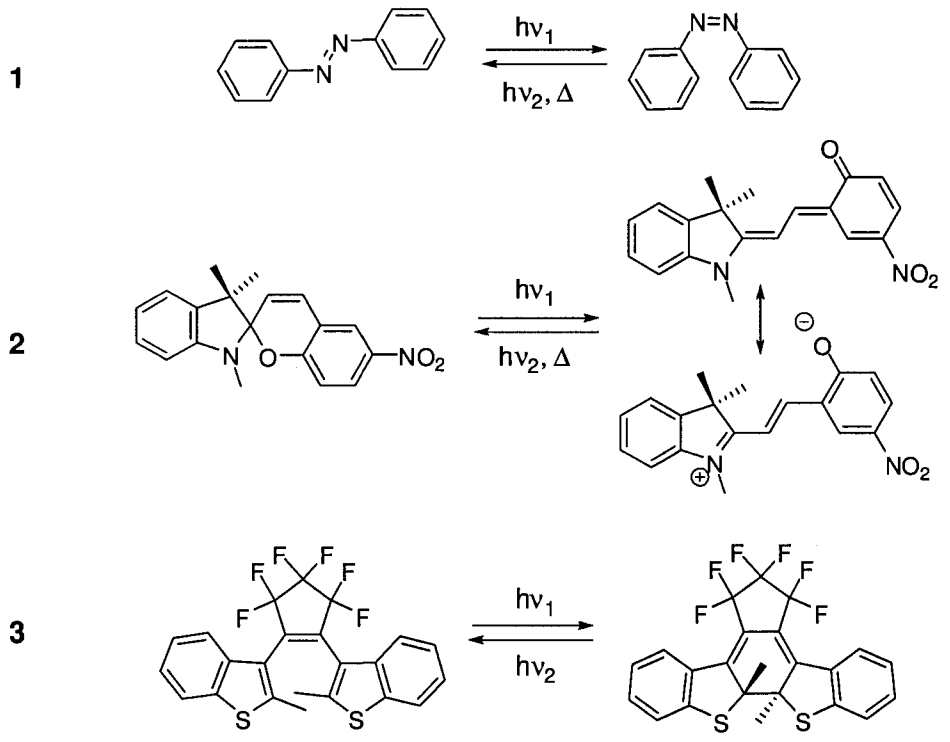

Scheme 1.1: Examples of common unimolecular photochromic systems: Azobenzene (**1**), spiropyran (**2**) and dithienylethene (**3**).[1]

1.3 Bimolecular photochromism

1.3.1 Common bimolecular systems

The most common bimolecular photochromic systems undergo either [2+2] or [4+4] cycloaddition reactions leading to dimerisation of the photochromic moiety when exposed to UV or visible light. Non-exhaustive lists of molecules known to undergo [2+2] and [4+4] cycloadditions are shown in Scheme 1.2 and Scheme 1.3 respectively.

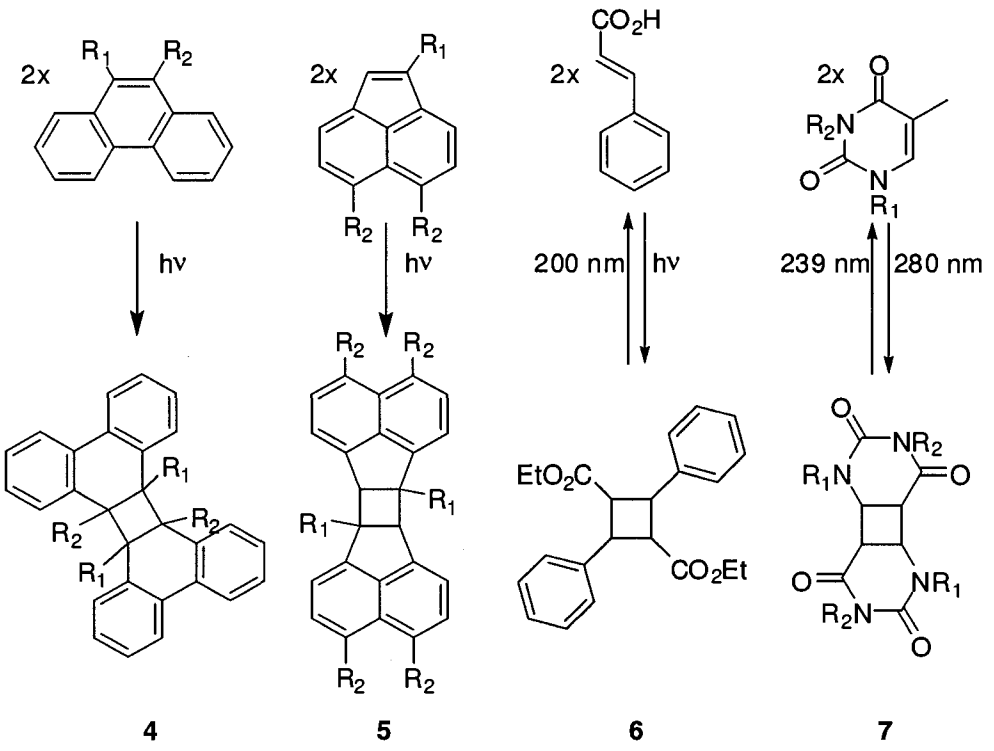

Scheme 1.2: Common systems undergoing [2+2]-photocycloaddition when exposed to UV irradiation: Phenanthrene (**4**), acetanaphthylene (**5**), cinnamate acid (**6**) and thymine (**7**).

Cycloaddition involving four π electrons, yielding a cyclobutane ring through a [2+2] cycloaddition of ethene containing chromophores, tends to induce only a small shift in absorption spectra.[1,9] This makes these systems less attractive for material applications such as photochromic lenses and optical data storage, which are focused on the change of colour. Materials containing cinnamate moieties (**6**) have been investigated for printing, lithography and photoresist applications.[10,11] The dimerisation of thymine (**7**) has been extensively investigated, as it has been shown to cause lesions in DNA leading to apoptosis, immuno-suppression and carcinogenesis.[12,13]

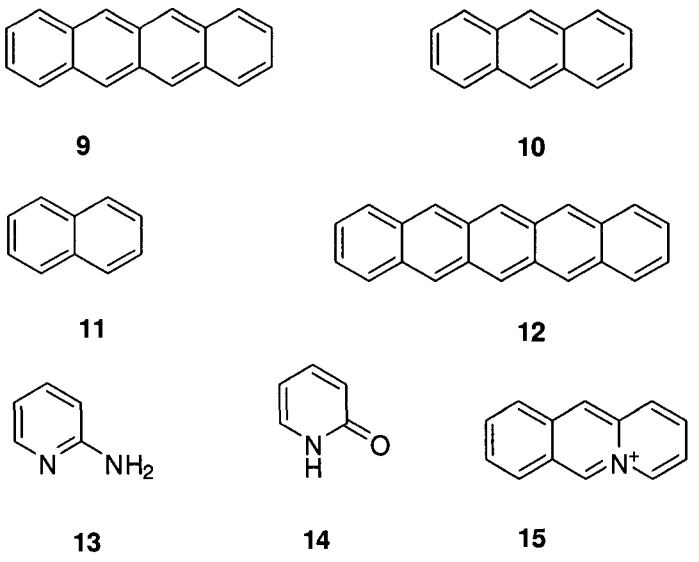

Scheme 1.3: Examples of molecules undergoing [4+4] cycloaddition under UV irradiation: Tetracene (**9**), anthracene (**10**), naphthalene (**11**), pentacene (**12**), 2-aminopyridine (**13**), 2-pyridone (**14**) and acridizinium (**15**).[1]

The first example of a [4+4] cycloaddition was reported for the dimerisation of tetracene (**9**) in 1867 by Fritzsche.[14] Since then, other conjugated systems such as naphthalene (**11**) and more recently pentacene (**12**), as well as heterocyclic systems such as acridizinium (**15**) were reported to undergo [4+4] photocycloaddition reactions.[15-17] Anthracene (**10**) and its derivatives remain the most studied systems and several reviews concerning their photochromic properties have been published.[18,19] Thus, anthracene will be used to illustrate the mechanism of [4+4] photocycloaddition reactions.

1.3.2 Anthracene photochemistry

The photochromic properties of anthracene were first reported by Fritzsche in 1867, when he exposed an extract of tar to sun light and observed an insoluble white powder adhering on the walls of the glassware.[14]

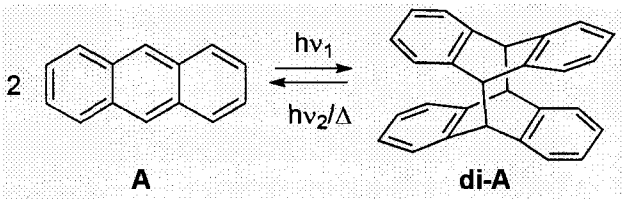

Equation 1.2: Formation of dianthracene (**di-A**) under UV light exposure of anthracene (**A**) and reversion from **di-A** to **A** through light $h\nu_1 > h\nu_2$ or heat.

Luther and Weigert reported the first investigation of the mechanism of dimerisation of anthracene in 1905.[20,21] However, it was not until the 1950's, along with the emergence of systematic studies on the mechanistic aspects of photochemical reaction processes, that Förster and Kasper discovered the formation of excimers (excited dimers).[22] The discovery of excimer formation combined with the Woodward-Hoffman rules in 1965 generated interest in the mechanism of anthracene dimerisation. As shown in Scheme 1.4, once a molecule of anthracene interacts with a photon, it is excited to the singlet state ^{1}**A*** which can then relax *via* several competing paths. Thus, as observed by Bowen and coworkers, an increase in dimerisation will be accompanied by a decrease in fluorescence.[23] The formation of an excimer during anthracene dimerisation was first proposed by Ferguson in 1974 and confimed by Cohen *et al.* in 1976.[24-26]

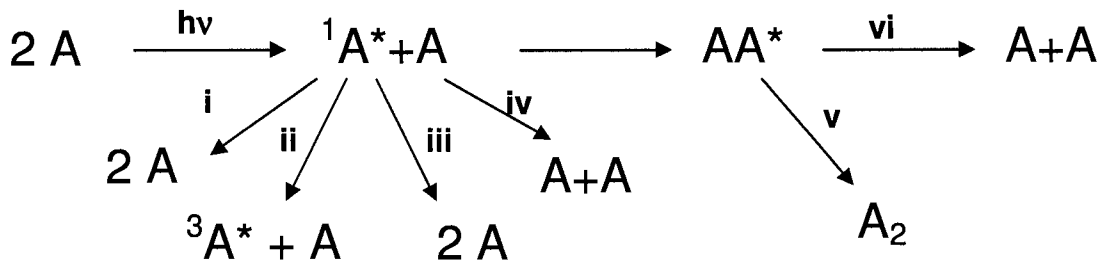

Scheme 1.4: Paths of relaxation of anthracene in its singlet excited state: (i) Internal conversion, (ii) Inter-system crossing, (iii) luminescence, (iv) non-radiative deactivation, (v) dimerisation and (vi) dissociation.

The [4+4] photocycloaddition across the central ring of two anthracenes results in the formation of two new sigma bonds at the 9- and 10-positions (Figure 1.1) which are the most reactive positions of the anthracene core as most of the electron density is located on the central ring.[27] Along with the competing photophysical processes shown in Scheme 1.4, other photochemical events can occur resulting in a reduction of the dimerisation efficiency.[18] It was demonstrated that when irradiated at low concentration in presence of molecular oxygen, anthracene undergoes photooxidation to yield 9,10-epidoxioanthracene (**AO_2** endoperoxide) (Scheme 1.5).[18] **AO_2** is formed by reaction of singlet oxygen, sensitised by the triplet state of anthracene, at the 9-and 10-positions of anthracene (Scheme 1.5).[27] Thus, to avoid the formation of the endoperoxide, the dimerisation of anthracene must often be carried out in a rigorously deoxygenated solvent, which makes anthracene dimerisation less attractive than other photochromic systems for practical applications such as holographic memory or photoinduced patterning.[16,28,29]

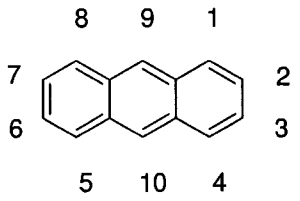

Figure 1.1: Numbering of positions of anthracene.

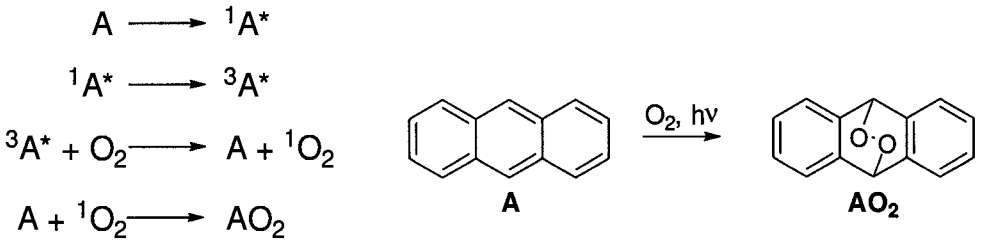

Scheme 1.5: Formation of endoperoxide (**AO_2**) when anthracene (**A**) is irradiated in presence of oxygen.

1.4 Reversibly cross-linked polymers

1.4.1 Applications of reversible photo-cross-linking

The changes of physical properties (*e.g.* refractive index or solubility) involved with the dimerisation *via* either [2+2] and [4+4] processes can be exploited for practical applications. For instance, Tomlinson and co-workers investigated the dimerisation of several systems for holographic applications with non-destructive read-out.[30,31] Kuckling and co-worker used the change in solubility associated with the dimerisation of acridizinium salt of a poly(N-isopropyl-acrylamide) to induce hydrogel formation and consequently photoinduced patterning of thin films at the picometer scale in aqueous media.[16,28] It should however be noted that the application of photochromic systems has to overcome several practical limitations including fatigue

resistance, competition of absorption between two or more chromophores species and thermal stability.[1]

1.4.2 Previous efforts towards photo-reversibly cross-linked polymers

The use of photodimerisation as a tool to induce cross-linking in polymers has been widely studied.[32] Most studies focused on the dimerisation of cinnamate-based polymers, which suffer from the competing E/Z isomerisation resulting in a decrease in dimerisation efficiency.[29,33] Other systems based on [2+2] photocycloaddition such as coumarin or thymine labelled polymers have been reported.[34] However, only a limited number of reports have described the [4+4] photocycloaddition of systems other than anthracene (Scheme 1.3).[16]

1.4.3 Anthracene containing polymers

Several anthracene-containing polymers have been reported to undergo successful cross-linking through [4+4] photocycloaddition in solution.[32,35-38] Coursan and co-workers reported the photoreversible cross-linking of anthracene end-capped polystyrene.[36] However, both Zheng and Matsui independently observed that the irradiation of the cross-linked polymer with shorter wavelengths (< 300 nm) only partially regenerated the anthracene.[29,37] Zheng and co-workers suggested that the lack of reversibility was due to the competing absorption by the carbonyl functionality, but the change from an ester to an ether functionality did not lead to improved reversibility.[29] They also observed a decrease in rate of photoreaction for both forward and backward reactions in solid thin films.[29] This

reduced photoreactivity was ascribed to the lack of flexibility in the solid state, where anthracene cannot align optimally for photodimerisation. In order to, one day, witness the use of anthracene dimerisation in practical applications, studies have been focusing in overcoming the limitations that have been presented earlier, that is to say, the limited efficiency of the dimerisation, the tendency to form photooxidation product and the high energy required for the photodissociation step.

1.4.4 Influence of the substitution pattern

Research on dimerisation of anthracene derivatives has focused on compounds with substituents at the 9- and 10- positions, which are generally the most synthetically accessible derivatives as the carbon atoms on the central ring are the most reactive positions.[19] However, it has been demonstrated that the added steric bulk at these sites reduces the thermal stability of the photoadduct; hence, 9,10-disubstituted anthracenes do not tend to form homodimers, whereas 9-substituted derivatives form only the less sterically encumbered of two possible regioisomers (Equation 1.3).[18,19] Thus, changing the substitution to the peripheral 1-8-position could potentially lead to more thermally stable dimers. However, functionalisation at the 2- and 3-positions is not straightforward since the peripheral positions of the anthracene core are not as reactive.[19] The development of a system with synthetically accessible functionalisation that also undergoes [4+4] cycloaddition would enable the design of a reversibly cross-linked polymer based on bimolecular photochromism.

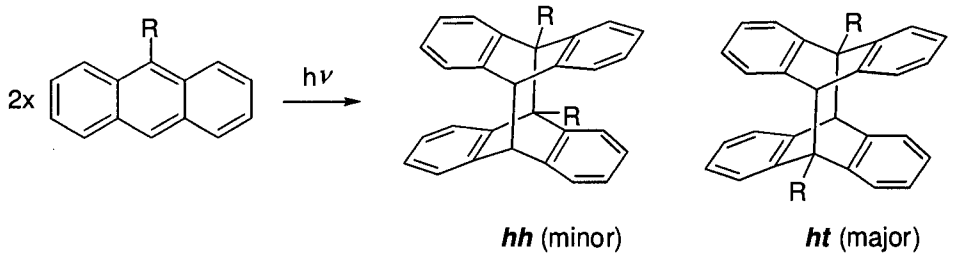

Equation 1.3: Possible isomers resulting from irradiation of a 9-substituted anthracene.

One potential solution to the lack of reversibility observed by Zheng [29] and Matsui [37] would be to tailor the anthracene moiety such that its dimer absorbs light above 300 nm. Indeed, reducing the energy necessary for the photodissociation would in turn decrease the number of possible photochemical events occurring upon irradiation and render the dissociation more efficient. As shown in Equation 1.3, groups at the 9- and 10- positions will only have a small effect on the absorption properties of the dimer since such groups do not contribute to the conjugated π-system in the dimer. Thus, substitution of the outer rings would be preferred to ensure the thermal stability of the dimer and red-shift its absorption as a result of the extended conjugated system. Such system would be more advantageous for material applications.

When a mixture of 2 anthracene compounds **A** and **B** is irradiated, three photoadducts can be formed: two dimers **AA** and **BB** and one cross-adduct **AB**. Previous work in our laboratory successfully exploited steric demands in anthracene dimerisation as a tool for selective photoadduct formation.[39] As part of this work, synthetic routes to peripherally substituted anthracene via Diels-Alder reactions of appropriate disubstituted sulfones or cyclopentadienones with

benzoquinones were developed.[40,41] These approaches were used to synthesise a variety of substituted anthracenes, albeit in low yields and over several steps. Such time-consuming synthetic routes combined with the low yields prevent such systems from being extensively investigated and in turns delays their use in material application. It is therefore necessary to develop a photochromic system that would be more synthetically accessible.

1.4.5 Possible heterocyclic candidates for bimolecular photochromism

Another approach to overcome the limitations of anthracene photochromism, is to introduce heteroatoms in the core while keeping it isoelectronic to anthracene. The most extensively studied nitrogen-containing analogues of anthracenes are acridiziums (**15**). Bradscher and co-workers reported that UV irradiation of a solution bromo acrizidinium salt yielded a photoadduct that was formed by [4+4] cycloaddition across the central ring of two acridizinium moieties.[42] Diazaanthracenes are systems where two carbons in the anthracene core were replaced by two nitrogens. To the best of our knowledge, only three isolated diazaanthracenes were reported to undergo successful [4+4] photocycloaddition in a similar manner to anthracene. Stimulated by the development of rigid framework containing pyrimidine base components, Warrener and co-workers reported dimerisation of 1,3-diazaanthracene (**16**) which was the first example of diazaanthracene [4+4] photocycloaddition.[43] However, neither the photodissociation of **16** nor the investigation of the photochemistry of its parent molecules was reported. Jouvenot and co-workers investigated the photochromic properties of 2,7-diazaanthracene **17** in an effort

to develop responsive ligands that could be employed to switch interactions between coordination centres.[44] More recently, Berni and co-workers reported the photochromic properties of 4,5-diazaanthracene **18** in an effort to capture helical foldamers in helice-like molecules.[45] Even though such diazaanthracenes possess interesting properties, their synthesis requires time-consuming multistep approach.

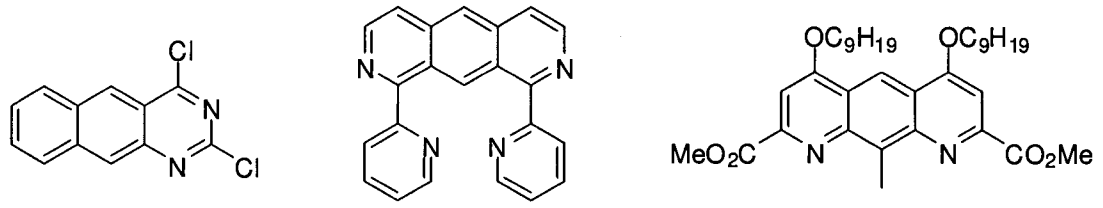

16 **17** **18**

Figure 1.2: Exhaustive list of diazaanthracene reported to undergo successful [4+4] photocycloaddition.

In order to develop a photochromic system that can be easily functionalised at the peripheral positions (*i.e.* not the 9- and 10-), we turned our attention to pyrazine containing polycyclic molecules. The structural similarity between benzo[2,3-*g*]quinoxaline (**BQ**), pyrazo[2,3-*g*]quinoxaline (**PQ**) and anthracene (**A**) led us to investigate the former two compounds as possible photochromic molecules (Figure 1.3). This work constitutes the major body of this thesis. The following sections will briefly introduce the chemistry of these and related molecules.

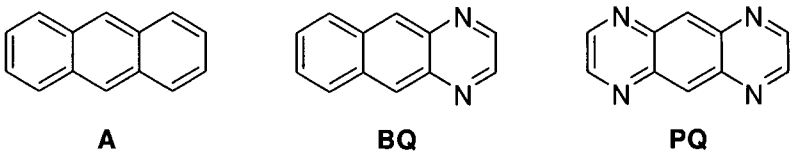

Figure 1.3: Structures of anthracene (**A**), benzo[2,3-*g*]quinoxaline (**BQ**) and pyrazo[2,3-*g*]quinoxaline (**PQ**)

1.5 Pyrazine-containing molecules

1.5.1 Common pyrazine containing molecules

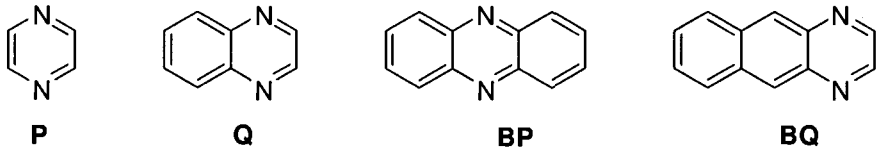

Figure 1.4: Different pyrazine (**P**) containing moieties, quinoxaline (**Q**), benzophenazine (**BP**) and benzo[2,3-*g*]quinoxaline (**BQ**).

Although pyrazines are synthetically accessible, their natural occurrence is fairly limited.[46] The dialkylated pyrazine rings are present in fused oils or flavour constituents in foodstuffs and these compounds are produced from proteins during fermentation.[47] Pyrazines represent important intermediates in fragrance or agricultural chemicals.[48]

The synthesis of pyrazine rings is typically achieved by condensation of unsaturated 1,2-diamine and a 1,2-diketone. For instance, refluxing a mixture of *o*-phenylenediamine and benzil in ethanol quantitatively yields 1,2-diphenylquinoxaline (Scheme 1.6).[49]

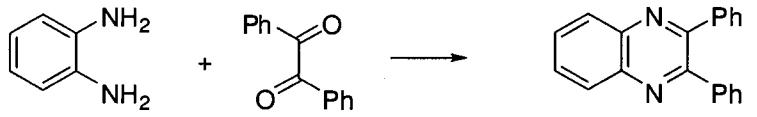

Scheme 1.6: Synthesis of 1,2-diphenylquinoxaline.

Symmetrically substituted pyrazines can also be obtained by self-condensation of α-amino carbonyl compounds.[50] This method is not optimum for unsymmetrical pyrazines as it yields a mixture of regioisomers. Thus, Buchi and Galindo developed a route to obtain alkylpyrazines from α-hydroxyimino ketones (Scheme 1.7).[51]

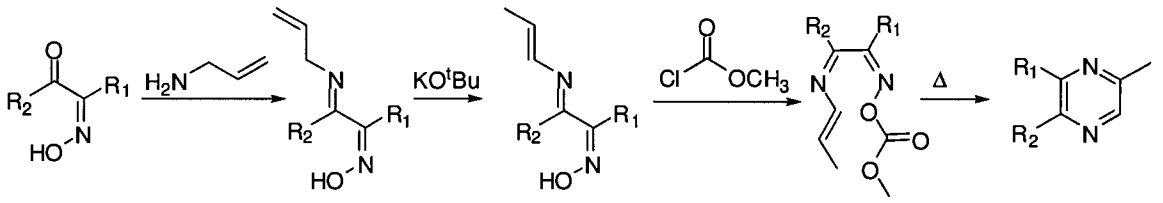

Scheme 1.7: Synthesis of alkypyrazines from α-hydroxyimino ketones.[51]

A wide variety of substituted pyrazines such as 2,3-substituted benzo[2,3-*g*]quinoxaline have been synthesised by condensation of 2,3-diaminonaphthalene with 2,3-diketones (Figure 1.5). The photochemistry of these compounds has yet to be reported.

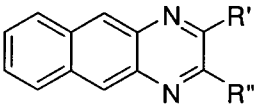

Figure 1.5: 2,3-substituted benzo[2,3-*g*]quinoxaline.

1.6 Objectives

This thesis will describe synthesis and the study of the photochromic properties of benzo[2,3-*g*]quinoxaline derivatives in an attempt to overcome the limitations encountered with the anthracene systems. 2,3-Diphenylbenzo[2,3-*g*]quinoxaline (**DPBQ**) will be synthesised and its photochromic properties investigated. To investigate the influence of substituents, the groups at the peripheral positions will be modified and their the photochemical properties will becompared to those of **DPBQ**. Finally, in order to develop a more selective photochromic system, the photochemical properties of tetraphenylpyrazo[2,3-*g*]quinoxaline will be investigated.

CHAPTER 2: PHOTOCHROMIC PROPERTIES OF SUBSTITUTED BENZOQUINOXALINE

2.1 Introduction

As was discussed in the previous chapter, bimolecular photochromic reactions offer unique opportunities for creating dynamic materials. Anthracene derivatives have been the most extensively studied bimolecular photochromic systems. However, these systems have many practical limitations, such as their often cumbersome synthesis and a tendency to form endoperoxides when irradiated in presence of oxygen.[18] The structural similarity between anthracene and benzo[2,3-*g*]quinoxaline, along with the relative ease of synthesis of the latter compound, led us to investigate the possible dimerisation of this class of heterocycles (Figure 2.1). The photochromic properties of a series of quinoxaline derivatives will be presented and will be compared with their anthracene analogues.

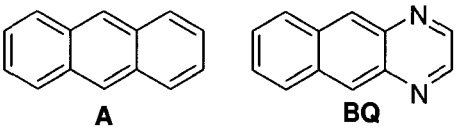

A **BQ**

Figure 2.1: Structure of anthracene (**A**) and benzo[2,3-g]quinoxaline (**BQ**).

2.1.1 Reactivity of benzo[2,3-*g*]quinoxalines

Prior to the synthesis of the targeted benzo[2,3-*g*]quinoxaline derivatives, the electron density of the HOMO and LUMO of benzo[2,3-*g*]quinoxaline (**BQ**) were calculated using semi-empirical calculations at the AM1 level and compared to those of anthracene. Like anthracene, both the HOMO and LUMO of **BQ** are predicted to have large coefficients at the 9- and 10- positions of the tricyclic core (Figure 2.2). This preliminary calculation suggested that **BQ** could undergo [4+4] cycloaddition upon irradiation.

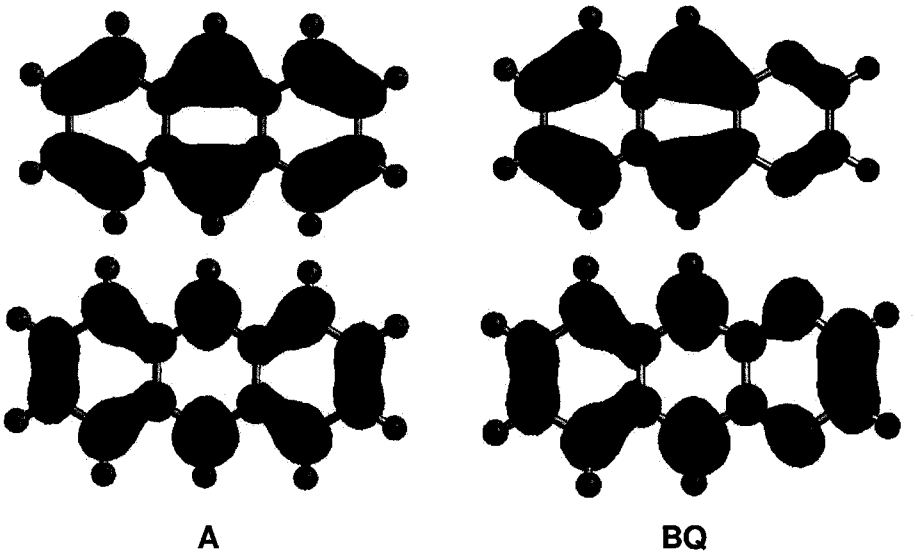

Figure 2.2: Orbital representation of HOMO (bottom) and LUMO (top) of anthracene (**A**) and benzoquinoxaline (**BQ**) calculated at the AM1 level.

2.1.2 Objectives

According to the information provided by the preliminary AM1 calculations, benzo[2,3-*g*]quinoxaline was expected to undergo [4+4] photocycloaddition across the central ring upon UV-irradiation. 2,3-Disubstituted benzo[2,3-

g]quinoxalines can potentially undergo [4+4] photocycloaddition to produce six isomers (Scheme 2.1).

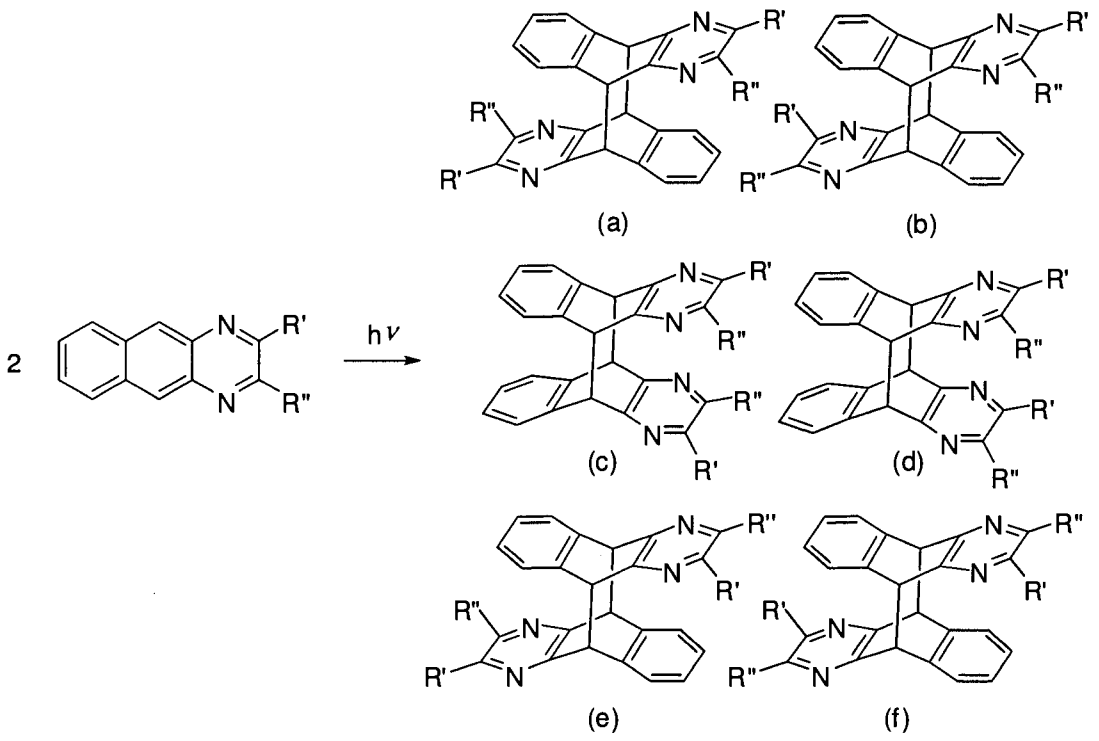

Scheme 2.1: Possible isomers resulting from [4+4] photocycloaddition of a 2,3-disubstituted benzo[2,3-*g*]quinoxaline.

When R' and R" are identical, the possible number of isomers is reduced to two stereoisomers, referred to as head-to-head ***hh*** (c and d) and head-to-tail ***ht*** (a, b, e and f). A previous study in our group demonstrated that irradiation of a degassed solution of 2,3-diphenylanthracene (**DPA**) in CH_3CN with 350 nm light led to the formation of only one photoadduct. It was suggested that the less sterically hindered ***ht***-photoadduct was formed (Scheme 2.2).[18,27,52] Hence, we could expect that irradiation of 2,3-disubstituted benzo[2,3-*g*]quinoxaline would also lead to the least hindered photoproduct.

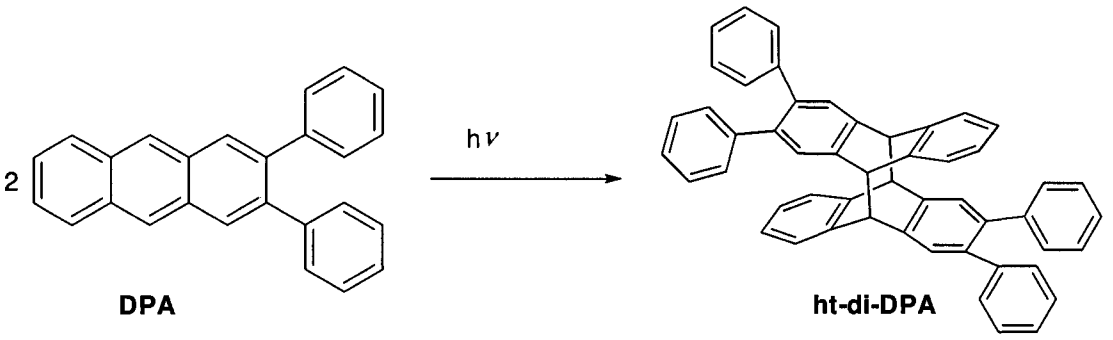

Scheme 2.2: Formation of *ht*-dimer after [4+4] photocycloaddition of 2,3-diphenylanthracene.

2.2 Results and discussion

2.2.1 Photochromism of 2,3-Diphenylbenzo[2,3-*g*]quinoxaline

2,3-Diphenylbenzo[2,3-*g*]quinoxaline (**DPBQ**) was chosen to investigate whether benzo[2,3-*g*]quinoxaline derivatives could undergo [4+4] photocycloaddition upon UV-irradiation as it was expected to lead to only two possible photoadducts (***hh*** and ***ht***). **DPBQ** was synthesised according to literature procedure by condensation of the commercially available 2,3-diaminonaphthalene and benzil[53] (Scheme 2.3) and characterised by ^{1}H-NMR and UV-Vis absorption spectroscopy as well MALDI-TOF mass spectroscopy. The UV-Vis absorption spectrum of this compound in CH_3CN reveals a strong absorbance centred at 270 nm and a less intense set of bands at longer wavelengths (λ_{max} = 380 nm)(Figure 2.4), which suggested that UV irradiation could lead to a photochemical reaction.

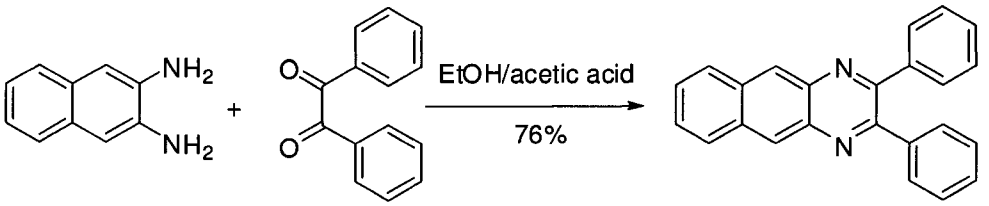

DPBQ

Scheme 2.3: Synthesis of **DPBQ**.

2.2.1.1 [4+4] Photocycloaddition of DPBQ

In order to study its photochemical behaviour, a 4.4 mM solution of **DPBQ** in CH_3CN was irradiated with 350 nm lamps in a Rayonet® photochemical reactor. After 2.5 h of irradiation, a white powder was formed on the side of the reaction vessel. This is consistent with the behaviour of anthracene dimers which tend to have lower solubility than their monomeric forms. Unlike anthracene dimers, which tend to be ionised and break apart during mass spectrometry experiments, the MALDI-TOF spectrum of the photoadduct of **DPBQ** exhibited a peak at m/z = 665, corresponding to the dimer (M+1) peak in addition to a more intense peak corresponding to **DPBQ**. The insoluble white powder was isolated from the reaction medium by decantation of CH_3CN and characterised by ^{1}H-NMR spectroscopy. The singlet corresponding to the protons at the 9- and 10-positions shifted from 8.75 to 5.06 ppm, which is consistent with the change of hybridization from sp^2 to sp^3 as a bridgehead was formed between the central rings in the benzo[2,3-*g*]quinoxaline moieties (Figure 2.3).[18] The presence of a single peak at 5.06 ppm is consistent with the presence of only one photoadduct, which was tentatively inferred to be the ***ht***-

dimer for steric reasons. The observed peak at 52.7 ppm in the ^{13}C-NMR spectrum of the photoadduct was consistent with the shift observed for **di-DPA** with respect to **DPA** (from 141.5 to 53.4 ppm).[39] The UV-Vis absorption spectrum of **di-DPBQ** is blue-shifted with respect to that of **DPBQ**, with an absorption maximum at 328 nm (Figure 2.4). This is consistent with the reduction of delocalisation of the π-electrons as the dimerisation results in a change of hybridisation of the carbon atoms in the central ring from sp^2 to sp^3. Like anthracene dimers, **di-DPBQ** does not absorb in the visible region, but its absorption is significantly red-shifted with respect to that of **di-DPA**.[39] Such red-shift in absorption represents an advantage over the anthracene analogue as the photodissociation would require less energy and in turn reduce the number of other possible photochemical events occurring in solution.

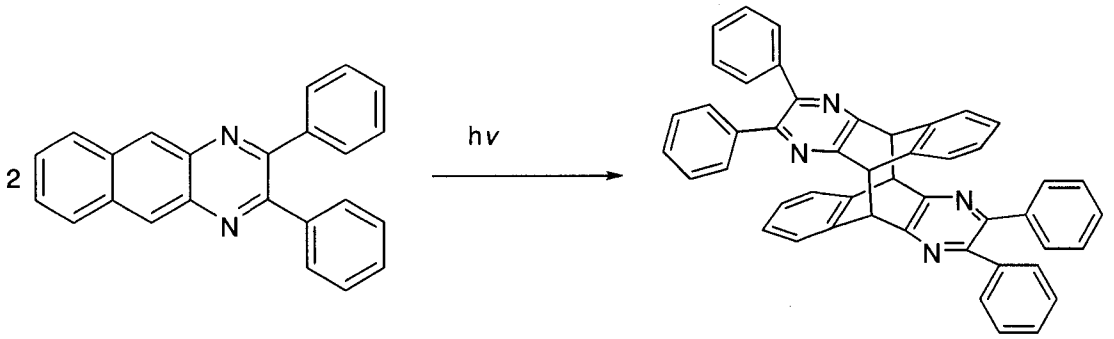

Scheme 2.4: Photodimerisation of **DPBQ.**

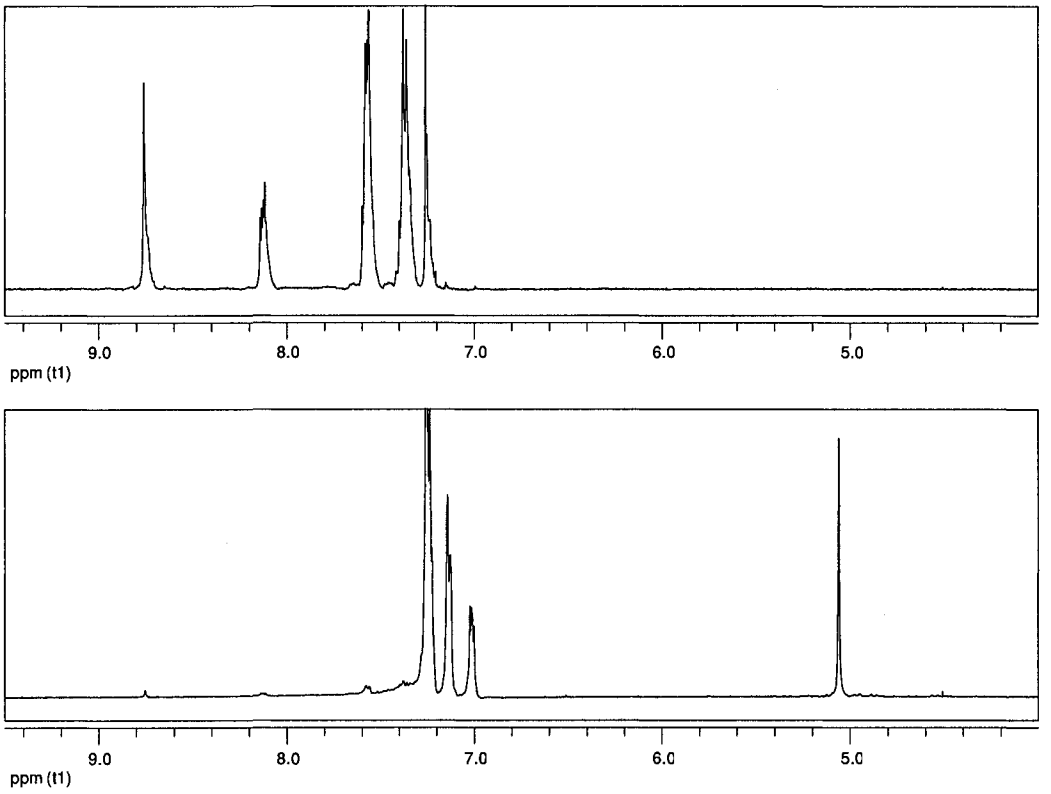

Figure 2.3: ^{1}H-NMR spectra of **DPBQ** recorded in $CDCl_3$ before (top) and white solid isolated by decantation of CH_3CN after 150 of irradiation (bottom).

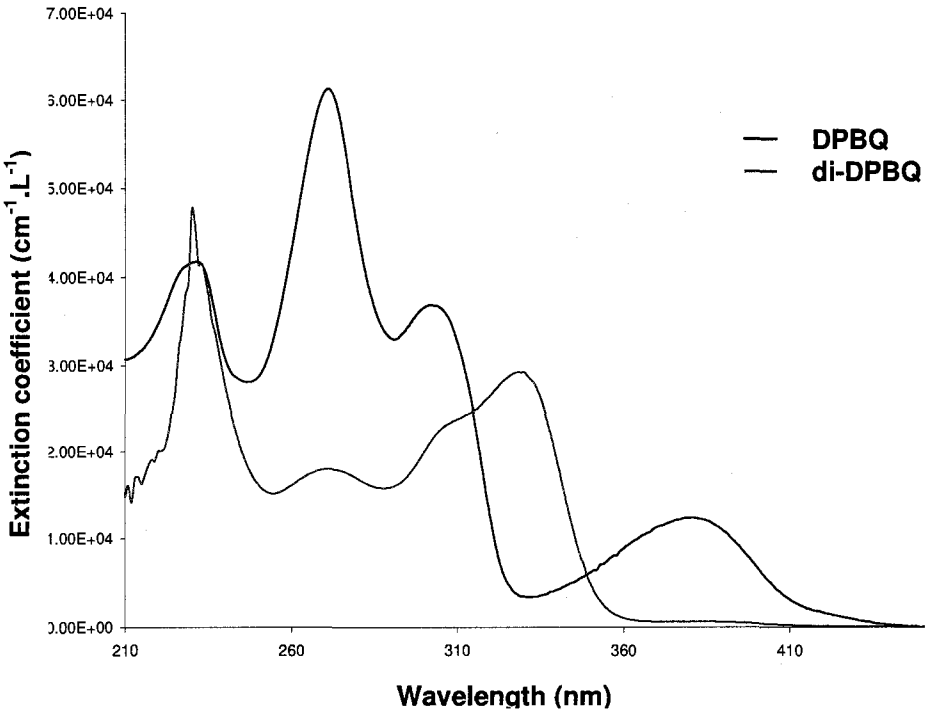

Figure 2.4: UV-Vis absorption spectra of a 5.0 μM solution of **DPBQ** and a 10.0 μL solution of **di-DPBQ** recorded at room-temperature in CH_3CN.

2.2.1.2 Crystal structure of di-DPBQ

The identification of this photoproduct as ***ht*-di-DPBQ** was confirmed by X-ray crystallography of single crystal obtained by slow evaporation of a 1:1 CH_3CN:$CHCl_3$ solution (Figure 2.5). Under these conditions, the **di-DPBQ** crystallizes in the monoclinic space group $P2_1\backslash n$. [a] The bond lengths between the sp^3-hybridized bridgehead carbons are 1.61(6) Å, which are longer than for a

[a] *Crystal data for* **di-DPBQ**: $C_{48}H_{32}N_4$, *M.W.* = 664.79, monoclinic, space group *P* 1 2_1/n 1, *a* 8.6132(9) , *b* = 18.4915(17), *c* = 10.9618(16) Å, β = 96.550(6), *V* = 1734.5(4) Å^3, T = 293 K, *Z* = 2, ρ_{calcd} = 1.273 g·cm^{-3}, μ(Cu-Kα) = 0.580, T = 293 K, 3014 unique reflections, 2639 observed ($I_o > 2.5\sigma(I_o)$). The final R_F = 0.0436 and R_{WF} = 0.0645 (observed data). Apendix I for full crystallographic data.

typical carbon-carbon single bond, but similar to the lengths of the corresponding bonds in dianthracene (1.624 Å) and related systems.[18]

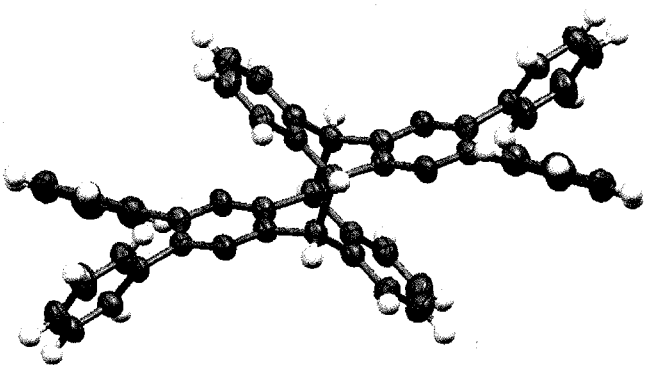

Figure 2.5: Crystal structure of **ht-di-DPBQ**

2.2.1.3 Formation of Endoperoxide

To test the sensitivity of **DPBQ** dimerisation to O_2, three samples of a 4.4 mM solution of **DPBQ** in CH_3CN were irradiated in the Rayonet® photochemical reactor with different levels of air in the reaction vessel. One sample was degassed by three freeze-pump-thaw cycles and irradiated under N_2, the second sample was not deoxygenated, but was irradiated under ambient conditions, while air was bubbled through the third sample during irradiation. The effect influence of oxygen was quantified by ^{1}H-NMR analysis of the concentrated solutions after 150 min of irradiation. Similar ratios of **DPBQ** to **di-DPBQ** in ^{1}H-NMR spectra of all three samples confirmed that unlike anthracene derivatives, the dimerisation of **DPBQ** was not sensitive to the presence of oxygen yielding only **di-DPBQ** (21 %). No additional products were observed in the presence of

O_2, suggesting that **DPBQ** can be irradiated in presence of oxygen without formation of endoperoxide or singlet oxygen, which represents a significant advantage in terms of fatigue resistance and performance relative to anthracene. The above results suggest that photodimerisation occurs from the singlet excited state, since triplets would likely undergo quenching by oxygen.[27] As shown in Scheme 1.5, the formation of endoperoxide is dependent on the sensitisation of O_2 by the excited molecule of **DPBQ** in its triplet state.

In an effort to better understand the mechanism of photodimerisation, the excited state lifetimes of **DPBQ** were determined by single-photon counting for the singlet excited state and by laser flash photolysis for the triplet state by Dr. Cornelia Bohne and Tamara Pace (University of Victoria, BC, Canada).[b54] The singlet state lifetime was found to be 1.9 ± 0.1 ns in CH_3CN and less than 0.5 ns in cyclohexane. The triplet lifetime is long (≥ 10 μs) in CH_3CN and cyclohexane. The singlet excited state of anthracene has a lifetime of approximately 5.3 ns. In comparison, the lifetime of the singlet excited state of **DPBQ** is very short, thus the efficiency of dimerisation is expected to be reduced. Indeed, when two degassed solutions of **A** and **DPBQ** are irradiated in the same conditions, **di-A** is formed in 86 %, whereas **di-DPBQ** is formed in 21 %. Even though the triplet lifetime of **DPBQ** is relatively long lived, the unsuccessful sensitisation of O_2 by

[bb] Fluorescence spectra were measured with a PTI QM-2 spectrometer and the singlet excited state lifetimes were measured with a OB920 single photon counter from Edinburgh. The excitation wavelength was 380 nm and emission spectra were collected between 395 and 700 nm (slit bandwidth of 3 nm), while decays were collected at 460 or 490 nm (slit bandwidth of 16 nm). For a description of the laser flash photolysis system.[54] Samples were excited with a Nd:YAG laser at 266 nm and the kinetics was monitored at 400-410 and 460 nm. For all photophysical experiments samples were deoxygenated by bubbling nitrogen for 20 min.

excited **DPBQ** in its triplet state can be rationalised by the fact that there are competing photophysical events occurring in solution (Scheme 1.4).

Assuming that the photodimerisation occurs through a singlet state, the efficency of dimerisation is dependent on the probability of an excited molecule ***A** interacting with another molecule in its ground state A to form the intermediate ***A-A**. This process, also called quenching, is diffusion limited.[55] Assuming a steady state of the concentration of ***A-A**, the rate constant for the dimerisation k_q can be expressed as followed:

$$*A + A \underset{k_d}{\overset{k_d}{\rightleftharpoons}} *A\text{-}A \xrightarrow{k_{de}} \text{dimer}$$

$$k_q = \frac{k_d k_{de}}{k_{-d} + k_{de}}$$

Assuming that the deactivation of the excited state ***A** is a competition between the monomolecular processes (fluorescence k_f and non-radiative processes k_{nr}) and bimolecular processes, the change of intensity of emission can be expressed by the Stern-Volmer equation expressed below:

$$\frac{I^0}{I} = 1 + \left(\frac{k_q}{k_0}\right)[A]$$

$$k_0 = k_f + k_{nr} = \frac{1}{\tau_0}$$

The Stern-Volmer constant K_{SV} is defined as:

$$K_{SV} = \frac{k_q}{k_0} = k_q \tau_0$$

Thus, the efficiency of the bimolecular reaction is directly proportional to the lifetime of the excited state τ_0. This may explain why less **di-DPBQ** was produced when two equimolar degassed solutions of **A** and **DPBQ** were irradiated simultaneously.

In order to rule out that dimerisation resulted from preassociation of **DPBQ**, UV-Vis absorption spectra of **DPBQ** in CH_3CN were recorded at concentrations ranging from 1.00 $x10^{-4}$ to 1.00 $x10^{-6}$ M. The linear plot of absorbance versus concentration confirmed that the Beer-Lambert law was obeyed, suggesting that no pre-association was taking place over this concentration range (Figure 2.6).

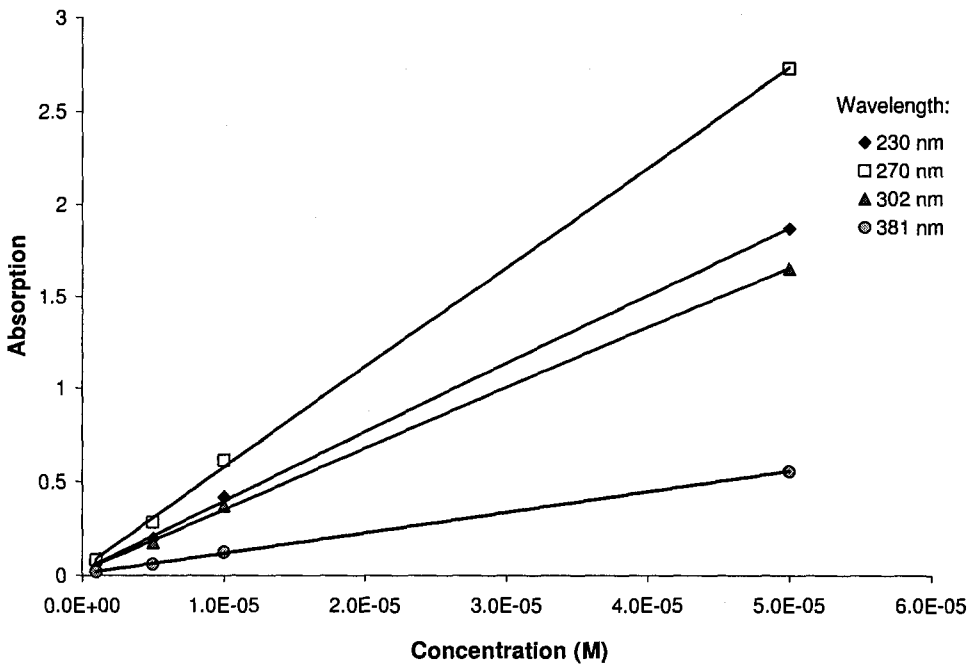

Figure 2.6: Plot of absorbance versus of concentration of **DPBQ** in CH_3CN recorded at 25 °C.

According to the Stern-Volmer equation, the amount of dimer formed should be proportional to the initial concentration of **DPBQ** in solution as well as

the number of incident photons. The 350 nm lamps that were used emit a non-negligible amount of light around 330 nm, the wavelength of light absorbed by the dimer. It is therefore possible that the dimer is being dissociated during the irradiation in the Rayonet® fitted with 350 nm lamps.

In an effort to further understand the effect of 350 nm lamps on the dimerisation of **DPBQ**, a solution of **di-DPQB** in CH_3CN was irradiated in the Rayonet® photochemical reactor. After 15 min, the dimer was fully dissociated back to the monomer. This result implied that the photoreactor produced enough light around 330 nm to dissociate the dimer during dimerisation of **DPBQ**, resulting in a reduced yield of dimerisation. It should however be pointed out that during the dimerisation experiments the lamps used also emits light at 350 nm where **di-DPBQ** has only a reduced absorption, which enables the formation of **di-DPBQ** which precipitated at of solution. Thus, the use of a monochromatic light source should improve the yield of the dimerisation of **DPBQ**. To that end, a 1.00 mM solution of **DPBQ** in CH_3CN was irradiated using a fluorimeter as a monochromatic light source (λ = 378 nm, slid width 5 nm). The progress of the reaction was followed by UV-Vis spectroscopy, which imposed a limitation on the concentration used for irradiation with the fluorimeter to 1.00 mM instead of 4.4 mM when the Rayonet® photoreactor was used. No change was observed in the UV-Vis spectrum with irradiation time; it therefore was concluded that the dimerisation using a selective light source was unsuccessful. The photodissociation studies of **di-DPBQ** (vide infra) demonstrated that the light source used for monochromatic irradiation was less effective than the Rayonet®

photoreactor® likely because of the lower flux. The lack of dimer formation of **DPBQ** under the same conditions can be associated with the reduced lifetime of the excited state with respect to anthracene. Consequently, the use of a more powerful monochromatic light source or the use of cut-off filters should improve the yield of dimerisation.

In order to demonstrate that the use of a cut-off filter would improve the yield of dimerisation **DPBQ**, a 2.00 M solution of KNO_3 in water was used to block wavelength under 340 nm.[56] In order to verify that the filter reduced the effectively prevented the dissociation of **di-DBPQ** in solution during the irradiation in the Rayonet®, a solution of **di-DPBQ** in CH_3CN was immersed in the KNO_3 solution and irradiated in Rayonet® photochemical reactor for 15 min. ^{1}H-NMR analysis of the concentrated solution did not show any **DPBQ**. A solution of **DPBQ** immersed in this filter solution was irradiated simultaneously with an identical sample without a filter solution in the Rayonet® photochemical reactor. After 150 min of irradiation, integration of the diagnostic peaks in ^{1}H-NMR spectra for **di-DBPQ** and **DPBQ**, at 5.1 and 8.8 ppm, respectively, in a ratio of 3.6: 1 indicated yield of photoadduct of 78 %, whereas irradiation without filter only yields 72 % of photoadduct with a peak ratio of 2.6 : 1. This confirmed that light under 340 nm influences the yield of photocycloaddition likely by partially dissociating **di-DPBQ** formed in solution.

In order to study the influence of the solvent used during irradiation of a **DPBQ** solution, **DPBQ** was dissolved in benzene, acetonitrile, chloroform, dichloromethane, deuterated chloroform and deuterated acetonitrile. A degassed

1.3 mM solution of **DPBQ** yielded 19 % of dimer in CH_3CN whereas only 14 % of dimer was formed in benzene when irradiated for 150 min in the Rayonet® photochemical reactor. However, irradiation of **DPBQ** in halogenated and deuterated solvent did not yield any dimer. The lack of any photoadduct formation after irradiation in halogenated solvent might be associated with the quenching of the excited **DPBQ** by the solvent. Dissociative charge transfer in halogenated solvents during photochemical reactions has been previously reported.[57,58] Hence, CH_3CN is better suited as a solvent for the dimerisation of **DPBQ.**

2.2.1.4 Photodissociation of di-DPBQ

In order to investigate the photodissociation of **di-DPBQ**, a 1.00 mM solution of **di-DPBQ** in CH_3CN was selectively irradiated with 328 nm light.[c] A continuous decrease in absorbance at 328 nm, along with an increase at 380 nm in the UV-Vis spectra demonstrated that **di-DPBQ** dissociates to the corresponding monomer when irradiated at 328 nm (Figure 2.7). After 240 min of irradiation, no more changes in absorption were observed, confirming that the dissociation had reached completion. The presence of isobestic points at 321 nm and 345 nm suggests that the dissociation from **di-DPBQ** to **DPBB** occurs in one step. This assumption is only valid if there are no other species absorbing in the region of the isobestic point generated during the photoreaction.

[c] This irradiation was carried out in 1 cm quartz cell and a fluorimeter was used as a selective light source allowing narrow excitation wavelength.

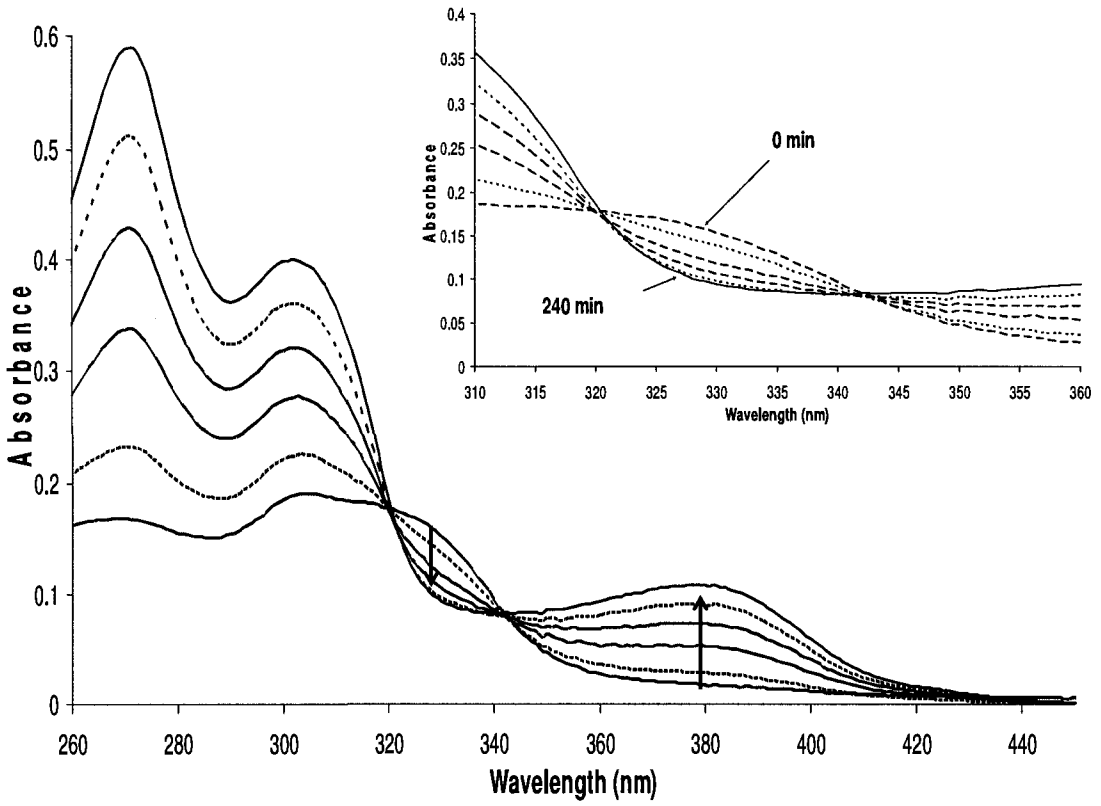

Figure 2.7: UV-Vis spectra monitoring the photodissociation of **di-DPBQ** when irradiated with 328 nm light at room temperature. Inset: zoom-in isobestic points.

2.2.1.5 Thermal dissociation of di-DPBQ

The thermal stability of **di-DPBQ** was studied by heating 25 mL aliquots of a 1 mM solution in DMSO at 80, 100, 120 and 150 °C. The effects of temperature were followed by UV-Vis absorption spectroscopy. For the samples heated for over five hours at 80, 100 and 120 °C, the lack of absorption in the 400 nm region associated with the absorption of the monomer indicated that **di-DPBQ** is stable at these temperatures for a prolonged period of time and did not undergo dissociation. As observed in the photodissociation study, the continuous decrease of absorption at 328 nm and a corresponding increase at 380 nm, with

increased heating time demonstrated that **di-DPBQ** started decomposing back to **DPBQ** after 1 h at 150 °C (Figure 2.8). After 150 min, a 73 % decrease in absorption at 328 nm and an increase at 380 nm in the UV-Vis spectrum were observed. Inconveniently, the thermal dissociation could not be carried out to completion as a result of an amount insufficient stock solution. None the less, the presence of two isobestic points at 323 nm and 347 nm shows that the dissociation of **di-DPBQ** proceeds without side product formation, similar to anthracene.[19] This suggested that longer exposure to heat would lead to full reversion of **di-DPBQ** to **DPBQ**.

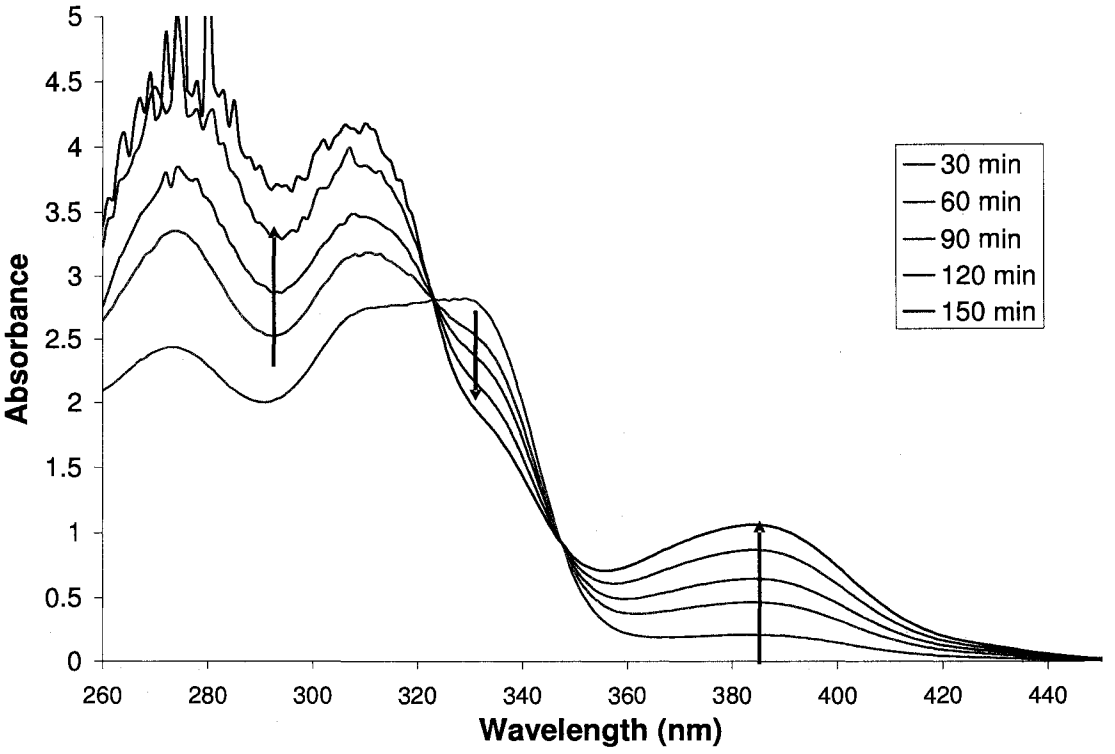

Figure 2.8: Variation of UV-Visible absorption spectra of a 1.0 mM solution of **di-DPBQ** in CH_3CN heated at 150 °C.

2.2.2 Influence of Substitution at the 2- and 3-positions

2.2.2.1 Phenyl groups

2.2.2.1.1 Synthesis

Once **DPBQ** was shown to undergo [4+4] photocycloaddition, we turned our attention to other derivatives. In order to further understand the influence of the substitution on the photodimerisation of benzo[2,3-*g*]quinoxaline derivatives, 2-phenylbenzo[2,3-*g*]quinoxaline (**PBQ**) and benzo[2,3-*g*]quinoxaline (**BQ**) were synthesised and their photochemical behaviours were investigated (Scheme 2.5 and Scheme 2.6) [59]

The unsubstitued benzo[2,3-*g*]quinoxaline core **BQ** was synthesised in two steps from glyoxal and 2,3-diaminonaphthalene (Scheme 2.5).[60]

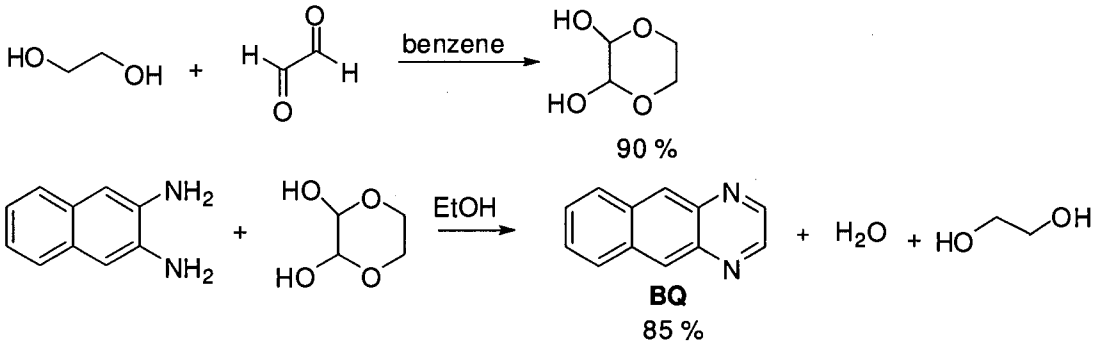

Scheme 2.5: Synthesis of **BQ**

The desired phenylglyoxal necessary for the synthesis of **PBQ** was synthesised by oxidation of acetophenone. Several literature procedures for the oxidation of benzophenone were examined. To avoid the use of carcinogenic

dioxane, the oxidation of benzophenone was achieved on silica using microwave irradiation, but separation of the phenylglyoxal from the silica was cumbersome.[61] The use of SeO_2 in dioxane solution [42] only yielded 35% of the target compound, which was not as attractive as the use of HBr as an oxidating agent, which led to the product in 87% yield.[59,62] **PBQ** was then obtained in 92% yield by condensation of phenylglyoxal with 2,3-diaminonaphthalene.

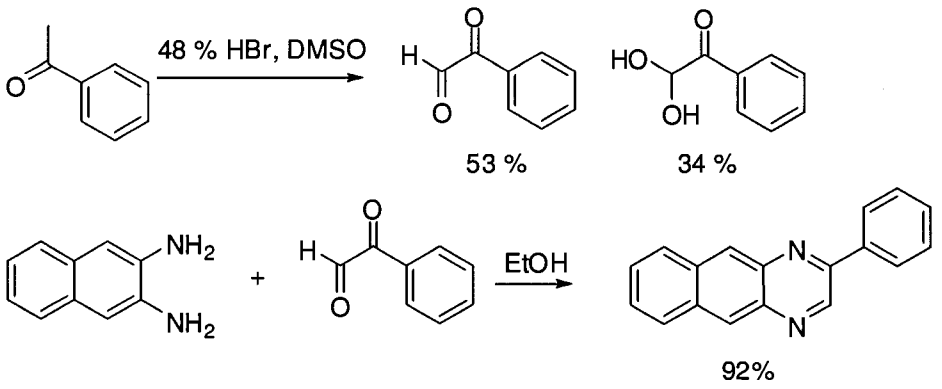

Scheme 2.6: Synthesis of **PBQ**

The UV-Vis absorption spectrum of **BQ** showed two strong peaks at 222 and 258 nm, and a less intense set of peaks centred at 359 nm, while the UV-Vis spectrum of **PBQ** was very similar to **DPBQ** (Figure 2.9). The absorption at the maximum wavelength of **PBQ** is less intense and blue-shifted relative to those of **DPBQ** but more intense and red-shifted with respect to **BQ**. This change in absorption is consistent with the reduced delocalisation of the π electrons. This shift to shorter wavelength from **DPBQ** to **BQ** was similar to the observations made between 2,3-diphenylanthracene and anthracene.[39]

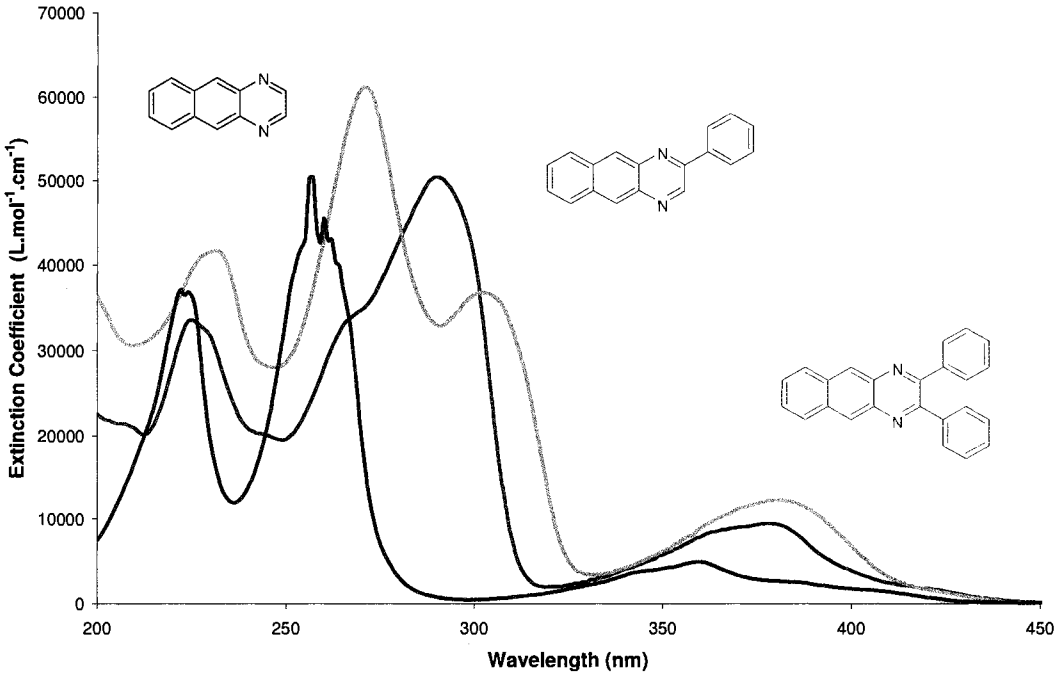

Figure 2.9: Comparison of UV-Vis spectra of **DPBQ, PBQ** and **BQ** recorded at room-temperature in CH_3CN

2.2.2.1.2 Photochemical studies

BQ exhibits a much lower solubility than **DPBQ** in CH_3CN, which necessitated carrying out photochemical experiments at lower concentrations than had been used for the latter compound. Irradiation of a 1.40 mM non-deoxygenated solution of **BQ** in spectral grade CH_3CN for 150 min did not lead to the formation of a precipitate. However, ^{1}H-NMR analysis of the concentrated reaction mixture showed a new peak at 4.41 ppm, which can be ascribed to a change of hybridisation of the central ring and new peaks in the aromatic region, demonstrating that **BQ** was reacting under UV-irradiation. Integration of the diagnostic peaks for **BQ** and the formed photoproduct at 8.77 and 4.85 ppm respectively, enabled us to determine that the photoproduct was formed in 41 %

yield, assuming that it was the dimer (Figure 2.10). MALDI-TOF MS showed two major peaks, the strongest at m/z = 180 corresponding to **BQ** and a second less intense peak at m/z = 391 associated with the M(**di-BQ**+K^+). Simultaneous irradiation of a 1.39 mM non-deoxygenated solution of **DPBQ** in CH_3CN in the same conditions yielded 40 % of **di-DPBQ**. This suggested that addition of phenyl groups at the peripheral position did not appreciably influence the photoreactivity of benzo[2,3-*g*]quinoxaline derivatives. Unfortunately, the low solubility of **BQ** also made isolation of the photoproduct more difficult. In the case **DPBQ**, isolation of the photoadduct was achieved by decantation of the solution containing the soluble unreacted monomer from the insoluble product. The similar solubility of the monomer and product precluded this approach, and isolating a sufficient amount of the photoproduct to carry out characterisation could not be achieved.

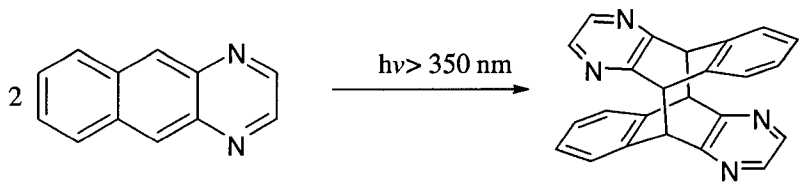

Scheme 2.7: [4+4]photocycloaddition of **BQ.**

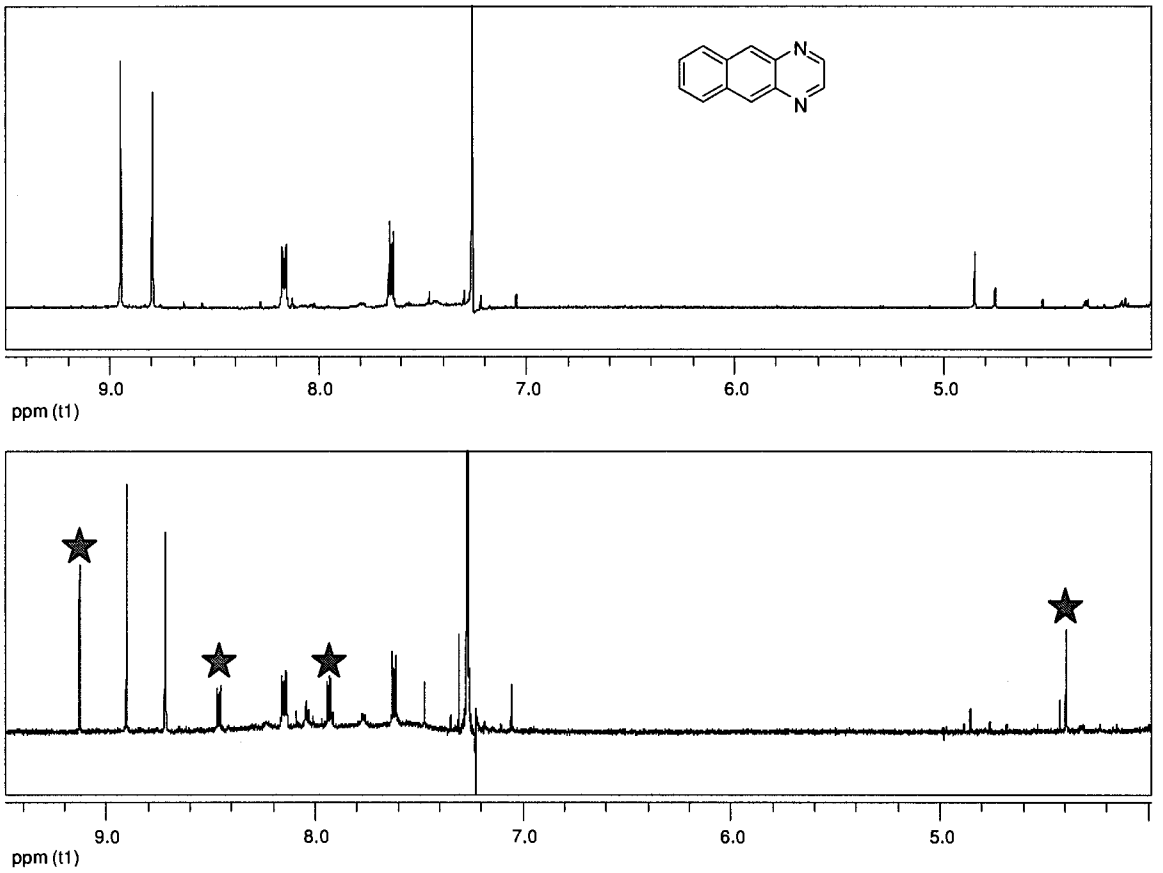

Figure 2.10: ^{1}H-NMR spectra of **BQ** recorded in $CDCl_3$ before (top) and after 150 min of irradiation (bottom). New peaks associate with the photoadduct are emphasised with stars.

Unlike **DPBQ,** no white solid was observed after irradiation of a 1.39 mM non-deoxygenated solution of **PBQ**. The MALDI-TOF mass spectrum of the solution showed two peaks; the heaviest fragment at m/z = 551 associated to M(**di-PBQ**+K)$^{+}$ (R.I= 117) and a more intense peak at m/z = 258 corresponding

to M(**PBQ**)$^+$ (R.I= 346), which is in accordance with results obtained after irradiation of a solution of **DPBQ** under the same conditions. ^{1}H-NMR analysis of the concentrated reaction mixture showed a new set of peaks in the aromatic region as well as two singlets at 5.1 and 5.09 ppm associated with the change a hybridisation on the central ring, which was consistent with the shifts observed for both **DPBQ** and **BQ** (Figure 2.11). The ^{1}H-NMR spectrum also showed another new peak at 9.5 ppm, which was assigned as the protons at the 3 and 3' position of the dimer. Assuming that the product was the dimer, integration of the diagnostic resonances of the **PBQ** at 9.3 ppm and the photoproduct at 9.5 ppm enabled us to determine a yield of 45 % for the product. On the other hand, integration of the two singlets (at 8.69 and 8.65 ppm) associated with **PBQ** versus the two singlets at 5.1 and 5.09 ppm associated with **di-PBQ** suggests a 13 % yield. It is therefore likely that another photoreaction is occurring under those conditions leading to a second photoproduct. Unfortunately, neither recrystallisation from acetone nor flash column chromatography were successful at separating **PBQ** from the photoproduct. Hence, the structures of the photoproducts could not be confirmed by X-ray crystallography. However, both MALDI mass spectrum and ^{1}H-NMR analysis suggest that the irradiation of a solution of **PBQ** in CH_3CN results in the formation of a **di-PBQ**. When irradiated in the same conditions, **DPBQ** and **A** yielded 40% and 44 % of dimer respectively but **A** also yielded 44 % of endoperoxide.

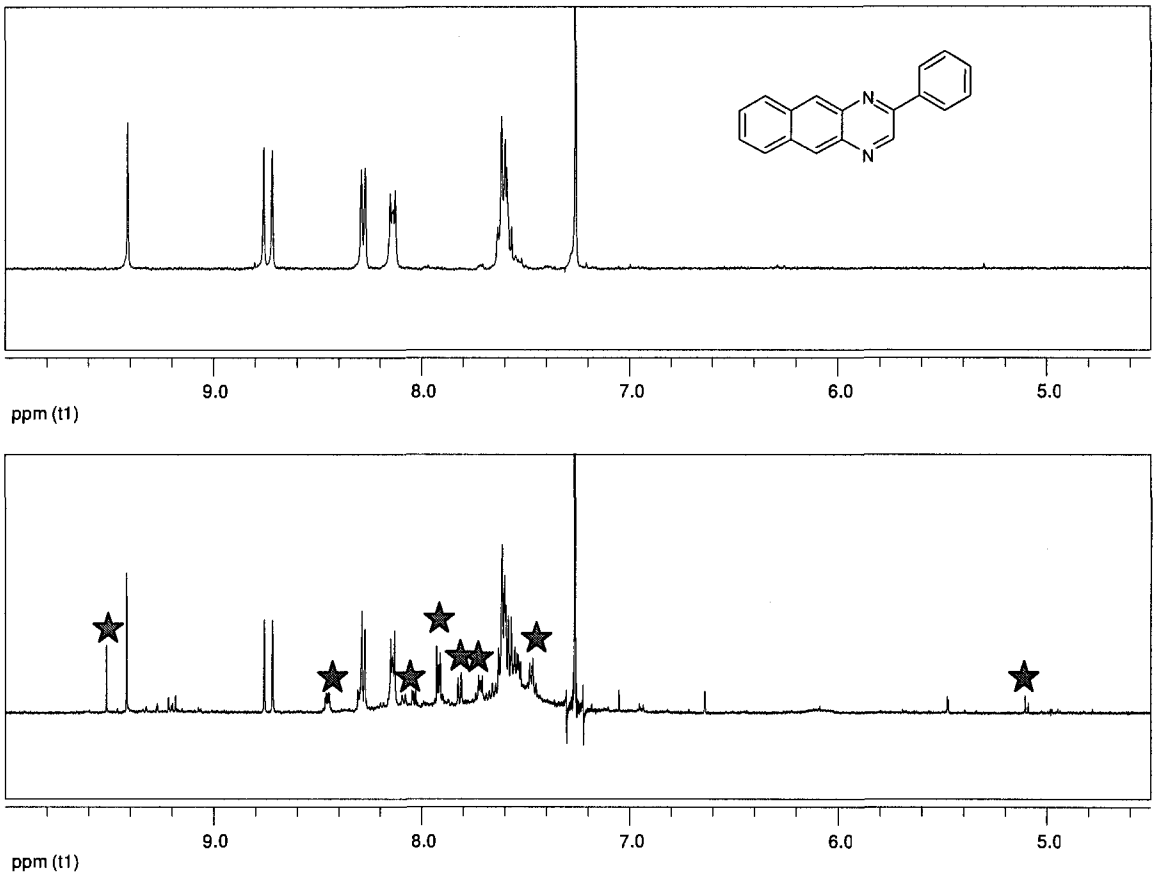

Figure 2.11: ^{1}H-NMR spectra of **PBQ** recorded in $CDCl_3$ before (top) and after 150 min of irradiation (bottom) (stars emphasise new peaks).

As a result of the unsymmetrical substitution pattern, the two protons on the central ring of **PBQ** are not equivalent. This difference in electronic environment was confirmed by ^{1}H-NMR analysis of **PBQ**, as two singlets were observed at 8.69 and 8.65 ppm. The formation of the bridgehead across the central rings of two molecules of **PBQ** would lead to two different kinds of sp^3 protons in the dimer. Thus, two doublets or two singlets would be expected between 6 and 5 ppm in ^{1}H-NMR spectrum of ***hh*-PBQ** and ***ht*-PBQ**, respectively. As observed in the ^{1}H-NMR spectrum of **PBQ**, the two protons are still in different environments with respect to each other but the lack of splitting suggest that the

photoadduct formed under these conditions is either ***ht*-di-PBQ** or ***hh*-di-PBQ** with X = Ph and Y = H (Scheme 2.8).

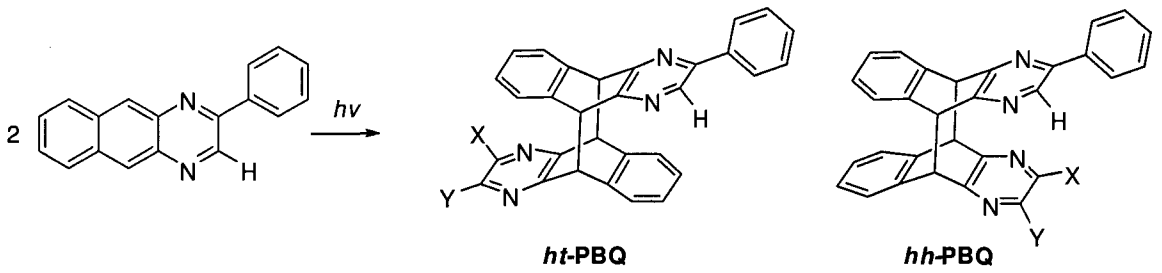

Scheme 2.8: Possible isomers resulting from dimerisation of **PBQ**.(X=Ph,Y=H or X=H,Y=Ph).

2.2.2.2 Influence of 4-methoxyphenyl groups

2.2.2.2.1 Synthesis

In order to use the photochromism of benzo[2,3-g]quinoxaline derivatives in practical applications such as optical data storage, such system should be incorporated in polymer matrices such as polystyrene and their reactivity in solid state should be investigated. In order to graft benzo[2,3-*g*]quinoxaline derivatives on polystyrene polymers 2,3-di(4-methoxyphenyl)benzo[2,3-*g*]quinoxaline (**DMoPBQ**) and 2-(4-methoxyphenyl)benzo[2,3-*g*]quinoxaline (**MoPBQ**) were synthesised as shown in Scheme 2.9 and Scheme 2.10, respectively. These methoxy groups have the advantage that they could act as synthetic "handles" for incorporating benzo[2,3-*g*]quinoxalines into polymers as well as allowing us to study the effect of functional groups, if any, on the photochemistry.

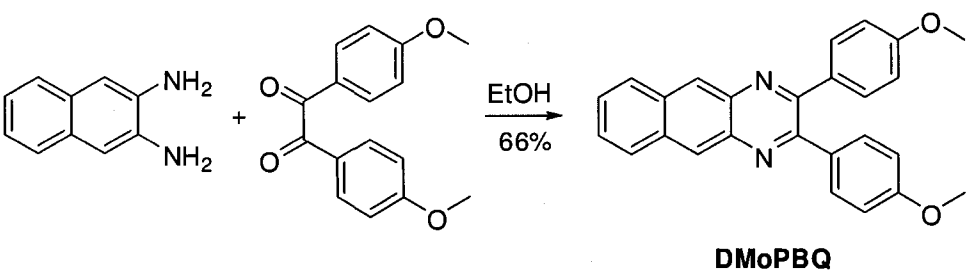

DMoPBQ

Scheme 2.9: Synthesis of **DMoPBQ.**

Like 2-phenylglyoxal, 2-(4-methoxyphenyl)glyoxal was synthesised by oxidation of 1-(4-methoxyphenyl)ethanone in a 48 % HBr solution. The resulting 2-(4-methoxyphenyl)glyoxal was then condensed with 2,3-diaminonaphthalene to form **MoPBQ** in 76 % yield.

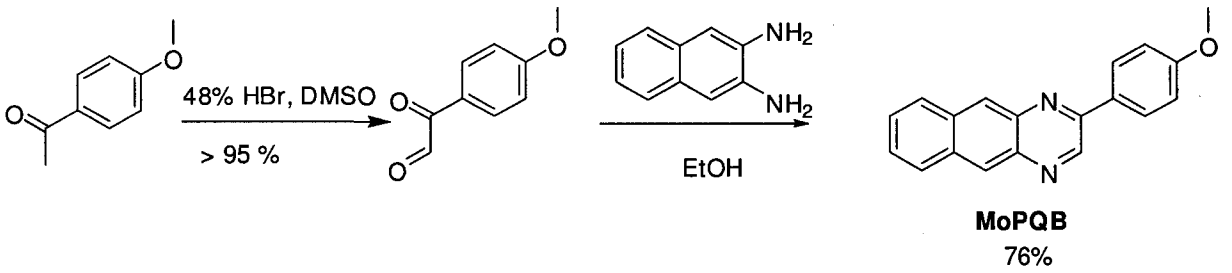

MoPQB
76%

Scheme 2.10: Synthesis of **MoPBQ**

As observed for **DPBQ**, **PBQ** and **BQ**, the extension of the π-conjugated system resulted in a shift of absorption towards longer wavelengths. The addition of methoxy groups on the phenyl substituent resulted in a shift of absorption from 381 to 396 nm for the disubstituted compound and from 379 to 384 nm for the monosubstituted derivatives (Figure 2.12 and Figure 2.9). This red-shift in the UV-Vis absorption is consistent with the addition of electron donating group on

benzene ring which results in a destabilisation of the HOMO and inducing a smaller HOMO-LUMO gap.[63-65]

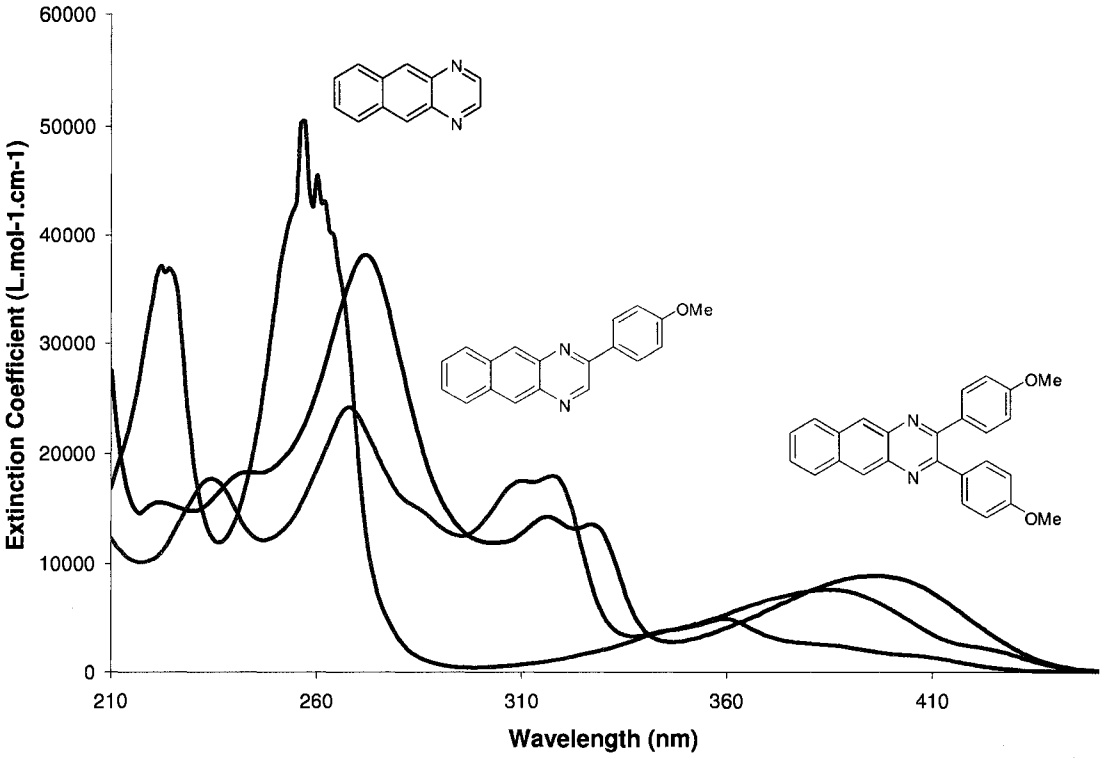

Figure 2.12: Comparison of UV-Vis spectra of **BQ, MoPBQ** and **DMoPBQ** recorded at room temperature in CH_3CN

2.2.2.2.2 Photochemical Studies:

Similarly to **PBQ** and **BQ**, after irradiation of a 1.33 mM non-deoxygenated solution of **DMoPBQ** in CH_3CN in the Rayonet® photoreactor for 150 min, no precipitate was observed. However, unlike the derivatives presented earlier in this chapter, MALDI- TOF MS did not show a peak related to **di-DMoPBQ**, which suggested that irradiation of **DMoPBQ** did not lead to any dimer. ^{1}H-NMR characterisation of the concentrated reaction mixture showed peaks corresponding to the starting material as well as a new set of peaks in the

aromatic region similar to the **di-DPBQ** and a new peak at 5.45 ppm (Figure 2.13). The presence of this new peak in the diagnostic region for bridgehead protons suggested that **DMoPBQ** was undergoing a photochemical reaction involving a change of hybrisation at the central ring. Assuming the photoproduct is the dimer, integration of the peak at 5.45 ppm versus the singlet at 8.27 ppm suggested a 10 % yield. However, the formation of a dimer could not be confirmed by MALDI-TOF MS. Moreover, attempts to separate the photoproduct from **DMoPBQ** via flash column chromatography were not successful; thus, further characterisation of the photoproduct using X-ray crystallography could not be achieved. It is therefore not possible at this time to confirm that **DMoPBQ** undergoes dimerisation when irradiated under the same condition as **DPBQ**, **PBQ**, **BQ** and **A**. However, efforts towards characterisation of the photoproduct should be pursued.

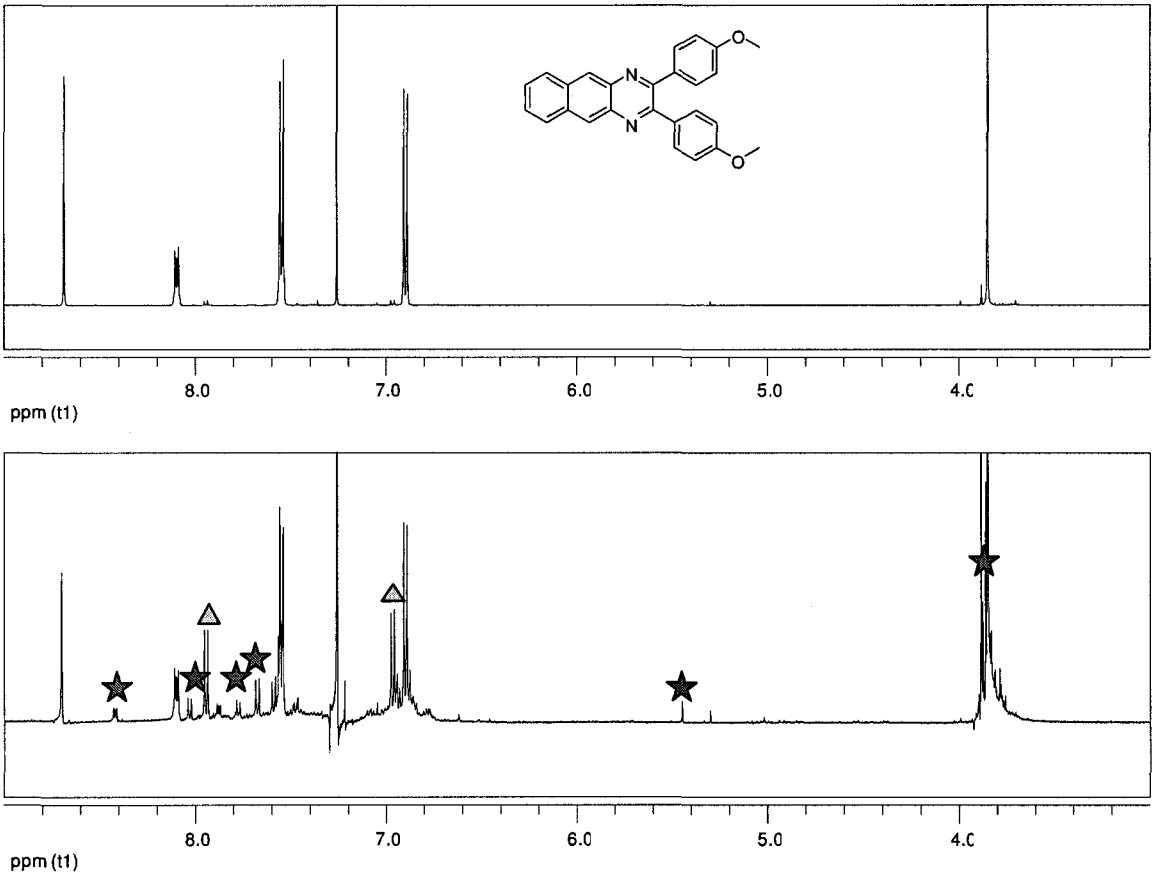

Figure 2.13: ^{1}H-NMR of **DMoPBQ** recorded in $CDCl_3$; (top), after 150min of irradiation (bottom). New peaks associated with the photoproduct are emphasised with stars, while the unidentified impurities present in traces prior to irradiation are emphasised by triangles.

Similarly to **DMoPBQ**, no precipitate was observed after irradiation of a 1.36 mM non-deoxygenated solution of **MoPBQ**. MALDI-TOF MS of the solution only showed the (**MoPBQ**)$^+$ and no (**di-MoPBQ**)$^+$ ion peak, which was consistent with the results obtained with the disubstituted analogue. ^{1}H-NMR characterisation of the concentrated reaction mixture showed peaks corresponding to the starting material as well as a new set of peaks in the aromatic region similar to that of **di-PBQ**. Two small singlets at 5.44 and 5.42 ppm within the diagnostic region for the bridge-head of photoproduct formed

suggest that **MoPBQ** undergoes a photoreaction that involves a change of hybridisation at the central ring of the benzo[2,3-*g*]quinoxaline moiety. For the unsymmetrical **MoPBQ**, similarly to **PBQ**, another new singlet at 9.4 ppm associated with the proton on the 3 position of the benzo[2,3-*g*]quinoxaline core of the photoproduct is observed (Figure 2.14). This new singlet at 9.4 ppm can therefore be used as the diagnostic peak to determine that the product was formed in 37 % yield, assuming that it was the dimer. However, integration of the singlets in the diagnostic region for bridgehead protons suggests that the photoproduct was only formed in 8 % yield. The lack of consistency between the singlet a 9.4 ppm and the singlets at 5.44 and 5.42 ppm implies that there were more than one photoproduct formed when **MoPBQ** was irradiated. Unfortunately, attempts to separate with photoproduct from **MoPBQ** by recrystallisation were not successful. Thus, the photoadduct could not be identified by X-ray crystallography. Other purification methods should be investigated in order to obtain the pure photoproduct and confirm that irradiation of a **MoPBQ** solution in CH_3CN results in **di-MoPBQ**. However, neither MALDI-TOF nor ^{1}H-NMR spectroscopy are sufficient to confirm that dimerisation is occurring in a similar fashion to **DPBQ**.

Unlike **DPBQ**, **DMoPBQ** only has limited absorption around 350 nm. Hence, the lack of reactivity of **DMoPBQ** could be rationalised by the use of the inappropriate energy to excite the molecule. Therefore, the effect of irradiation with a light source centred at longer wavelength should be investigated. As demonstrated with **DPBQ**, the use of a filter was necessary to prevent the

photodissociation of **di-DPBQ** in solution during the irradiation experiments. The addition of methoxy groups results in red-shift in absorption in the monomeric unit from **DMoPBQ** to **DPBQ** and from **MoPBQ** to **PBQ**, such shift should also be reflected in their respective dimers. Therefore, it is possible that both **DMoPBQ** and **MoPBQ** form dimers that absorb light around 350 nm, leading to their photodissociation in solution. Considering that **DMoPBQ** and **MoPBQ** did not behave as ideally as **DPBQ**, and due time to constraints, their photochemistry was not studied as thoroughly as the latter. Nonetheless, further studies should be carried out to understand the influence of methoxyphenyl groups on the photochemistry of benzo[2,3-*g*]quinoxaline.

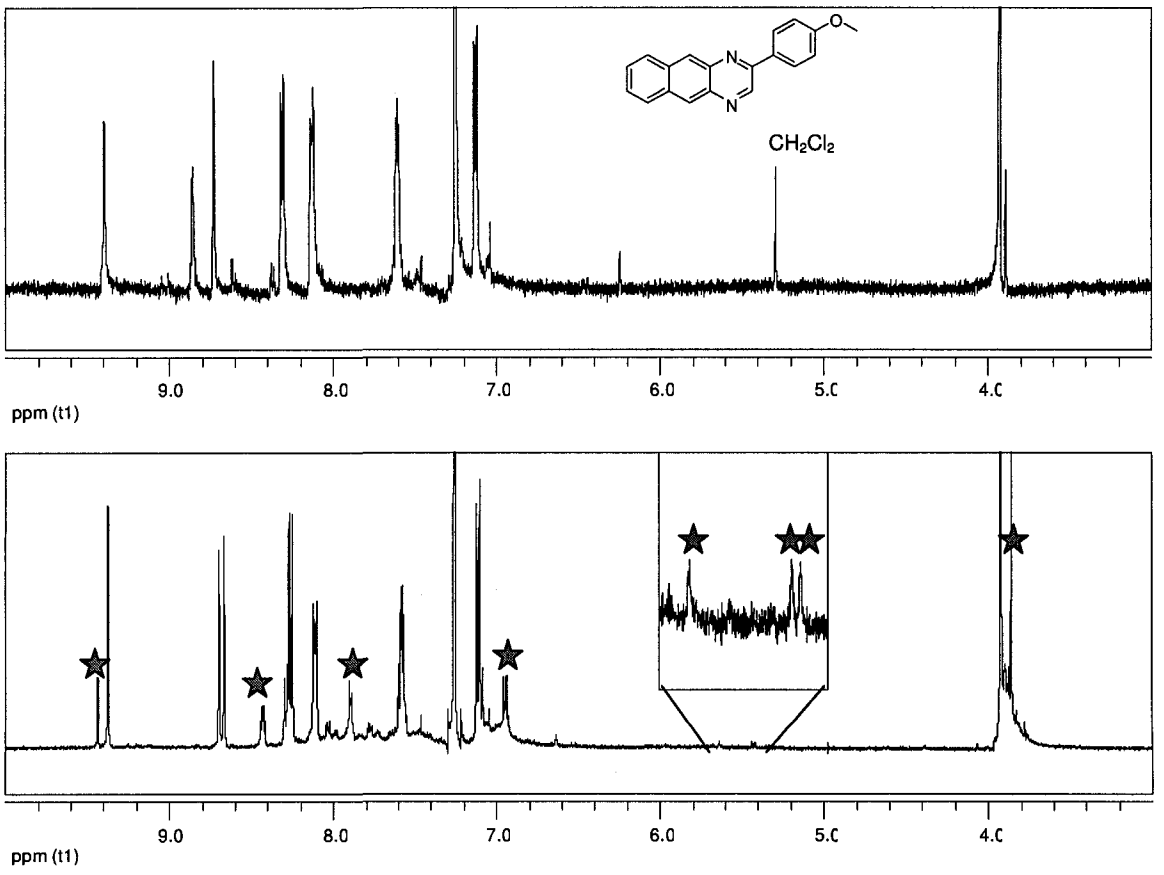

Figure 2.14: ^{1}H-NMR spectrum of **MoPBQ** recorded in $CDCl_3$ before (top) and after 150 min of irradiation (bottom). New peaks are emphasised with stars.

2.2.3 2,3-Di(pyridin-2-yl)benzo[2,3-*g*]quinoxaline

2,3-Di(pyrid-2-yl)benzo[2,3-*g*]quinoxaline was synthesised in order to investigate the influence of heteroatoms on the photochemical properties of a benzo[2,3-*g*]quinoxaline. As shown in Scheme 2.11, 1,2-dipyridylethanedione was synthesised by oxidation of the product of the benzoin condensation of picolinaldehyde. The dione was then condensed with 2,3-diaminonaphthalene to yield 2,3-di(pyrid-2-yl)benzo[2,3-*g*]quinoxaline (**DPyBQ**) in 73 % yield.

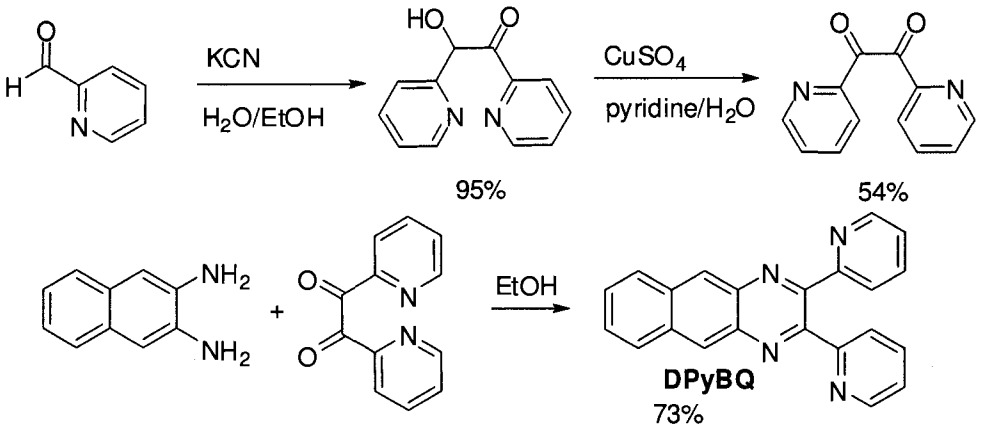

Scheme 2.11: Synthesis of **DPyBQ**

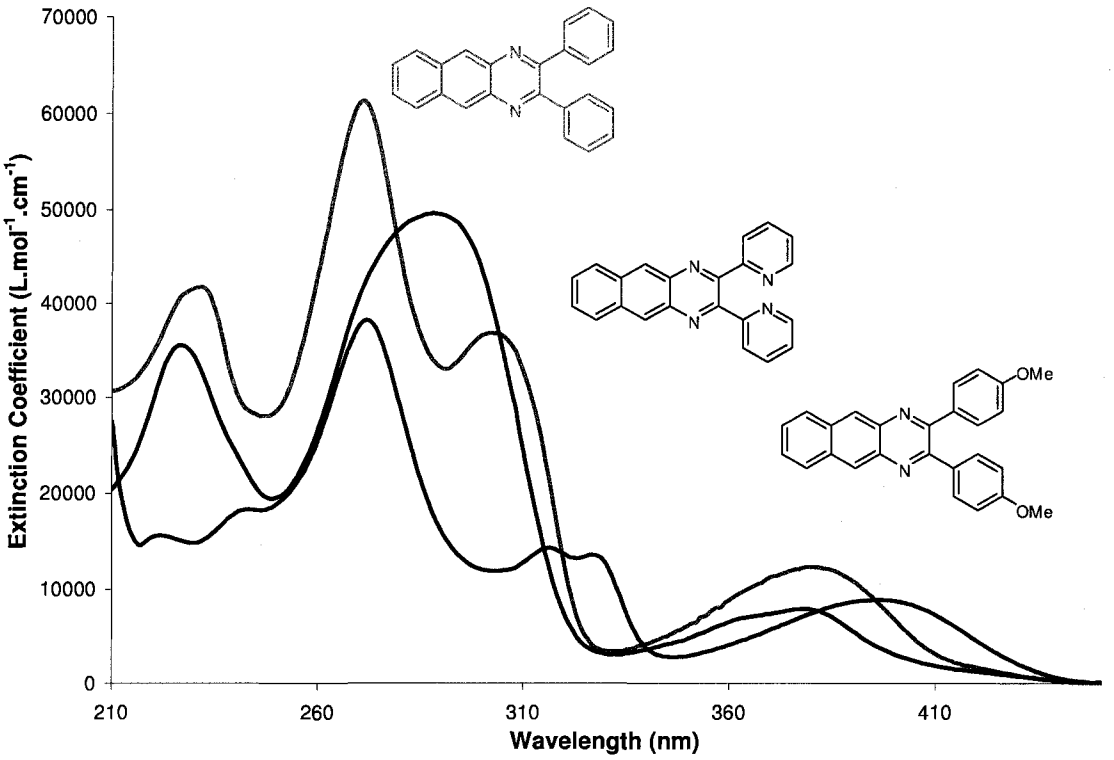

Figure 2.15: UV-Vis absorption spectra **of DPBQ, DPyBQ** and **DMoBQ** solutions in CH_3CN recorded at room-temperature.

In order to investigate whether **DPyBQ** would undergo [4+4] photocycloaddition in a similar manner to anthracene and **DPBQ**, a solution of

1.33 mM of **DPyBQ** in CH_3CN was irradiated in the Rayonet® photoreactor for 2.5 h. Similarly to **DPBQ**, MALDI TOF MS of the solution showed the m/z 668 (R.I= 461) corresponding to the M(**di-DPyBQ**)$^+$, and a more intense peak a m/z = 336 (R.I= 665) corresponding to M(**DPyBQ**+2)[d]. ^{1}H-NMR analysis of the evaporated reaction mixture showed a new set of peaks in the aromatic region and accompanied by a singlet at 5.15 ppm associated with the formation of the bridgehead protons across the central ring of two benzo[2,3-g]quinoxaline moieties (Figure 2.16). The ^{1}H-NMR analysis combined with the MALDI-TOF mass spectrum confirmed that irradiation of solution of **DPyBQ** in CH_3CN was undergoing [4+4] photocycloaddition in a similar manner to that of anthracene. The photoadduct formed could be separated from **DPyBQ** on slow evaporation of CH_3CN.

[d] The uncertainty may result from a calibration error

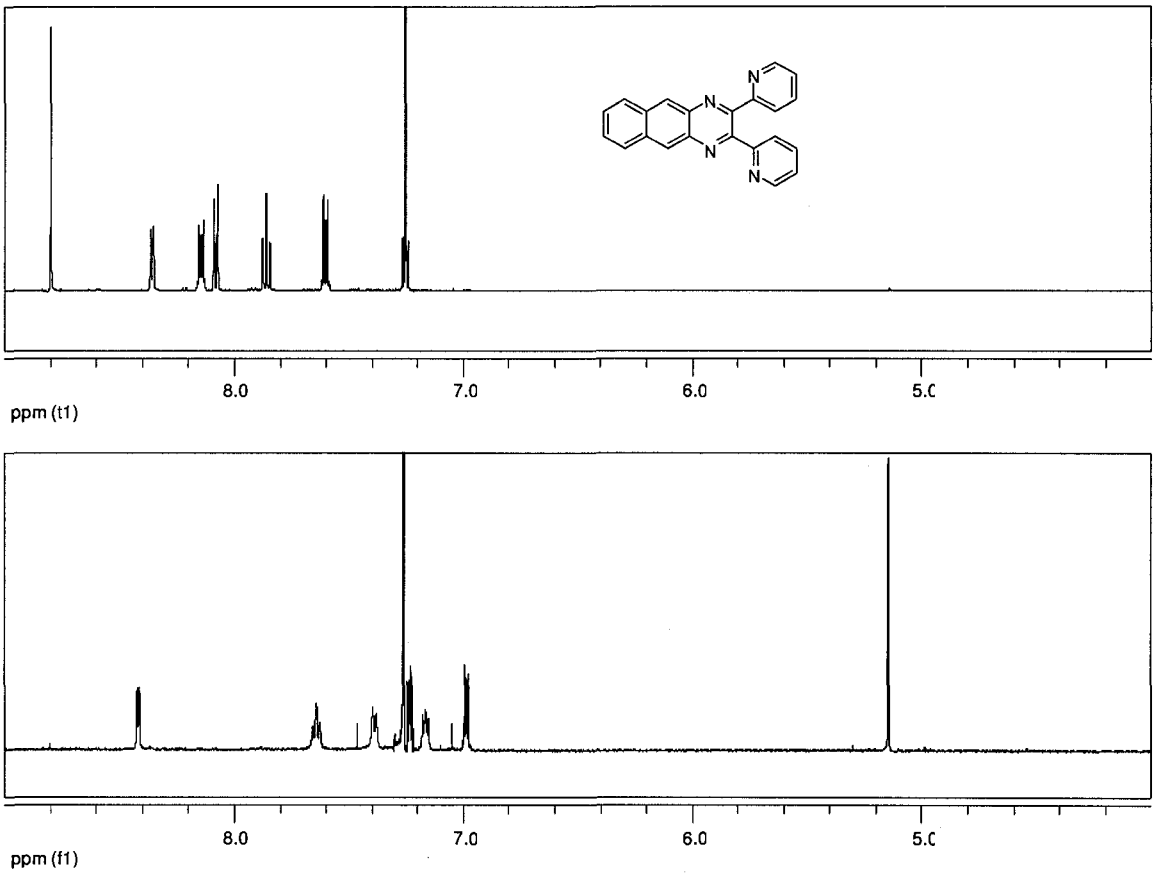

Figure 2.16: ^{1}H-NMR spectrum of **DPyBQ** recorded in $CDCl_3$ before (top) and white solid isolated after 150 min of irradiation (bottom).

2.3 Conclusion

We demonstrated that benzo[2,3-*g*]quinoxaline derivatives with phenyl and pyridyl substituent on the 2- and 3- positions, which are more synthetically accessible than their anthracene equivalents, can undergo dimerisation when irradiated in the Rayonet® photochemical reactor. X-ray diffraction studies enabled us to determine that irradiation of a solution of **DPBQ** results in the [4+4] photocycloaddition across the central ring of two benzo[2,3-*g*]quinoxaline derivatives to yield the ht-dimer. MALDI-TOF MS suggested that **PBQ** and **BQ** also formed dimers upon irradiation however, their structures could not be fully

characterised as a result of the limited solubility of the starting materials, which complicated their separation from their photoproducts. MALDI-TOF MS of **MoPBQ** and **DMoPBQ**, on the other hand, did not show the presence of any dimer but ^{1}H-NMR spectroscopy showed that both produced a photoproduct upon irradiation that could not be isolated or fully characterised. The absence of dimer after irradiation could be due the failure to excite the chromophore as both **MoPBQ** and **DMoPBQ** absorb at longer wavelengths than the other benzo[2,3-*g*]quinoxaline derivatives studied. The red-shift in absorption could also be observed in the dimer. This would lead to photodissociation during the irradiation experiments. When irradiated under the same conditions (without prior deoxygenation), anthracene forms dianthracene in similar yields, but 44 % of endoperoxide is also formed. Moreover, their facile synthesis enables the electronic properties of 2,3-benzo[2,3-*g*]quinoxaline to be tuned by variation of the substituents. Other derivatives should be synthesised and their photochemical properties should also be investigated. Such systematic studies will deepen the understanding of the influence of substitution on the photochemistry of benzo[2,3-g]quinoxalines and enable the rational design of a new sub-class of photochromic system based on this type of [4+4] cycloaddition reaction.

CHAPTER 3: TOWARDS STIMULI-RESPONSIVE PHOTOCHROMISM

3.1 Introduction:

The presence of the pyridine substituents on the benzo[2,3-g]quinoxaline, enables **DPyBQ** to coordinate to metals to form transition metal complexes.[44,66-69] The potential ability to modify the efficiency of the photodimerisation of **DPyBQ** by the addition a transition metal species could lead to the development of a new class of hybrid photochromic systems. Even though some of the binding properties of **DPyBQ** has been previously reported, the influence of chemical species on its photochemical properties has not been investigated.[70,71] In order to develop a photochromic system whose reactivity could be tuned by the presence of other chemical species, we investigated the influence of a variety of cations on the photophysical properties and efficiency of the dimerisation of **DPyBQ**.

3.2 Result and Discussion:

An excited molecule can relax to its ground state through different paths (*e.g.* fluorescence) or undergo chemical reactions (*e.g.* dimerisation). Prior to investigating the influence of cations on the photodimerisation of **DPyBQ**, we observed their influence on the luminescence of a stock solution of **DPyBQ** in CH_3CN. After qualitative investigation of the effect of different cations on the luminescence of a solution of **DPyBQ** in CH_3CN, it was concluded that Zn^{2+}

affected the optical properties of **DPyBQ** most dramatically as the luminescence was visibly increased (Figure 1.1).

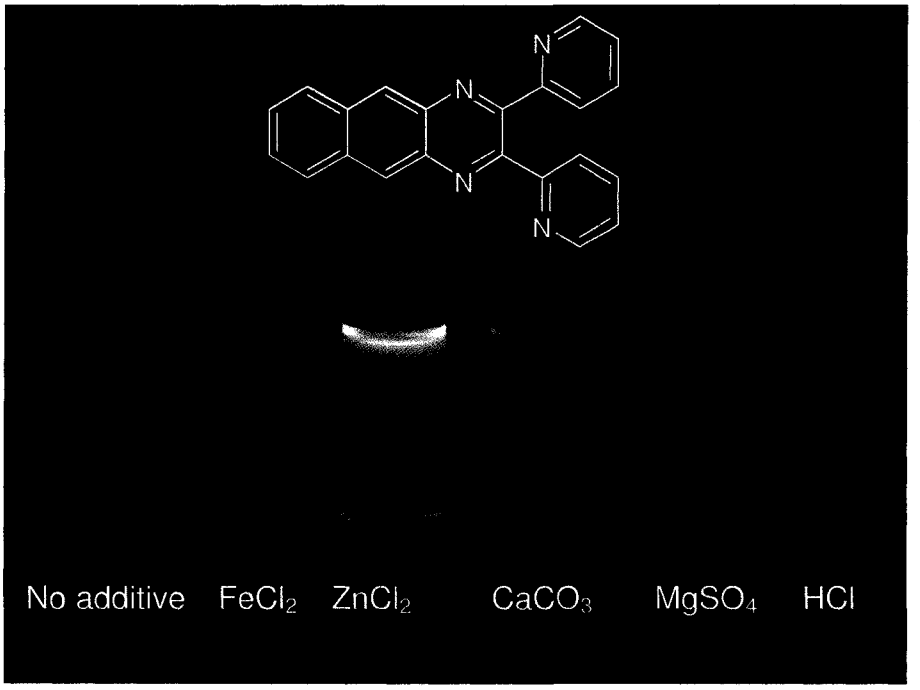

Figure 3.1: Influence of chemicals on the luminescence of a solution of **DPyBQ** in CH_3CN (3.02×10^{-4} M). Samples viewed under UV light.

3.2.1 Influence on optical properties

In order to better understand the interaction between **DPyBQ** and Zn^{2+}, the variation in luminescence with increasing amount of Zn^{2+} was investigated. A series of solutions was prepared by mixing aliquots of equimolar solutions of **DPyBQ** and $ZnCl_2$ in CH_3CN to maintain a total molarity $[Zn^{2+}]+[\mathbf{DPyBQ}]$ constant while varying $[Zn^{2+}]/[\mathbf{DPyBQ}]$.[72] This was achieved by mixing a volume *x* of a 0.1 mM solution of **DPyBQ** in CH_3CN with a volume (1-*x*) of a 0.1 mM solution of $ZnCl_2$ in CH_3CN. The UV-Vis absorption spectra of this series were recorded. As shown in Figure 3.2, increasing the ratio of Zn^{2+} resulted in a

decrease of absorption intensity, which is expected due to the dilution of **DPyBQ**. This reduction in absorption is also accompanied by a shift towards longer wavelengths that is consistent with enhanced conjugation of **DPyBQ** as a complex is formed with Zn^{2+}. Figure 3.3 shows the variation at the maximum absorption wavelength λ = 380 nm with molar ratio. This continuous addition method, also known as Job's method, enables us to determine that the complex formed in solution was the major absorbing specie when the concentration of Zn^{2+} represent 50 % of the total molarity of Zn^{2+} + **DPyBQ**.[72]

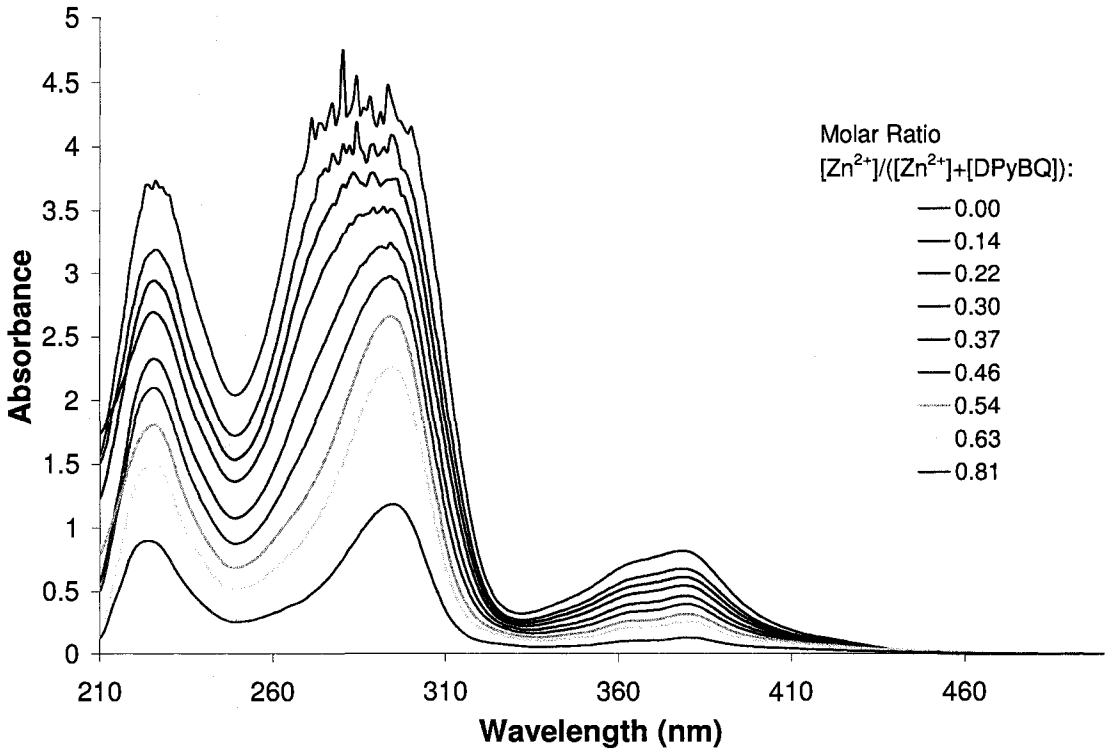

Figure 3.2: Absorption spectra of a solution of 0.1 mM = [**DPyBQ**] + [$ZnCl_2$] with varying [Zn^{2+}]/[**DPyBQ**] in CH_3CN measured at room temperature.

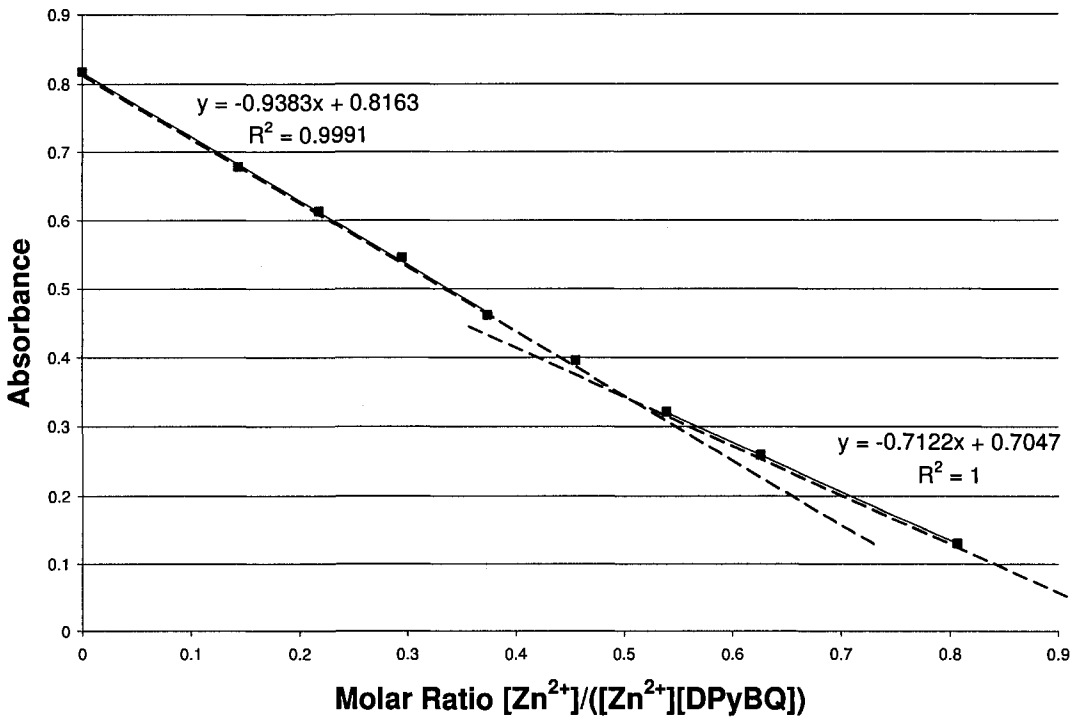

Figure 3.3: Job's plot obtained from the change of absorption intensity at 380 nm of a solution of **DPyBQ** and $ZnCl_2$ measured at room temperature.

In order to study the influence of $ZnCl_2$ on the luminescence of a 0.1 mM solution of **DPyBQ**, a series of solutions containing $ZnCl_2$ and **DPyBQ** were prepared such that $[Zn^{2+}]$/[**DPyBQ**] varies but $[Zn^{2+}]$+[**DPyBQ**] stays constant and their luminescence was measured.[72] Similarly to the UV-Vis absorption, the fluorescence intensity decreased with increasing molar ratio of Zn^{2+} (Figure 3.4). As shown in Figure 3.5, the change in luminescence enabled us to determine that under these conditions, the major complex is formed when $ZnCl_2$ and **DPyBQ** are present in equal ratio in solution, which is consistent with the absorption data.

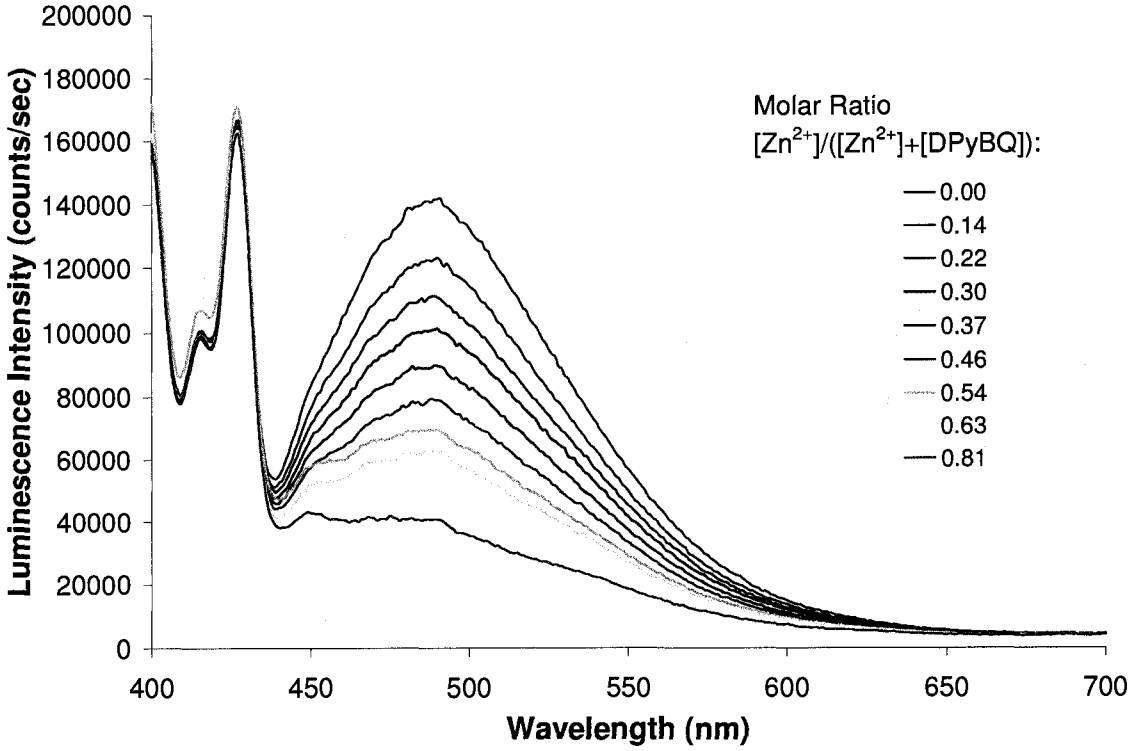

Figure 3.4: Emission spectra of a series of solutions made of 0.1 μM solution of **DPyBQ** and $ZnCl_2$ in CH_3CN excited at 380 nm with varying molar ratio of $ZnCl_2$ such that [**DPyBQ**] + $[Zn^{2+}]$ = 0.1 μM but $[Zn^{2+}]$/[**DPyBQ**] varies measured at room-temperature.

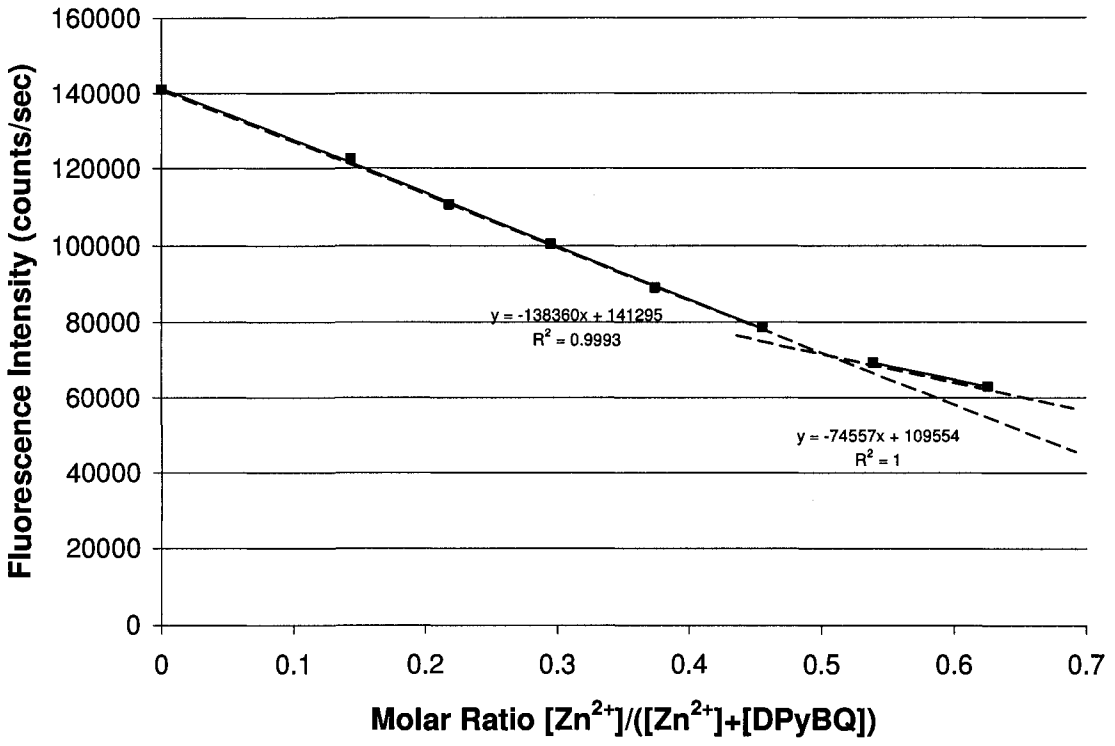

Figure 3.5: Job's plot obtained from change of luminescence intensity at 486 nm of a 0.1 μM of **DPyBQ** in CH_3CN with addition of $ZnCl_2$ measured at room temperature.

In order to confirm the data obtained above, the addition of a small volume of a 0.2 mM solution of $ZnCl_2$ in CH_3CN to a constant volume (3.00 mL) of a 0.1 mM solution of **DPyBQ** in CH_3CN was monitored by UV-Vis spectroscopy. As shown in Figure 3.6, addition of $ZnCl_2$ resulted in an increase in absorption at 295 nm. However, after addition of 225 μL of $ZnCl_2$ solution, further addition of $ZnCl_2$ solution resulted in a reduction of absorption at 295 nm. Figure 3.7 shows that the maximum change of absorption was reached at an equimolar ratio of $ZnCl_2$ to **DPyBQ**. Thus, we concluded that the complex formed between Zn and **DPyBQ** was $ZnCl_2$(DPyBQ). Attempts to further characterise the structure of the complex were not successful. Indeed, the isolated precipitate formed if a large

amount of Zn^{2+} is added to a solution of **DPyBQ** did not crystallise. Hence, the structure could not be confirmed by X-ray crystallography. Figure 3.7 also shows that a change in absorption of less than 5 % was observed with a molar ratio of 10 part **DPyBQ** to 1 part $ZnCl_2$. Thus, this system would not likely be useful in sensor applications.

The change in luminescence of a constant volume of **DPyBQ** solution in CH_3CN (1×10^{-6} M) with addition of a small volume of $ZnCl_2$ solution (1×10^{-5} M) in CH_3CN can be seen in Figure 3.8. In agreement with the UV-Vis absorption, the luminescence increases upon the addition of $ZnCl_2$ to a solution of **DPyBQ**, presumably due to an increase of rigidity in the $ZnCl_2$(DPyBQ) complex (Figure 3.8). After addition of 1 equivalent of $ZnCl_2$ for 1 **DPyBQ**, the fluorescence increased to such an extent that the upper limit of the detector was reached, thus the formula of the complex formed in these conditions could not be extrapolated using the Job's plot. The small change of fluorescence intensity observed at low molar ratio of Zn^{2+} was consistent with the UV-Vis data discussed above and confirmed that such a system would not be optimal for sensing applications.

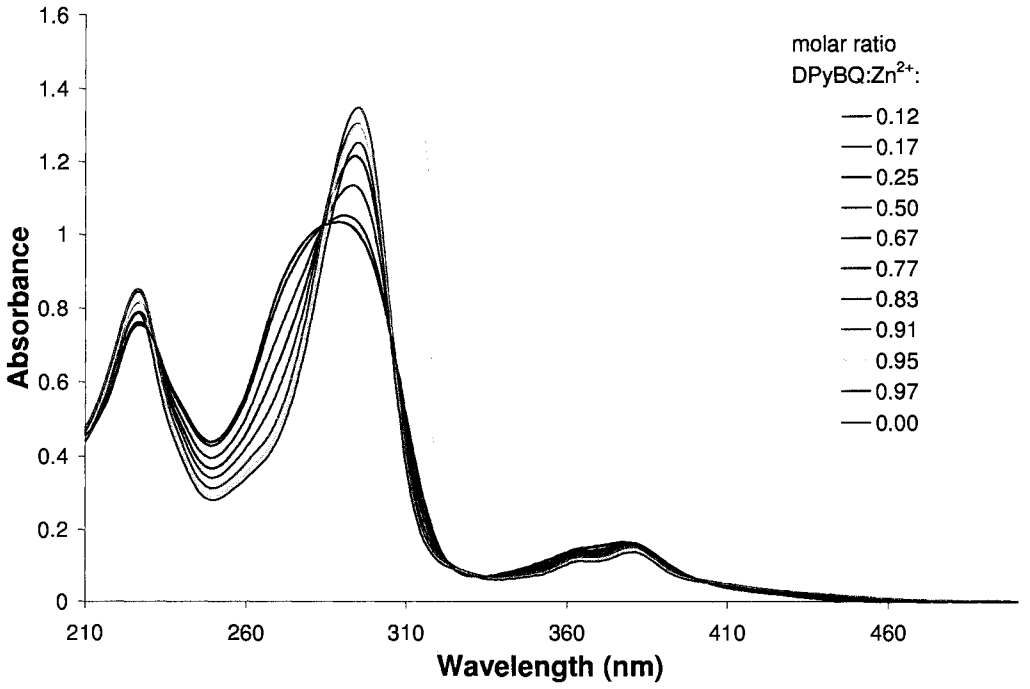

Figure 3.6: Influence of $ZnCl_2$ on the absorption of a 1.07 x 10^{-4} M solution of **DPyBQ** in CH_3CN measured at room-temperature.

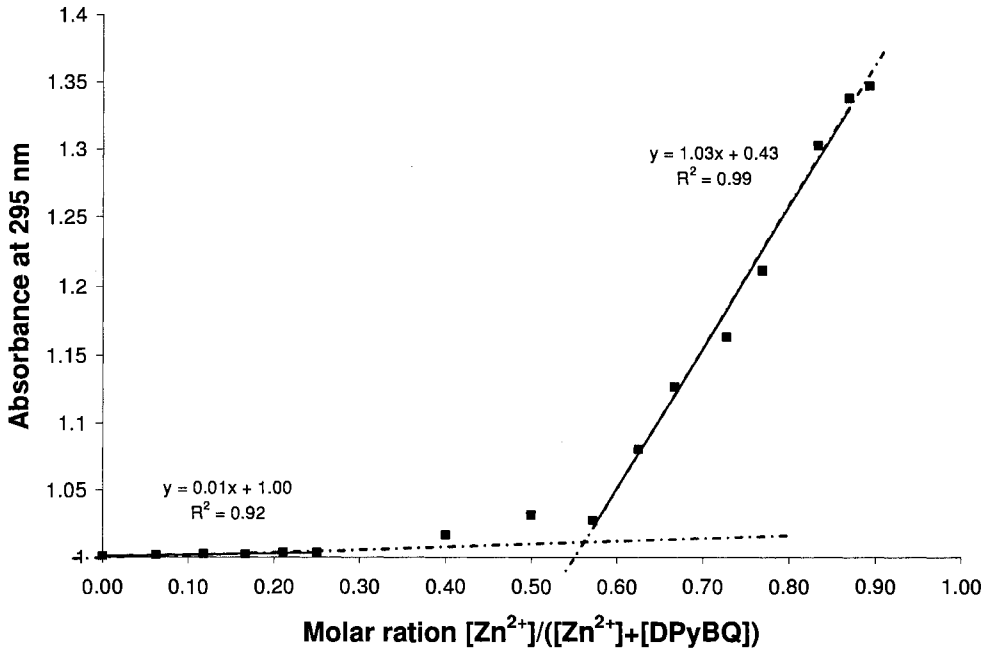

Figure 3.7: Job's plot of change of absorbance at 295 nm with molar fraction of Zn^{2+} added to a constant volume of **DPyBQ** solution (1 x 10^{-4} M).

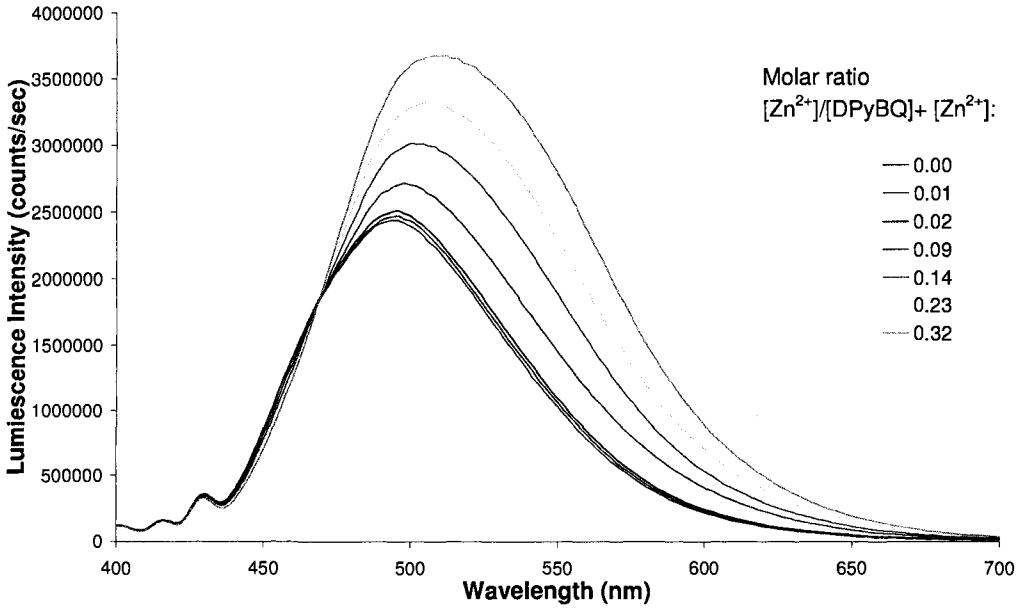

Figure 3.8: Fluorescence titration of a constant volume of **DPyBQ** solution ($1x10^{-6}$ M) in CH_3CN with addition of a small volume of $ZnCl_2$ solution (1×10^{-5} M) measured at room-temperature.

In order to study the influence of the counter-ion on the fluorescence of a solution **DPyBQ**, a series of solutions were prepared by mixing equimolar solutions of $Zn(OAc)_2$ and **DPyBQ** in CH_3CN such that $[Zn(OAc)_2]/[\mathbf{DPyBQ}]$ varies but $[Zn(OAc)_2]+[\mathbf{DPyBQ}] = 0.1$ mM. As shown in Figure 3.9, a decrease in absorbance is observed with increasing ratio of $Zn(OAc)_2$ which is consistent with the dilution of **DPyBQ**. As was the case for $ZnCl_2$, a shift to longer wavelengths in the UV-Vis spectrum with increasing concentration of $Zn(OAc)_2$ was observed, perhaps as a result of the increased conjugation of **DPyBQ** induced by the formation of a complex. Figure 3.10 shows that the absorption at 379 nm decreases with increasing molar ratio of $Zn(OAc)_2$ and enables us to determine that the major complex formed under those experimental conditions is present when $Zn(OAc)_2$ and **DPyBQ** in equimolar amount in solution. Attempts to isolate

the complex formed in solution were not successful. Indeed, attempts to crystallize the formed complexes by slow diffusion in order to further understand the coordination of **DPyBQ** to Zn^{2+} were not successful. Hence, the structure of the complex cannot be confirmed to be Zn(**DPyBQ**)$(OAc)_2$. However, this experiment did not show that the counter-ion had a specific influence on the complex formed in solution.

In order to confirm the results obtained from the continuous addition method, a small volume of $Zn(OAc)_2$ solution in CH_3CN ($1x10^{-6}$ M) was added to a constant volume of **DPyBQ** in CH_3CN ($1x10^{-7}$ M). As shown in Figure 3.11, addition of $Zn(OAc)_2$ resulted in an increase in fluorescence, accompanied by a shift to longer wavelength, which is again consistent with the formation of a complex with increased planarity.

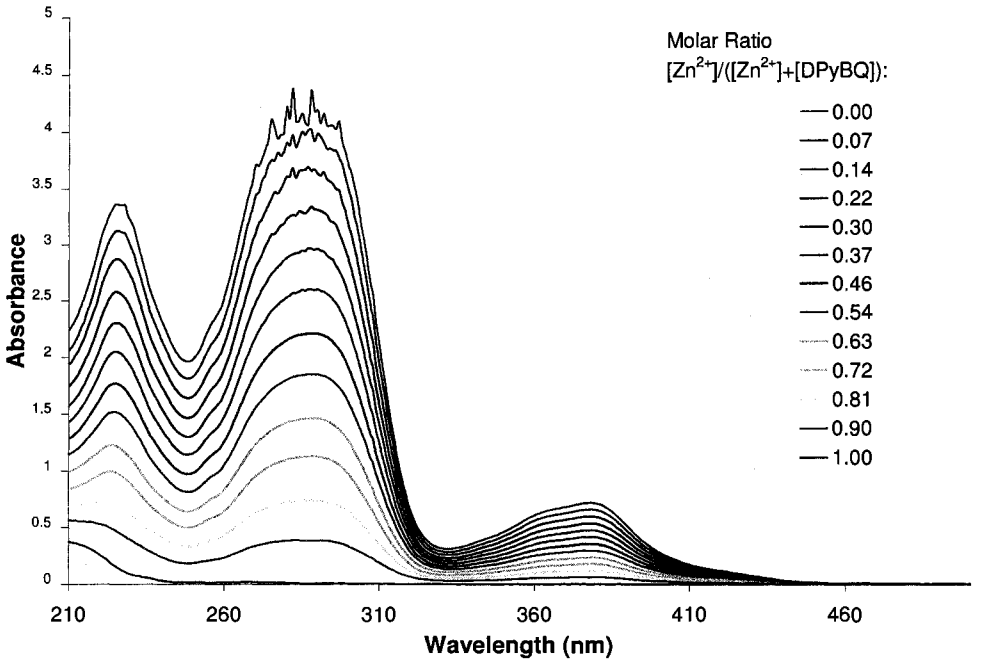

Figure 3.9: Absorption spectra of a solution of 0.1 mM = [**DPyBQ**] + $[Zn(OAc)_2]$ with varying $[Zn^{2+}]$/[**DPyBQ**] in CH_3CN measured at room temperature.

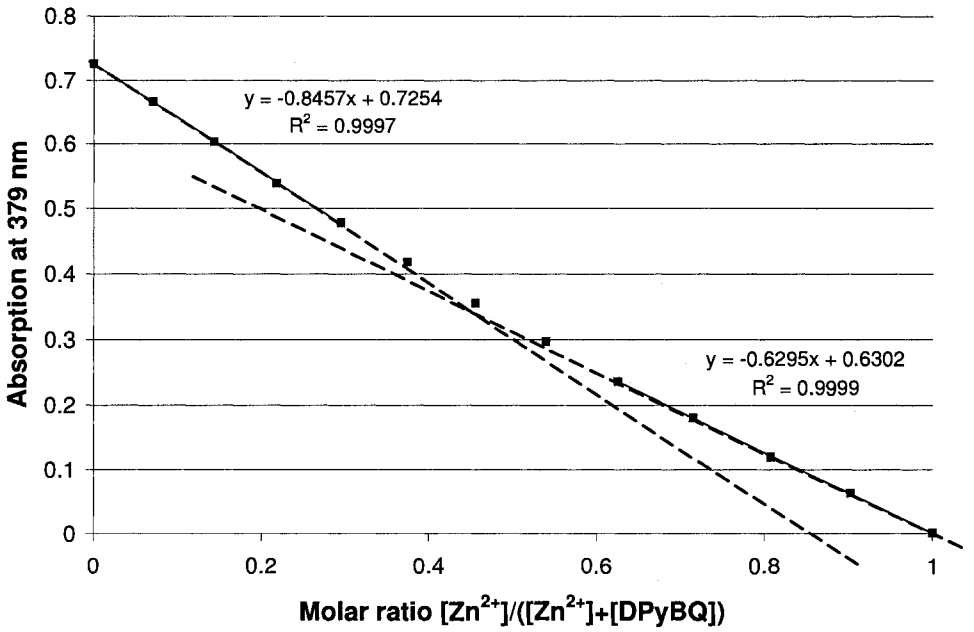

Figure 3.10: Job's plot obtained from the change of absorbance at 380 nm of a 0.1 mM solution of **DPyBQ** in CH_3CN measured at room-temperature.

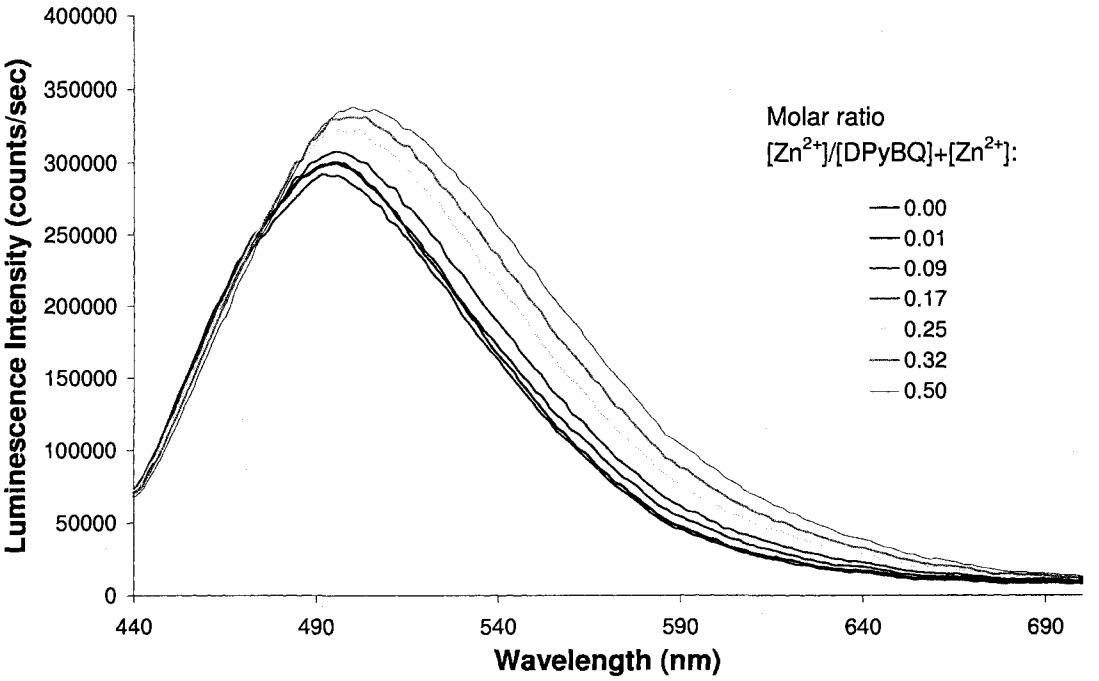

Figure 3.11: Change of luminescence of a constant volume of **DPyBQ** solution in CH_3CN with addition of a solution of $Zn(OAc)_2$ in CH_3CN, recorded at room-temperature.

3.2.2 Photochemical studies

The titration studies of a solution of **DPyBQ** in CH_3CN with zinc in the presence of different counter-ions discussed above showed that both $ZnCl_2$ and $Zn(OAc)_2$ resulted in an increase in the fluorescence. A series of solutions containing different molar ration of Zn^{2+} to **DPyBQ** was prepared by mixing 0.1 M solutions DPyBQ and Zn^{2+} in CH_3CN such that $[Zn^{2+}]/[$**DPyBQ**$]$ varies but ($[Zn^{2+}]+[$**DPyBQ**$]$) stays constant (0.1 mM) was irradiated in the Rayonet® photochemical reactor for 150 min. As shown in Figure 3.12and Figure 3.13, UV irradiation resulted in a decrease in absorption at 280 and 380 nm for both series. This decrease in absorption can be ascribed to the dimerisation of **DPyBQ** in solution.

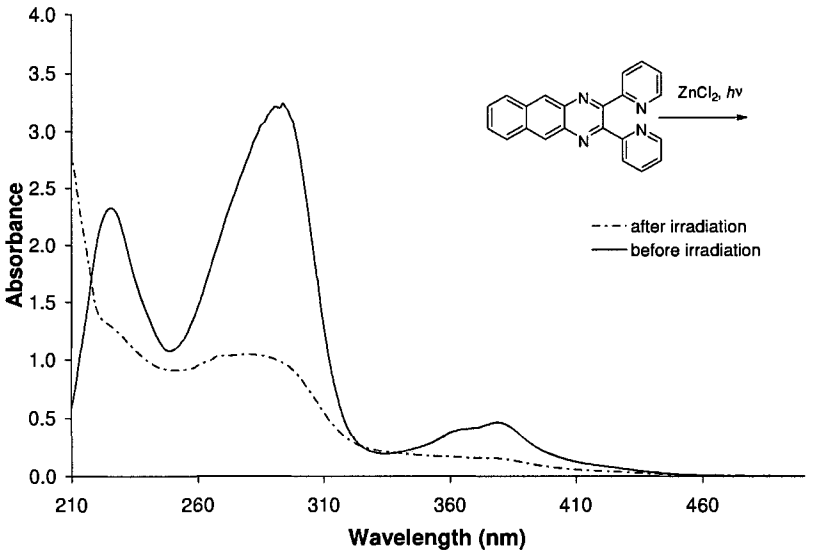

Figure 3.12: UV-Vis absorption spectra a solution of **DPyBQ** and $ZnCl_2$ in CH_3CN containing 0.37 molar ratio of $ZnCl_2$ before (full line) and after (dashed line) irradiation, measured at room-temperature.

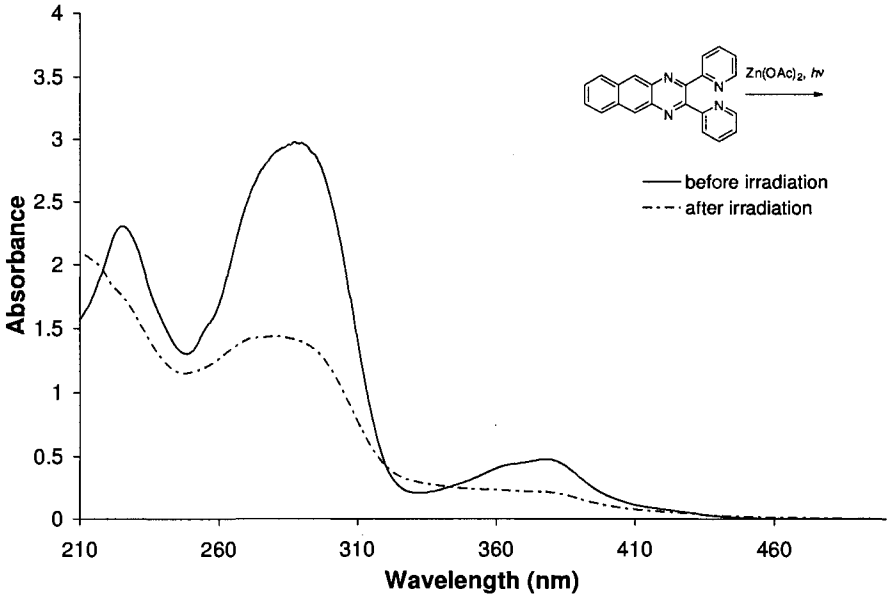

Figure 3.13: UV-Vis absorption spectra of a solution of **DPyBQ** and $Zn(OAc)_2$ in CH_3CN containing 0.30 molar ratio of $Zn(OAc)_2$ before (full line) and after (dashed line) irradiation (150 min), measured at room-temperature.

Assuming that no other species absorbs at 380 nm, the efficiency of dimerisation can be calculated by comparison of the absorbances of the

solutions of **DPyBQ** before and after irradiation. The percent conversion of **DPyBQ** for both $ZnCl_2$ and $Zn(OAc)_2$ series discussed earlier, were calculated by dividing of absorbance of the solution by the initial absorbance at 380 nm. As shown in Figure 3.14, irradiation of a solution of **DPyBQ** in CH_3CN at initial concentrations $[\mathbf{DPyBQ}]_i$ ranging from 0.05 mM to 0.1 mM yielded 55-70 % of dimer. However, when irradiated in the same conditions in presence of 10-50 mol% of Zn^{2+}, dimerisation efficiency was reduced to 40-55% for $Zn(OAc)_2$ and 50-55 % for $ZnCl_2$. No significant difference was observed between $Zn(OAc)_2$ and $ZnCl_2$ over the studied range of concentrations, suggesting that the counter ion does not appreciably influence the photochemistry of **DPyBQ** in presence of Zn^{2+}. Figure 3.14 also shows that the difference in conversion stays almost constant between each series. This suggests that the increasing molar ratio of Zn^{2+} does not influence the dimerisation efficiency of **DPyBQ**, nor does the change in concentration of **DPyBQ** alter the results appreciably over this concentration range. However, the luminescence studies discussed above revealed that the addition Zn^{2+} to a solution of **DPyBQ** resulted in an increase in luminescence (Figure 3.8). In the dimerisation process, one molecule of **DPyBQ** in its ground state acts as a quencher to another molecule of **DPyBQ** in its excited state. However, when Zn^{2+} acts as a competing quencher for the excited state, a concentration increase in Zn^{2+} would be expected to reduce the dimerisation efficiency as the efficiency of dimerisation is dependent on the efficiency of the other photochemical events occurring in solution (Chapter 1:). Irradiation studies in different conditions such as keeping a constant

concentration of one of the components or working with more concentrated solutions should be undertaken in order to better understand the influence of Zn^{2+} on the dimerisation of **DPyBQ**. It is also important to replicate these experiments to establish the experimental error.

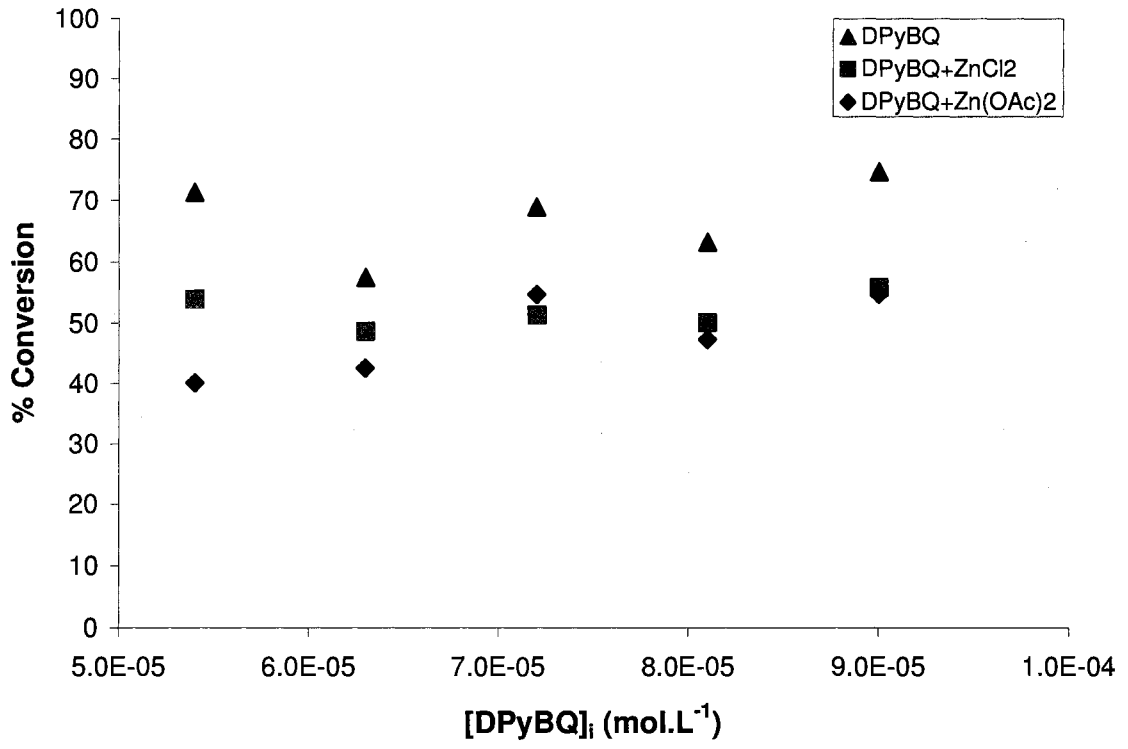

Figure 3.14: Percent conversion of **DPyBQ** after 150 min of irradiation in the Rayonet photoreactor without filter.

As shown in Figure 3.1, the addition of HCl resulted in the quenching of the fluorescence of a solution of **DPyBQ**. Thus, HCl was chosen in order to study the influence of acid on the dimerisation of **DPyBQ**. After 150 min of irradiation, a solution of **DPyBQ** in CH_3CN (0.81 mM) containing 10 mol% of HCl yielded 12 % of **di-DPyBQ**. Irradiation under the same conditions of a control solution of **DPyBQ** in CH_3CN (0.81 mM) yielded 20 % of **di-DPyBQ**. Thus, it was

concluded that the presence of a small amount of HCl during the irradiation of a **DPyBQ** solution did not result in a significant decrease in the amount of **di-DPyBQ** formed. Other chemical stimuli should be investigated in order to better understand the factors affecting the dimerisation of **DPyBQ**.

3.3 Conclusion:

In an attempt to develop a stimuli-responsive photochromic system based on the [4+4] photocycloaddition reaction, we investigated the influence of $ZnCl_2$ and $Zn(OAc)_2$ on the optical properties of **DPyBQ**, which was shown to undergo dimerisation upon irradiation. Addition of Zn^{2+} ion to a solution of **DPyBQ** results in a red shift in the UV-Vis absorption as well as an increase of absorbance at 290 nm, which is ascribed to the formation of a complex. Job's method enabled us to determine that a complexes of Zn:**DPyBQ** were formed when both species are in equal concentration in solution.

In order to assess the influence of Zn^{2+} on its photochemical properties, a solution of **DPyBQ** was irradiated in the presence of different molar ratios of Zn^{2+}. These preliminary studies revealed that the dimerisation of **DPyBQ** was slightly reduced by the presence of $ZnCl_2$ and $Zn(OAc)_2$ when present in 10-50 mol% in solution, however the nature of the counter ion did not appear to affect the yield of dimerisation. The results discussed earlier demonstrate that addition of Zn^{2+} did not result in complete suppression of the dimerisation of **DPyBQ**.

In order to gain a better understanding of the quenching mechanism of Zn^{2+} taking place during the dimerisation of **DPyBQ**, the complex formed in solution

should be isolated and its photochemical and photophysical properties investigated. To that same purpose, the photochemical properties of solutions of **DPyBQ** containing 51-99% of Zn^{2+} should also be investigated. Working to the limit of solubility of complex should clarify whether the quenching in caused by the sole presence of the complex having competing photochemistry or if the reduced efficiency of dimerisation is only caused by the decreased amount of **DPyBQ** present in solution as the complex crashes out of solution.

CHAPTER 4: SELECTIVE FORMATION OF PHOTOADDUCT

4.1 Introduction:

Recently, the Williams' group reported a method for enforcing the selectivity of [4+4] photocycloadditions through careful control of steric interactions.[52] 9,10-Dimethylanthracene (**DMA**) is known to not form a stable photodimer due to high steric hindrance across the newly formed sigma bond in the dimer.[73] Similarly, 2,3,6,7-tetraphenylanthracene (**TPA**) does not readily form its photodimer due to the steric bulk associated with the phenyl groups.[52] However, when **DMA** and **TPA** were irradiated together in solution with 350 nm lamps, a cross-photoadduct **DMA-TPA** was produced as the exclusive product, as shown in Equation 4.1.[52] Stimulated by this selective photoadduct formation, the photochromic properties of tetraphenylpyrazo[2,3-*g*]quinoxaline (**TPPQ**) as a heterocyclic equivalent to **TPA** were initiated (Figure 4.1).

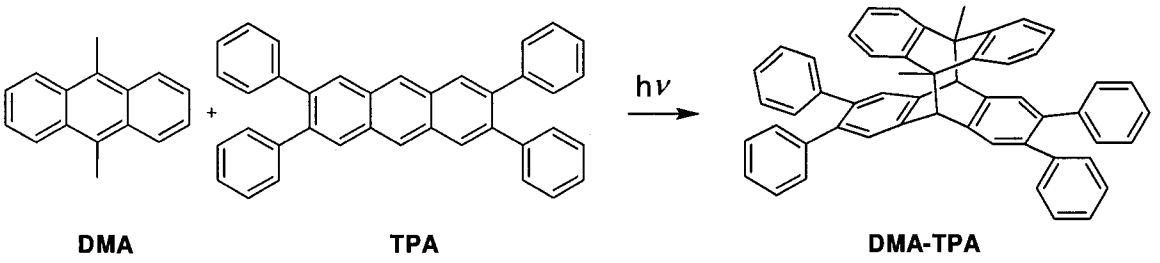

Equation 4.1: Photocycloaddition of 9,10-dimethylanthracene and 2,3,6,7-tetraphenylanthracene.

Modelling of the HOMO and LUMO of pyrazo[2,3-*g*]quinoxaline (**PQ**) were carried out at the AM1 level and were found to be qualitatively similar to those of anthracene (Figure 4.2). Thus it was anticipated that pyrazo[2,3-*g*]quinoxaline would undergo [4+4] cycloaddition across the central ring when irradiated with UV light.

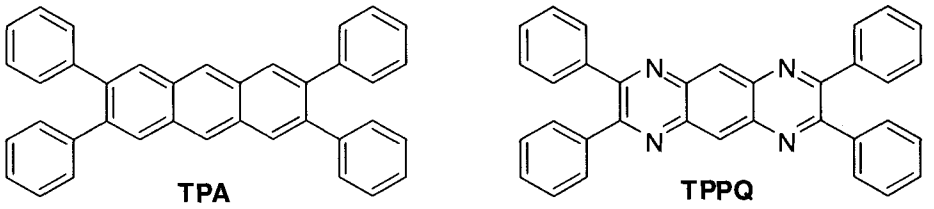

Figure 4.1: 2,3,6,7-Tetraphenylanthracene (**TPA**) and 2,3,7,8-tetraphenylpyrazo[2,3-*g*]quinoxaline (**TPPQ**).

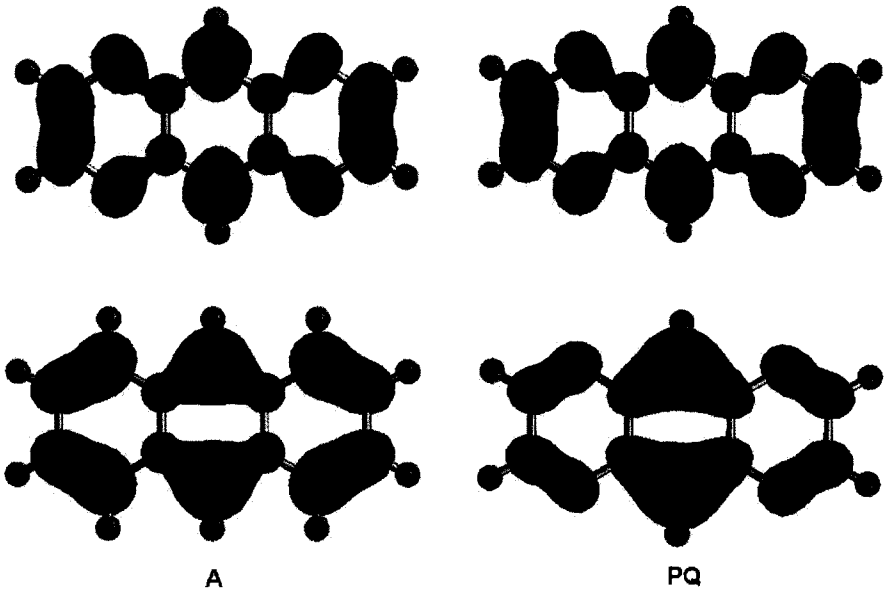

Figure 4.2: HOMO (bottom) and LUMO (top) of A and PQ calculated at the AM1 level.

Like the benzo[2,3-*g*]quinoxaline derivatives discussed in Chapter 2:, tetra-substituted pyrazo[2,3-*g*]quinoxalines were more synthetically accessible than their peripherally functionalized anthracene counter-parts. In this chapter, our attempts to demonstrate that **TPPQ** undergoes [4+4] phototocycloaddition with anthracene compounds substituted at the 9- and 10-positions will be described.

4.2 Results and Discussion:

In order to test the photoreactivity of the pyrazo[2,3-*g*]quinoxaline core, **PQ** was synthesized following a literature procedure.[74] Similarly to **BQ**, **PQ** could not be purified to the same extent as the substituted quinoxaline derivatives and the final product was a dark brown solid instead of the yellow product reported in the literature.[74] Unfortunately, the exceedingly low solubility of **PQ** rendered the investigation of its photochromic properties impractical.

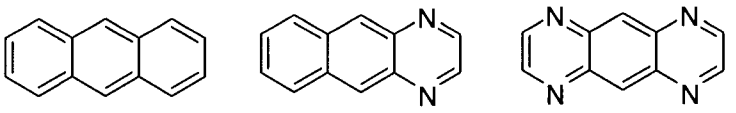

A **BQ** **PQ**

Figure 4.3: Structural similarities between anthracene (**A**), benzo[2,3-*g*]quinoxaline (**BQ**) and pyrazo[2,3-*g*]quinoxaline (**PQ**).

TPPQ was synthesized in one step by condensation of benzil with tetraaminobenzene tetrahydrochloride salt (Equation 4.2) in 84 % yield.[75] The UV-Vis absorption spectra in CH_3CN revealed a strong absorption at 264 nm and a set of less intense peaks with a maxima at 406 nm (Figure 4.4).

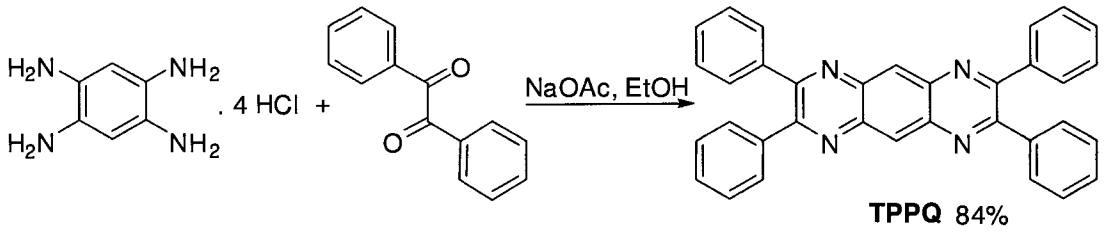

Equation 4.2: Synthesis of **TPPQ**.

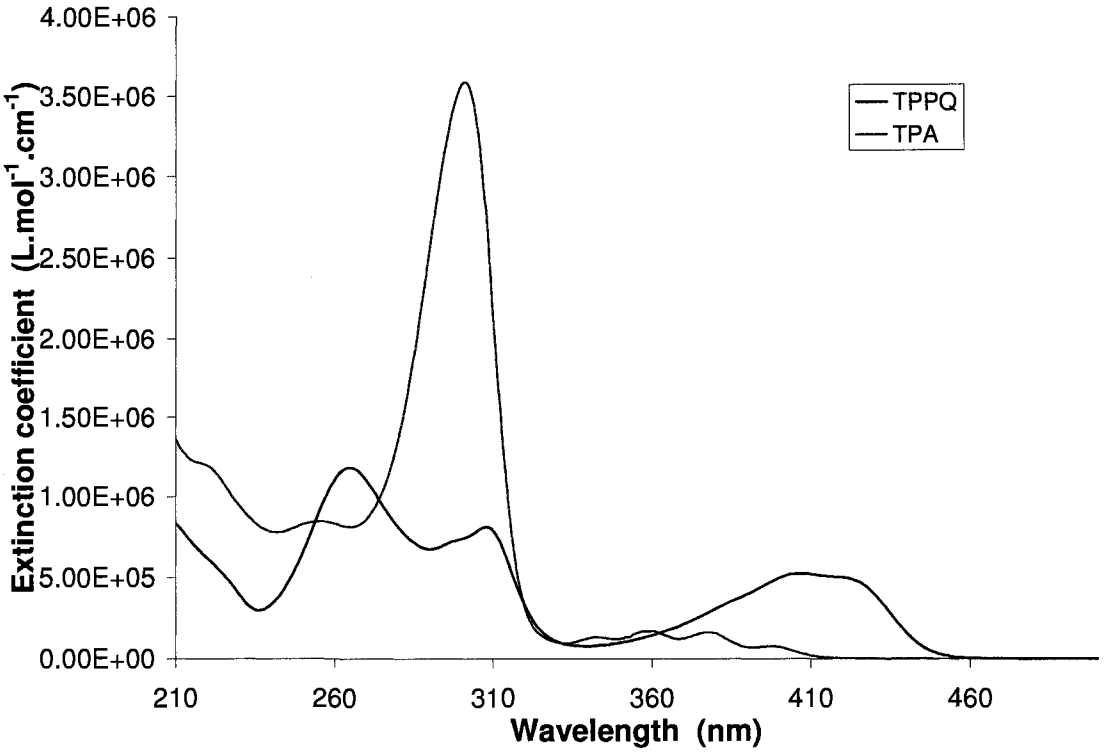

Figure 4.4: UV-Vis absorption spectra of **TPPQ** and **TPA**.

4.2.1 [4+4] Photocycloaddition

4.2.1.1 [4+4] Photocycloaddition

A 1.96 mM solution **TPPQ** in CH_3CN was irradiated in the Rayonet® photochemical reactor fitted with 350 nm lamps. After 2.5 h of irradiation, no photoproducts were observed. This lack of reactivity could be caused by the low

concentration that was necessitated by the low solubility of **TPPQ** in CH_3CN. This compound was much more soluble in benzene; hence irradiation of a 3.82 mM benzene solution was also examined. After 2.5 h of irradiation, no photoadduct was isolated suggesting that the reactivity of **TPPQ** was similar to that of **TPA**. In order to verify that the apparent lack of reactivity was not caused by cycloreversion of the dimer, a 0.1 mM solution of **TPPQ** in CH_3CN was irradiated in the Rayonet® photochemical reactor fitted with 419 nm lamps. After 2.5 h of irradiation, no photoadduct was observed by ^{1}H-NMR spectroscopy. The absence of photoadduct suggested that the enhanced steric bulk present at the peripheral positions inhibits the formation of photodimer (Equation 4.3). Thus, **TPPQ** could potentially be used to form cross-dimer in a similar manner as **TPA**, when irradiated in the presence of anthracene or **DMA**.

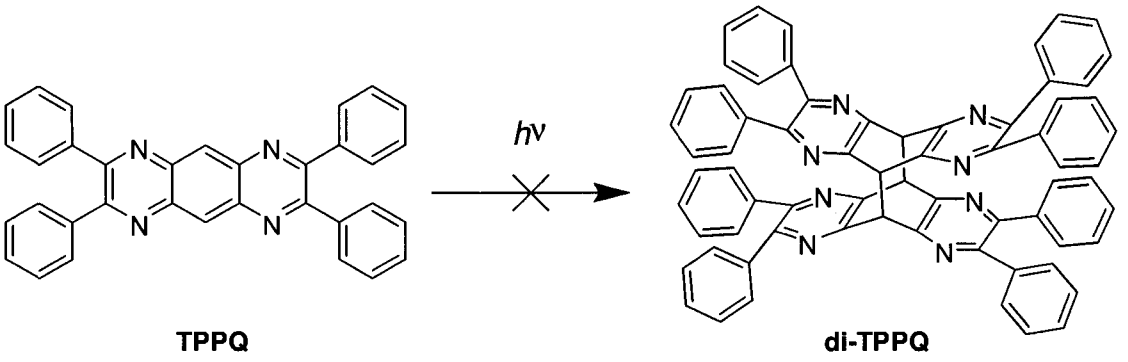

Equation 4.3: Result of UV exposure of **TPPQ**.

In order to improve the solubility of **TPPQ**, 2,3,7,8-tetrakis(3,4-bis(hexyloxy)phenyl)-pyrazo[2,3-*g*]quinoxaline (**THPQ**) (Figure 4.5) was synthesised by condensation of 1,2,4,5-tetraminobenzene tetrahydrochloride and 3,3',4,4'-tetrahexyloxylbenzil. However, the solubility of **THPQ** in CH_3CN was not

improved compared to **TPPQ**. After a 1.34 x 10^{-4} M solution of **THPQ** was irradiated in the Rayonet® photochemical reactor for 170 min, no photoadduct was observed by ^{1}H-NMR spectroscopy. While this compound does not appear to undergo [4+4] photocycloaddition, **THPQ** was found to be liquid crystalline. DSC analysis showed that **THPQ** was liquid crystalline between 90 and 109 °C (see appendix 2). Polarised optical microscopy indicated that this liquid crystalline phase was columnar hexagonal (col_h) phase. X-Ray crystallography data confirmed the hexagonal packing during slow cooling of **THPQ** from its isotropic liquid state. The relative accessibility of this new mesogenic compound combined with high fluorescence makes tetradialkoxyphenylpyrazo[2,3-*g*]quinoxaline derivatives potentially attractive for electroluminescent devices applications.[76]

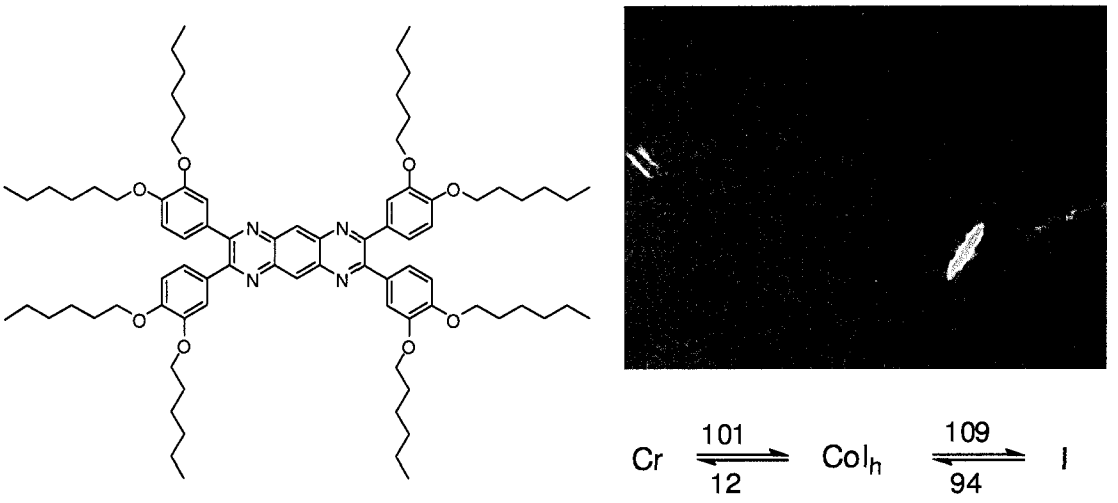

Figure 4.5: 2,3,7,8-Tetrakis(3,4-bis(hexyloxy)phenyl)-pyrazo[2,3-*g*]quinoxaline (**THPQ**) and polarised micrograph showing the C_6 symmetry taken at 106 °C with 400 x magnification.

4.2.1.2 Cross [4+4] photocycloaddition

To investigate whether **TPPQ** could react like **TPA**, a 0.1 mM of **TPPQ** (5.00 mL) and a 0.1 mM solution of anthracene (**A**) (5.00 mL) in CH_3CN were mixed and irradiated in the Rayonet® photochemical reactor with 350 nm lamps for 2.5 h without prior deoxygenation. MALDI-TOF mass spectrum showed peaks at m/z=177, 489 and a less intense peak at m/z=664 corresponding to M(**A**)$^+$, M(**TPPQ**+3)[e] and M(**A-TPPQ**)$^+$, respectively. The last peak suggested that UV-irradiation of a concentrated solution containing equimolar amounts of **TPPQ** and **A** yielded and **TPPQ-A** cross-dimer. ^{1}H-NMR analysis of the concentrated solution revealed peaks associated with **TPPQ** but only traces of **A**. Another set of peaks composed of two peaks in the aromatic region at 8.3 and 7.8 ppm and a singlet at 4.1 ppm, were ascribed to the formation of anthracene

[e] Improper calibration of the MALDI instrument lead to a margin of error the ion peaks observed.

endoperoxide. A singlet at 4.55 ppm along with two peaks at 6.86 and 6.70 ppm suggested that **di-A** was also present in solution. When a 0.05 mM solution of **A** (10.00 mL) was irradiated simultaneously, endoperoxide was also produced quantitatively. This suggests that deoxygenating will be necessary for future photochemical studies of a mixture of **TPPQ** and **A** at millimolar concentration. ^{1}H-NMR analysis of the concentrated solution also showed two doublets in a 1:1 ratio at 3.75 and 3.20 ppm suggesting that a fifth species present after irradiation posses two adjacent sp^3 carbons in different environments which is consistent with the bridgehead protons of **TPPQ-A** (Equation 4.4). As seen in Figure 4.6, this third photoproduct is only present in minute amounts, thus attempts to assign the remaining peaks in the aromatic region were not successful. As encountered in earlier chapter, the lack of solubility of the starting material prevented separation of the photoproduct from the starting materials through crystallisation or column chromatography. Although MALDI-TOF MS suggested that **TPPQ** and **A** formed **TPPQ-A** upon irradiation, ^{1}H-NMR spectroscopy did not provide enough evidence to confirm that this photoadduct results from the [4+4] photocycloaddition across the central rings of both **TPPQ** and **A**. Irradiation of larger volumes of more concentrated solution of **TPPQ** and **A** should be carried out in order to separate sufficient amounts of the photoadduct and determine its structure.

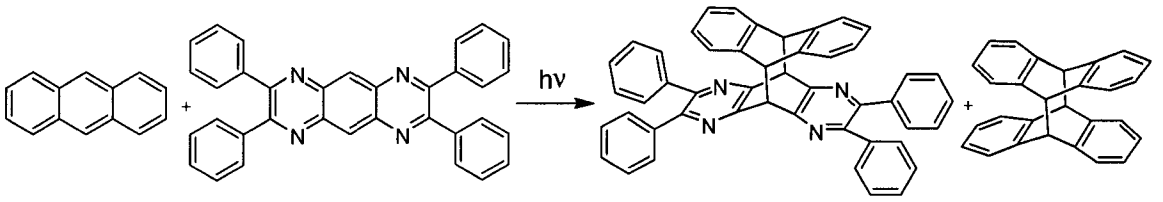

Equation 4.4: Cross-dimer formation resulting from irradiation of a mixture of **TPPQ** and **A**.

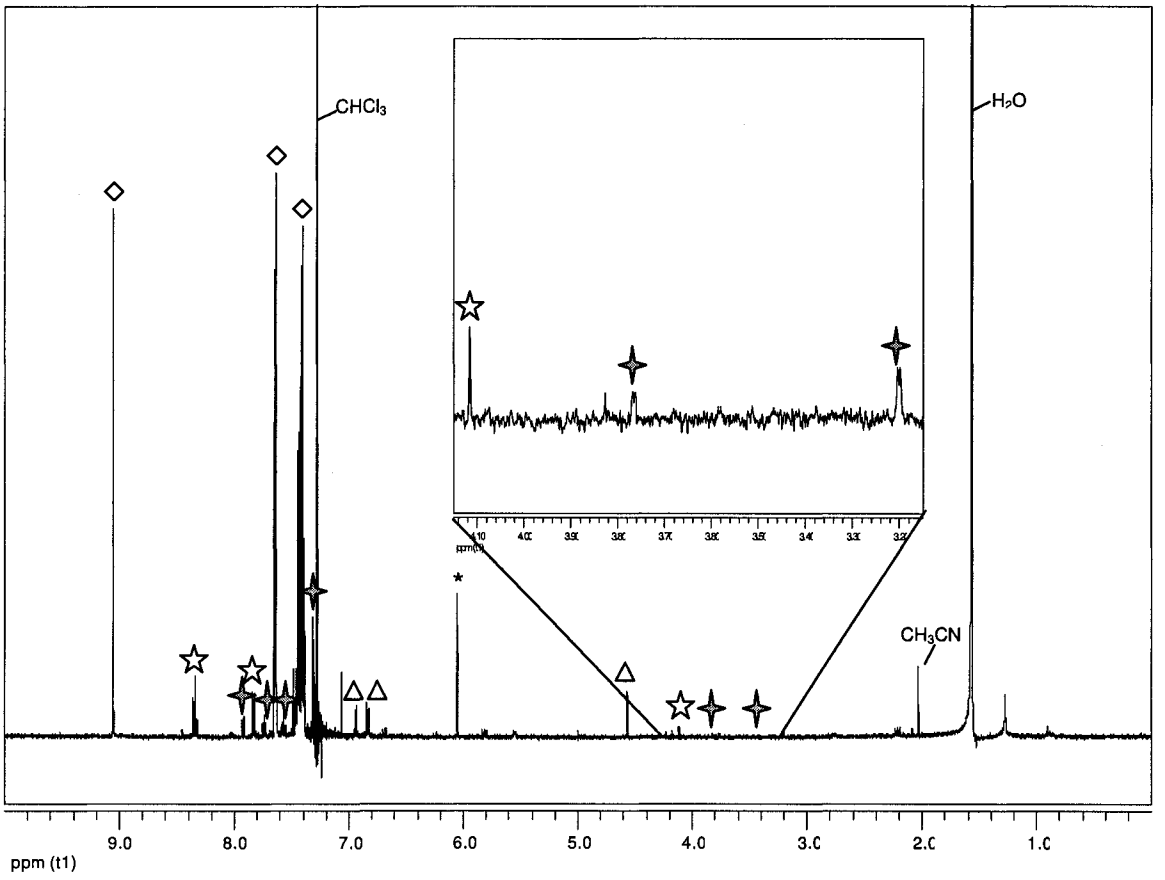

Figure 4.6: ^{1}H-NMR of a mixture of 0.2 mM solutions of **TPPQ** and **A** (5.0 +5.0 mL) in CH_3CN after 150 min of irradiation, dried *in vacuo* and recorded in $CDCl_3$. **TPPQ** (diamond), **AO_2** (five-point star), **di-A** (triangle), new photoproduct (four-point star), unknown impurity (*)

To demonstrate that **TPPQ** could form a heterodimer with **DMA** in a similar manner to **TPA**,[52] a 0.1 mM solution of **TPPQ** in CH_3CN (5.00 mL) was mixed

with a 0.1 mM solution of **DMA** in CH_3CN (5.00 mL) and irradiated for 2.5 h in the Rayonet® photochemical reactor. MALDI-TOF MS showed peaks at m/z = 206 and 489 associated with **DMA** and **TPPQ** respectively, and a peak at m/z= 698 which corresponds to the **TPPQ-DMA** cross-cyclomer (Equation 4.5). ^{1}H-NMR spectroscopy revealed that the major species present in solution was unreacted **TPPQ**. The ^{1}H-NMR spectrum also showed a set of peaks composed of a singlet at 2.95 ppm and two peaks at 8.30 and 7.80 ppm corresponding to **DMA**. Other peaks were also present in the ^{1}H-NMR spectra, but due to the high signal-to-noise ratio the structure could not be further characterised (Figure 4.7). Once again, the low solubility of **TPPQ** limited the characterisation of the photoproduct formed upon irradiation however trace amounts a third compound were present. When 0.05 mM solutions of **TPPQ** and **DMA** where irradiated under the same conditions, no photoadduct was observed for either sample. Thus, the unknown photoadduct was associated with the photoreaction of **TPPQ** with **DMA**. The lack of characteristic peak in the diagnostic bridgehead region suggests that another kind of photoreaction is occurring under these experimental conditions. Similar to the previous experiment, the low solubility of **TPPQ** represents the main limitation to the characterisation of the photoproduct; hence, the use of more concentrated solution or larger volumes for irradiation should be attempted to form larger amounts of the product.

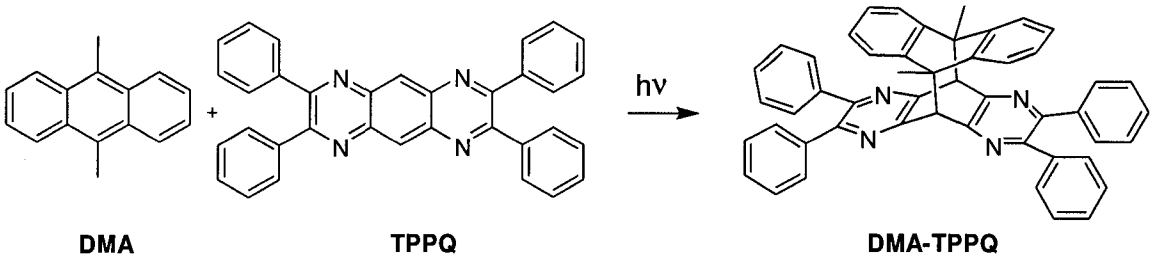

Equation 4.5: Cross-dimer formed from irradiation of a mixture of **DMA** and **TPPQ**.

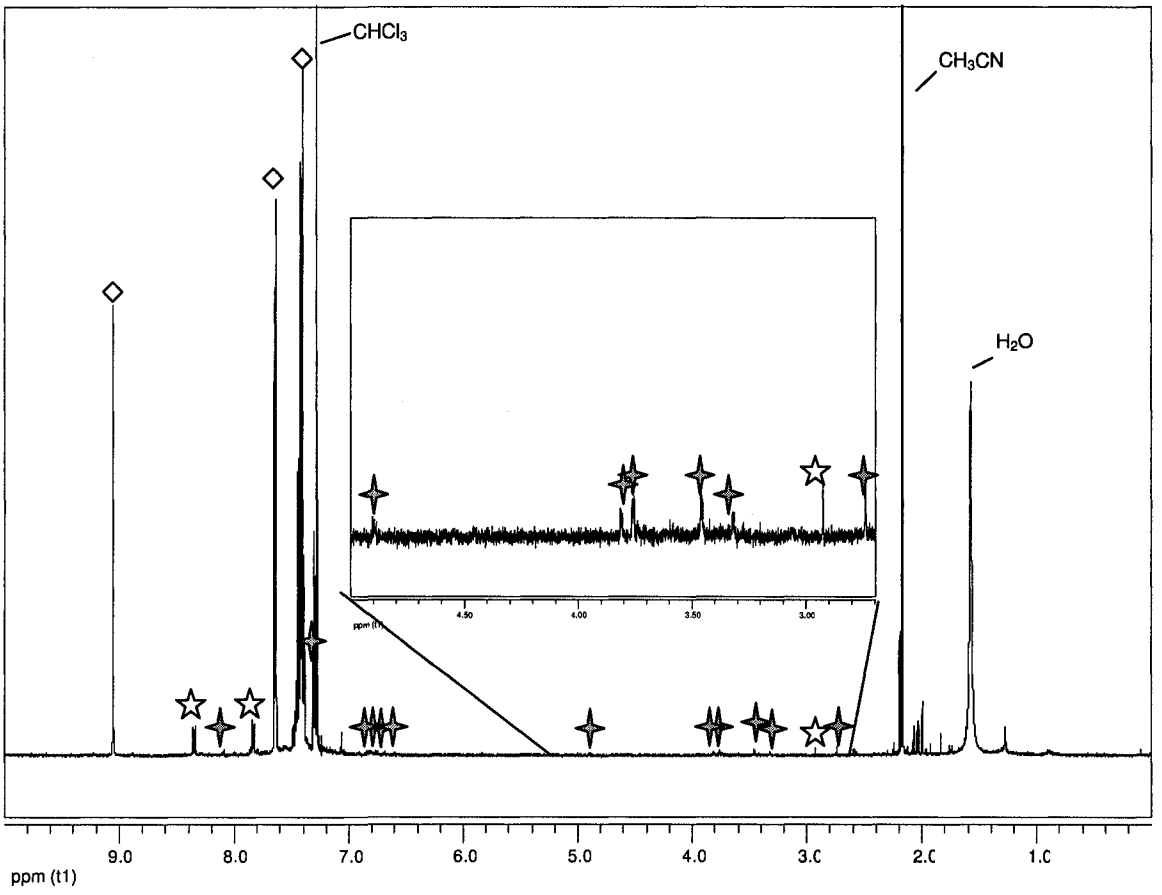

Figure 4.7: ^{1}H-NMR of a mixture of 0.2 mM solutions of **TPPQ** and **DMA** (5.0 +5.0 mL) in CH_3CN after 150 min of irradiation, concentrated *in vacuo* and recorded in $CDCl_3$. **TPPQ** (diamond), **DMA** (five-point star), new photoproduct (four-point star).

4.3 Conclusion

Similar to its anthracene analogue **TPA**, **TPPQ** did not yield any photoproduct when irradiated by itself. This suggested that the steric bulk at the peripheral positions prevented its dimerisation although at this point, we cannot rule out its lack of reactivity on electronic grounds as we still have not measured the lifetime of its excited state. Motivated to develop a selective photochromic system based on the control of steric interactions, **TPPQ** was irradiated in the presence of **A** and **DMA**. **TPPQ** was shown to undergo a photoreaction upon irradiation when equimolar amounts of **A** were present in solutions. However, the low solubility of **TPPQ** limited us to work at low concentrations, which in turn impeded the isolation and characterisation of the photoproduct.

CHAPTER 5: EFFORTS TOWARDS PHOTORESPONSIVE MATERIALS CONTAINING BENZO[2,3-*g*]QUINOXALINES

5.1 Benzo[2,3-*g*]quinoxaline-functionalised polymer

5.1.1 Introduction

The readily accessible benzo[2,3-*g*]quinoxaline derivatives discussed in Chapter 2 were shown to have similar photochromic properties to their anthracene analogues. However, the absorption spectra for these systems were red-shifted, which could be advantageous when used in a polystyrene matrix. Indeed one of the reasons preventing anthracene functionalized polystyrene-based materials from being used in practical applications is the poor efficiency of the backward reaction (photodissociation); in fact, the polystyrene backbone and the incorporated dianthracene both absorb at similar wavelength (light under 300 nm) rendering the photodissociation inefficient.

Our approach was to graft benzo[2,3-*g*]quinoxaline derivatives on a polystyrene backbone and compare the photochromic properties of this photoactive polymer with an anthracene analogue.

5.1.2 Result and Discussion

The benzo[2,3-*g*]quinoxaline moiety potentially can be grafted onto a polystyrene backbone by nucleophilic substitution on the benzylic position. To that purpose two polymers with different 4-chloromethylstyrene content were synthesised.

Our attempts to chloromethylate a commercially available polystyrene (PS) of known chain length and polydispersity using monochloromethyl ether were unsuccessful.[77,78] Thus, a polydisperse polymer was synthesised via free radical polymerisation of styrene and 4-chloromethystyrene (Equation 5.1).[79,80] After 18 h at 100 °C, a white solid was formed in the reaction vessel. ^{1}H-NMR spectroscopy of this product (**PS1**) revealed a peak at 4.5 ppm which was associated with the benzylic position of the vinylbenzyl chloride unit of the polymer. Integration of this diagnostic peak with respect to the proton at the 4-position of the styrene repeat unit enabled us to determine a ratio of one chloromethylstyrene unit per two styrene units. GPC analysis determined an average molecular weight of 38 kDa and a polydispersity of 1.69. The high chloromethyl content would then lead to high level of cross-linking. In order to obtain a polymer with lower chloromethylstyrene content and the temperature of polymerisation was decreased to 70 °C and AIBN was added as a radical initiator. These experimental conditions yielded a copolymer **PS2** composed of one unit of chloromethyl styrene per fifty unit styrene, with an average molecular weight of 71 kDa with a polydispersity of 1.74.

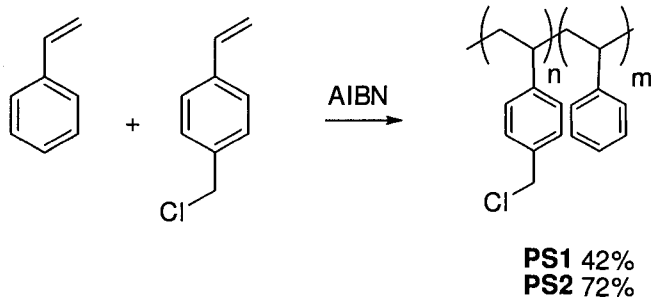

PS1 42%
PS2 72%

Equation 5.1: Synthesis of poly(styrene-*co*-4-vinylbenzyl chloride) by free-radical polymerization.

In order to functionalise the **PS2** with a benzo[2,3-*g*]quinoxaline, 4-(benzo[2,3-*g*]quinoxalinyl)phenol (**BQP**) was synthesised by demethylation of **MoPBQ** with 48 % HBr solution.[81] Polymer **PS2** of known chain length and broad polydispersity was then grafted with **BQP** in the presence of a base (Scheme 5.1). The obtained polymer was however very insoluble and tended to form gels in several solvents such as acetonitrile, chloroform, benzene, dichloromethane, cyclohexane and toluene. The low insolubility suggested that other reactions occurred during the functionalisation of the polymer backbone resulting in a high cross-linking density within the polymer.

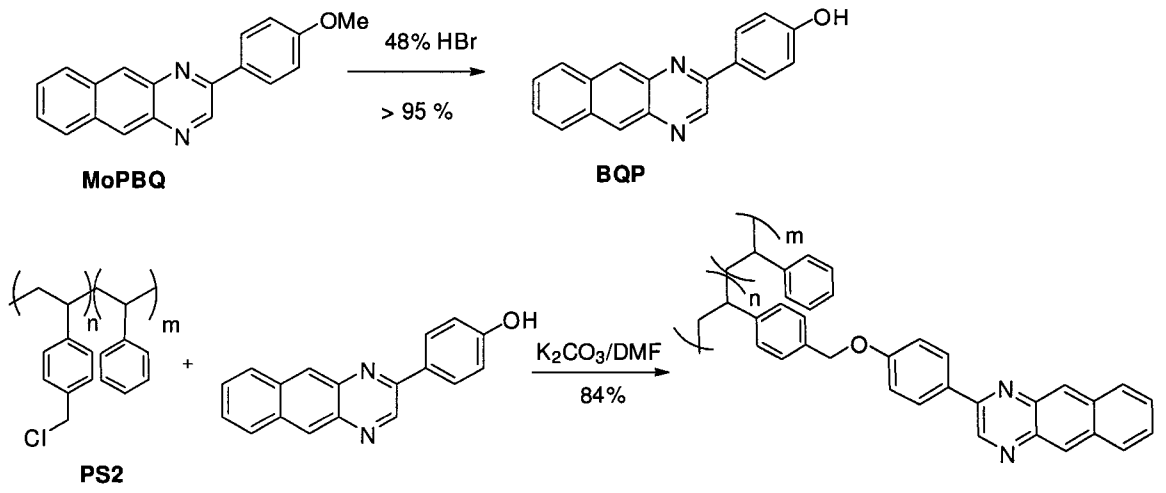

Scheme 5.1: Synthesis of benzo[2,3-*g*]quinoxaline functionalised polystyrene.

As a result of its poor solubility, the solution photochemistry of the modified polymer could not be investigated. Prior to the investigation of the photochemical properties of benzo[2,3-*g*]quinoxaline functionalised polystyrene, other synthetic routes such as polymerisation of functionalised monomer or inserting ethylene glycol chain in the back bone to increase the solubility should be investigated.

CHAPTER 6: CONCLUSION AND FUTURE WORK

6.1 Conclusion

The synthesis and studies of the photochemical properties of a series of benzo[2,3-*g*]quinoxaline and pyrazo[2,3-*g*]quinoxaline derivatives were described in this thesis. The 2,3-disubstitutedbenzo[2,3-*g*]quinoxaline derivatives represent easily synthetically accessible heterocyclic analogue to 2,3-disbustituted anthracene compounds, and were found to display similar photochromic properties. Such compounds therefore allow a facile investigation of the factors influencing the photochemistry of compounds undergoing [4+4] photocycloaddition upon irradiation.

Upon irradiation, anthracene derivatives are known to undergo [4+4] photocycloaddition to form a dimer. The dimer can then be dissociated back to the monomer using light of higher energy, which also promotes other photochemical events that prevent systems based on the photochromism of anthracenes to be used in practical applications. To overcome such phenomenon anthracene can be substituted on the peripheral ring rather than at the central ring using cumbersome multistep synthesis. A series of peripherally substituted benzo[2,3-*g*]quinoxaline derivatives was synthesised. As predicted, extension of the conjugation on the benzo[2,3-*g*]quinoxaline core resulted in a shift in UV-Vis absorption towards longer wavelengths. The effect of UV irradiation of these

compounds was investigated in solution and monitored by NMR spectroscopy, UV-Vis absorption spectroscopy and MALDI-TOF MS. All compounds synthesised underwent photoreactions upon UV-irradiation however, only the photoadducts of **DPBQ** and **DPyBQ** could be isolated and were confirmed to be dimers. The photochemistry of **DPBQ** was studied in more detail than the other derivatives. Both **PBQ** and **BQ** formed photoadduct upon irradiation however, the structure of the photoadduct could not be identified due their poor solubility. The addition of methoxy group resulted in a red-shift in UV-Vis absorption but no dimer was observed for both **DMoPBQ** and **MoPBQ**. This lack of reactivity could be associated to the photodissociation of the dimers being formed during irradiation. Indeed, the addition of the methoxy group would lead to a red-shift in the dimers and the light source used during the irradiation experiment could provide enough energy to dissociate the photoadduct.

Table 6-1: Summary of characterisation of benzo[2,3-*g*]quinoxaline derivatives synthesised.

Monomer	**Yield** (%)	**Mw** (g/mol)	**m.p** (^{o}C)	λ_{max} (nm)	ε ($M^{-1}.cm^{-1}$)	δ^{a} (ppm)
DPBQ	72	332	185-186	381	12349	8.87
DPyBQ	73	334	185-187	378	7922	8.83
DMPBQ	66	392	185-187	396	8899	8.72
MPBQ	76	286	179 (d)	384	7612	9.37
PBQ	92	256	155-157	379	9502	9.34
BQ	> 95	180	125-126	360	4899	8.77

[a] diagnostic peak in ^{1}H-NMR spectrum

Table 6-2: Characterisation of concentrated solutions of benzo[2,3-g]quinoxaline derivatives after 150 min of irradiation.

monomer	Mw ($g.mol^{-1}$)	MALDI-TOF m/z	M	δ^b (ppm)	yield %
DPBQ	664	665	M+	5.06	40
DPyBQ	668	668	M+	5.17	40
DMoPBQ	784	394	M+2	5.45	10
MoPBQ	572	288	M+2	5.42	8
PBQ	512	551	M(K+)	5.1	13
BQ	360	182	M+2	4.41	41
A	356	180	M+2	4.57	44

[b] diagnostic peak in the ^{1}H-NMR spectrum.

The pyridyl substituent enabled the study of the influence of Zn^{2+} on the dimerisation efficiency of **DPyBQ**. The presence of Zn^{2+} in solution decreased the efficiency of dimerisation, but changing the counter-ion did not have any detectable effect.

In order to develop more selective systems based on the dimerisation of anthracene derivatives, tetrasubstituted pyrazo[2,3-*g*]quinoxaline derivatives were synthesised and their ability to undergo [4+4] cycloaddition was investigated. Similarly to its anthracene analogue, **TPPQ** did not undergo dimerisation when irradiated in solution. However, when **TPPQ** was irradiated in the presence of less sterically hindered anthracene derivatives, cross-photoadduct were observed by ^{1}H-NMR-spectroscopy.

The studies described above demonstrate that benzo[2,3-*g*]quinoxaline derivatives possess interesting photochemical properties that had not been reported prior to this work. They proved to be a viable alternative to anthracene

derivatives and have many advantages over them such as the ease of their synthesis, their tolerance to the presence of oxygen during dimerisation, and the fact that their dissociation is triggered at longer wavelengths.

6.2 Future Work

6.2.1 Benzo[2,3-*g*]quinoxaline-functionalised polymers

In the interest of further understanding the photochemistry of benzo[2,3-*g*]quinoxalines, more derivatives should be synthesised and their photochemistry should investigated. More precisely, the influence of electron donating and/or drawing groups, and the effect of polarisation and steric hindrance should be investigated.

In order to further understand the influence of transition metals and other chemicals on the dimerisation of **DPyBQ**, the isolation and characterisation of the complex formed with Zn^{2+} should be pursued. To that same purpose, the influence of pH on this compound and its photochemistry should also be further investigated. Such chemo-responsive systems could lead to the use of [4+4] cycloaddition as a sensor.

In an effort to develop light responsive materials based on the photochemistry of benzo[2,3-*g*]quinoxaline, future research should focus on trying to implement polymeric materials functionalised with benzo[2,3-*g*]quinoxalines. Indeed, most applications using photochromic systems require solid state devices.

Our preliminary efforts to functionalise polystyrene did not lead to a processable polymer. In order to yield more soluble benzo[2,3-*g*]quinoxaline functionalised polystyrene materials, polyethylene glycol chains could be added between the chromophore and the vinylic backbone. Other synthetic approaches to obtain anthracene-functionalised polysterene should be investigated. One possible alternative route could be to include the **DPBQ** in the polymer backbone by co-polymerising styrene with a vinylic derivative of **DPBQ** (Figure 6.2). Polyamide polymers could also represent a new variety of photoresponsive polymer (Figure 6.3).

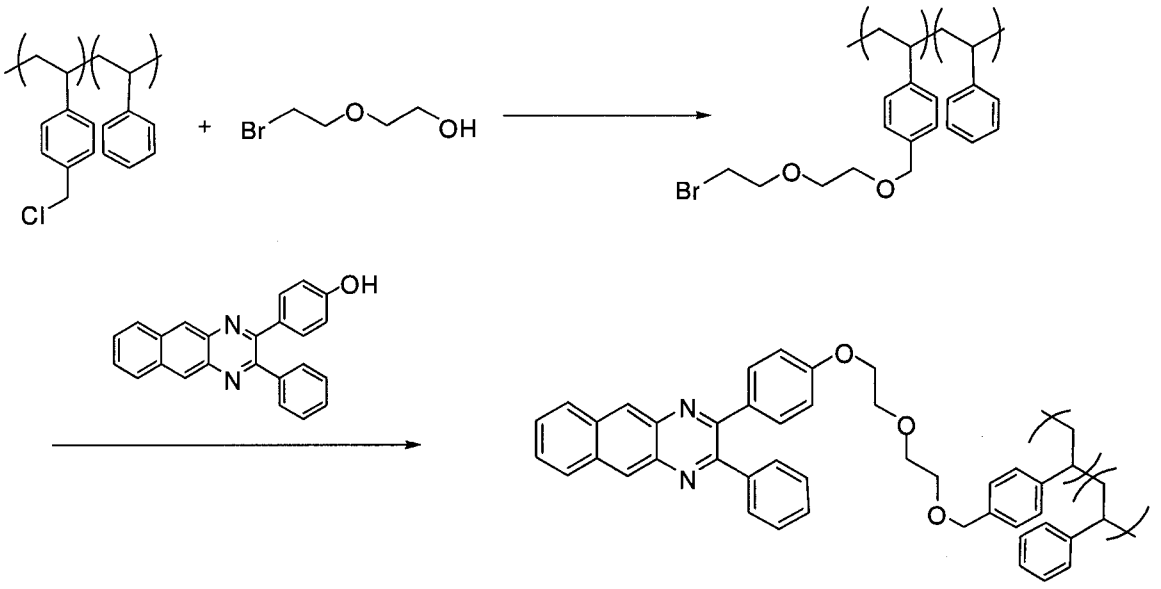

Figure 6.1: Synthesis of **PS** functionalised with a benzo[2,3-*g*]quinoxaline with a glycol linkage.

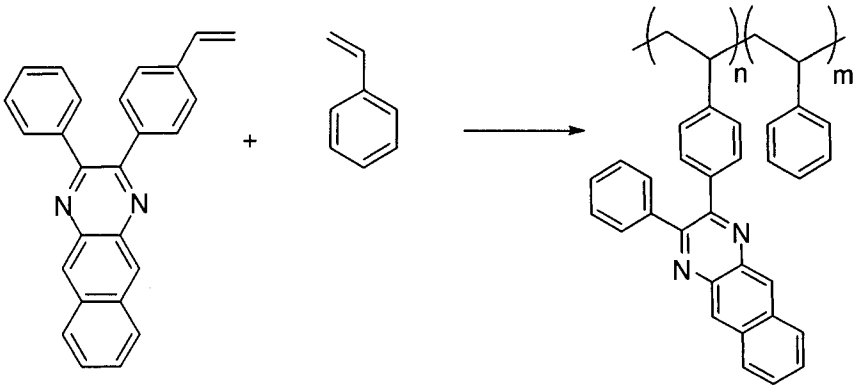

Figure 6.2: Proposed synthesis of co-benzoquinoxaline styrene polymer

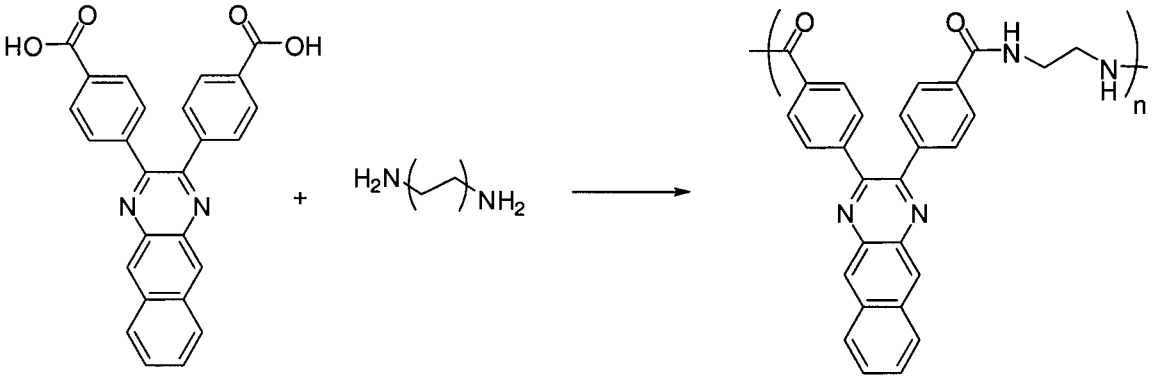

Figure 6.3: Proposed synthesis of polyamide polymer based on 2,3-diphenylbenzo[2,3-g]quinoxaline.

6.2.1 Stimuli responsive gels

The ability to reversibly change the state of matter using external stimuli has motivated chemists and material scientists to develop photoresponsive gels. Serendipitously, Bouas-Laurent and Desvergne discovered the gelating properties of 2,3-dialkoxyanthracenes (**DAOA**) in different polar solvents.[82] Replacing two CH groups in the central ring of anthracene by two N atoms to form phenazine also resulted in an effective gelator. Dialkoxyphenazine was also reported to be pH-sensitive.[83] Inspired by the theoretically easily accessible

dialkoxybenzoquinoxalines (**DABQ**), we attempted to develop photoreversible gelator (Figure 6.4).

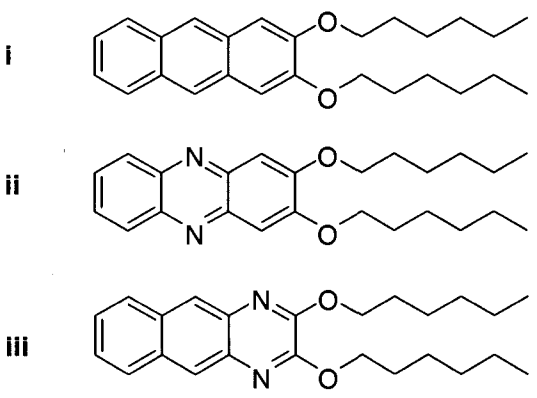

Figure 6.4: Structural similarities between (i) dialkoxyanthracene (**DAOA**), (ii) dialkoxyphenazine and (**iii**) dialkoxybenzoquinoxaline (**DABQ**).

In order to study the photochemical properties of **DABQ**, a systematic synthetic route should be developed. After overcoming those synthetic limitations, a series of **DABQ** derivatives should be synthesised in order to study the influence of alkoxy chains in systematic manner and the gelling properties of these compounds. This would in turn, allow the rational design of photoresponsive gels based on the underexploited dimerisation of anthracene-like molecules.

CHAPTER 7: EXPERIMENTAL:

The methods used in synthesis, purification; and characterisation of the compounds reported in the previous chapters is presented in this chapter.

7.1 Materials and methods

All chemicals were used as purchased from supplier without further purification. Benzil was purchased from Matheson Colemann & Bell and Potassium cyanide from Merck. All other chemicals were purchased from Aldrich.

NMR characterisation of products was carried out using either a Bruker AMX-400 400MHz spectrometer (400 MHz ^{1}H and 100 MHz ^{13}C) or a Varian Unity Inova 500 MHz spectrometer equipped with a 5 mm inverse detection probe (500 MHz ^{1}H and 125 MHz ^{13}C) as specified. Low resolution mass spectra were recorded on a Hewlett Packard 5985 mass spectrometer (EI 70 eV) by Mr. Philip Ferreira and Mr. Simon Wong. MALDI-TOF mass spectra were performed using a Perspective Voyager-DE STR from PE Applied Biosystems with a nitrogen laser (337 nm) and using 2,5-dihydroxybenzoic acid as the matrix. Melting points were determined either on a Fisher Johns or a Gallenkamp melting point apparatus. Fluorimetry was performed on a PTI C60

spectrofluorimeter and UV-Visible spectroscopy was recorded on a Cary 100 UV-Vis spectrophotometer. Microanalyses (C,H and N) were performed at Simon Fraser University by Mr. Miki Wang and Mr Simon Wong. Infrared spectra were recorded with a Thermo Nicolet Nexus 670 FT-IR E.S.P. spectrometer; samples were prepared as compressed KBr pellets.

All calculations were performed using the Spartan '02 molecular modeling program.[23] Geometry optimizations were performed at the AM1 semiempirical level.[24] Structures were optimized without any constraints. Calculation of the HOMO/LUMO potential surfaces were performed at the AM1 level using geometry-optimized structures.

7.2 Experimental for chapter 2

7.2.1 Synthesis of diketone derivatives

7.2.1.1 Symmetrical precursor

Apart from benzil, which was commercially available, all symmetrical diketones were synthesised by benzoin condensation of the corresponding aryl-aldehyde followed by oxidation.[84] 4,4'-(Dimethoxy)benzil was graciously provided by Dr. Daniel Spantulescu.

2-Hydroxy-1,2-di(pyridine-2-yl)ethanone: Picolinaldehyde (3.22g, 30.0 mmol), and potassium cyanide (1.92 g, 30.0 mmol) were dissolved in ethanol (5 mL) and water (20 mL) and heated to reflux. After 4h, TLC analysis (hexane: ethyl acetate 1:1) showed that all picolinaldehyde was consumed and the hot reaction mixture was poured over crushed ice. The resulting brown suspension

was filtered with a Buchner funnel and washed with cold ethanol to yield 2-hydroxy-1,2-di(pyridine-2-yl)ethanone (3.07 g, 14.3 mmol, 95 %) which was used without further purification. ^{1}H NMR (500 MHz, $CDCl_3$) δ_H (ppm) = 8.47 (d, J = 5.0 Hz, 2.0 H), 7.93-7.88 (m, 2 H), 7.84 (dt, J_1 = 8.2, J_2 = 1.8 Hz, 2 H), 7.19 (ddd, J_1 = 7.3, J_2 = 5.0, J_3 = 1.2 Hz, 2 H)

1,2-di(pyridin-2-yl)ethane-1,2-dione: 2-Hydroxy-1-(pyridine-2-yl)ethanone (1.61 g, 7.50 mmol) was dissolved in pyridine (25 mL). To this solution was added a solution of $CuSO_4$ (1.87 g, 7.50 mmol) in H_2O (10 mL). Once the addition was completed, the reaction mixture was stirred at reflux for 1 h. The hot reaction was poured over crushed ice and filtered using a Buchner funnel yielding 0.857 g of pure 1,2-di(pyridine-2-yl)ethane-1,2-dione (0.86 g, 4.04 mmol, 54%) as a shiny yellow crystalline solid. ^{1}H-NMR (500 MHz, $CDCl_3$) δ_H (ppm)= 8.60 (d, J = 4.7 Hz, 2.0 H), 8.23 (d, J = 7.8 Hz, 2 H), 7.94 (dt, J = 7.7, 1.8 Hz, 2 H), 7.50 (ddd, J_1 = 7.6, J_2 = 4.8, J_3 =1.2 Hz, 2 H); m.p. = 155-157 °C (*Lit.*[85] 156-157 °C) m/z (EI) = 213 (M+1)

1,4-Dioxane-2,3-diol: 1,4-dioxane-2,3-diol was prepared as per literature procedure.[60] Oxalaldehyde (5.31 g, 91.5 mmol) and ethane-1,2-diol (2.33 g, 37.5 mmol) were dissolved in benzene (10 mL) in a 25 mL round bottom flask fitted with a Dean-Stark trap and a condenser and heated to reflux. After removal of 2.7 mL of water, the reaction was cooled down to room temperature. The top layer formed in the round bottom flask was decanted and the viscous lower layer

was triturated with acetone (6 mL). The resulting syrupy suspension was filtered to yield the target compound as a shiny white powder (4.50 g, 37.5 mmol, quant.) that was used without further purification. ^{1}H-NMR (400 MHz, DMSO-d_6) δ_H (ppm) = 6.45 (d, J = 5.6 Hz, 2 H), 4.29 (d, J = 5.5 Hz, 2 H), 3.80 (d, J = 8.5 Hz, 2 H,), 3.38 (d, J = 8.5 Hz, 2 H); m.p. = 101-103 °C (*Lit.*[60] 100-103 °C).

7.2.1.2 Unsymmetrical diketones

2-Oxo-2-phenylacetaldehyde: 48% aqueous HBr (17.0 mL, 150 mmol) was slowly added to a stirred solution of acetophenone (6.0 g, 50.0 mmol) in DMSO (85 mL). The reaction mixture was then heated in an oil bath at 55 °C. After 25 h, no more starting material was observed by TLC (hexane: ethyl acetate 2:3), the hot reaction mixture was poured over crushed ice. The resulting suspension was extracted with EtOAc (3 x 100 mL). The combined organic extract were dried over $MgSO_4$ and evaporated *in vacuo* yielding a mixture anhydrous 2-oxo-2-phenylacetaldehyde and 2-oxo-2-phenylacetaldehyde monohydrate in a 3:2 ratio (5.80 g, 43.2 mmol, 87%) as a yellow viscous liquid, which was used immediately without further purification.[86] ^{1}H-NMR (500 MHz, $CDCl_3$) δ_H (ppm) = 9.68 (s, 1 H), 8.16-8.10 (m, 2 H), 8.21 (dd, J_1 = 8.3, J_2 = 1.4 Hz, 3 H), 8.00 (dd, J_1 = 8.3, J_2 = 1.4 Hz, 4 H), 7.53 (dd, J_1 = 9.5, J_2 = 6.2 Hz, 1 H), 5.97 (s, 3 H), 7.70-7.60 (m, 1 H).

2-(4-Methoxyphenyl)2-oxoacetaldehyde: 48% aqueous HBr (8.5 mL, 75.0 mmol) was slowly added to a stirred solution of 1-(4-methoxyphenyl)ethanone (3.75 g, 25.0 mmol) in DMSO (42.5 mL). The reaction

mixture was then heated in an oil bath at 55 °C. After 24 h, no more starting material was observed by TLC (1:1 hexane:ethyl acetate), the hot reaction mixture was poured over crushed ice. The resulting suspension was extracted with EtOAc (3 x 100 mL). The combined organic extract were dried over $MgSO_4$ and evaporated *in vacuo* yielding the target compound (3.57 g, 21.7 mmol, 87%) as a yellow solid, which was used without further purification. ^{1}H-NMR (500 MHz, $CDCl_3$) δ_H (ppm) = 8.10 (d , J = 9.4 Hz, 2 H), 6.93 (d, J = 9.4 Hz, 2 H), 6.30 (s, 1 H), 3.86 (s, 3 H); m.p.= 95-98 °C (*Lit.*[87] 96-99 °C) m/z (EI) = 165 (M^+)

7.2.2 Synthesis of benzoquinoxaline derivatives:

2,3-Diphenylbenzo[2,3-*g*]quinoxaline (DPBQ): A solution of 2,3-diaminonaphthalene (0.316 g, 2.000 mmol) and benzil (0.423 g, 2.000 mmol) in acetic acid (10 mL) was heated under reflux overnight. Reaction progress was monitored by TLC (toluene). Once all 2,3-diaminonaphtalene was consumed, the hot reaction mixture was poured over crushed ice. The resulting brown suspension was then neutralised with saturated aqueous solution of $NaHCO_3$. The aqueous solution was extracted with dichloromethane (3 x 80 mL). The combined organic extracts were dried over $MgSO_4$, filtered and evaporated *in vacuo* yielding a dark yellow powder (0.585 g, 88%). The product was purified by flash column chromatography (silica gel, dichloromethane) and recrystallised from hot ethanol to yield **DPBQ** (0.497 g, 75%) as a yellow crystalline powder. ^{1}H-NMR (400 MHz, $CDCl_3$) δ_H (ppm) = 8.75 (s, 2 H), 8.13 (dd, J_1 = 3.3, J_2 = 6.4 Hz, 2 H), 7.57 (m, 6 H), 7.37 (m, 6 H); m.p. = 184-185 °C (*Lit.*[53] 187-189 °C).

Benzo[2,3-*g*]quinoxaline (BQ): BQ was synthesised as per literature procedure.[60] The product was purified by flash column chromatography (silica gel, ethyl acetate: dichloromethane 1:3) and recrystallised from hot ethanol to yield the target compound (85%) as brown powder. ^{1}H-NMR (400 MHz, $CDCl_3$) δ_H (ppm) = 8.95 (s, 2 H), 8.80 (s, 2 H), 8.17 (dd, J_1 = 3.3, J_2 = 6.5 Hz, 2 H), 7.65 (dd, J_1 = 3.2, J_2 = 6.6 Hz, 2 H); m.p. = 126-130 °C (*Lit.*[60] 125-126 °C).

2-Phenylbenzo[2,3-*g*]quinoxaline (PBQ): PBQ was synthesised as per literature procedure.[88] The product was purified by flash column chromatography (silica gel, ethyl acetate) yielding **PBQ** (92%) as shiny yellow needles. ^{1}H-NMR (400 MHz, $CDCl_3$) δ_H (ppm) = 9.41 (s, 1 H), 8.76 (s, 1 H), 8.72 (s, 1 H), 8.28 (d, J = 7.0 Hz, 2 H), 8.14 (dd, J_1 = 4.0, J_2 = 5.6 Hz, 2 H), 7.65-7.60 (m, 5 H); m.p. = 155-157 °C (*Lit.*[88] 163 °C); m/z (CI) = 256 (M+1)

2,3-Di(pyridin-2-yl)benzo[2,3-g]quinoxaline (DPyBQ): DPyBQ was synthesised as per literature procedure.[66] The product was recrystallised from hot ethanol yielding **DPyBQ** (73%) as shiny yellow crystals. ^{1}H-NMR (400 MHz, $CDCl_3$) δ_H (ppm) = 8.80 (s, 2 H), 8.36 (d, J = 4.8 Hz, 2 H), 8.15 (m, 2 H), 8.09 (d, J = 7.8 Hz, 2 H), 7.87 (dt, J_1 = 1.7, J_2 = 7.7 Hz, 2 H), 7.61 (m, 2 H), 7.26 (m, 4 H); m.p. = 183-185 °C (*Lit.*[66] 184-185 °C); m/z (CI) = 335 (M+1)

2,3-di(4-methoxyphenyl)benzo[2,3-g]quinoxaline (DMoPBQ): **DMoPBQ** was prepared as per literature procedure.[89] **DMoPBQ** (66%) was obtained as a shiny crystalline product. No further purification was necessary. ^{1}H-NMR (400 MHz, $CDCl_3$) δ_H (ppm) = 8.68 (s, 2H), 8.09 (m, 2 H), 7.55 (m, 6 H), 6.89 (m, 4 H), 3.84 (s, 6 H); m.p. = 183-186 °C (*Lit* 185-187 °C);[89] MALDI-TOF m/z = 361 (M-OMe)

2-(4-methoxyphenyl)benzo[2,3-*g*]quinoxaline (MoPBQ): MoPBQ was prepared according to the method described for **DMoPBQ**. **MoPBQ** (76%) was isolated as a yellow-greenish powder was obtained. EA found (*submitted* C, ;H, ;N;) Calc for $C_{19}H_{14}N_2O$ C, 79.7;H, 4.93;N, 9.78; ^{1}H-NMR (500 MHz, $CDCl_3$) δ_H (ppm) = 9.4 (s, 1 H), 8.86 (s, 1H), 8.73 (s, 1 H), 8.31 (d, J = 8.2 Hz, 2 H), 8.13 (m, 2H), 7.61 (m, 2 H), 7.13 (d, J = 8.4 Hz, 2 H), 3.93 (s, 3 H); ^{13}C-NMR (125 MHz, $CDCl_3$) δ_C (ppm) = 161.9, 151.6, 144.7, 139.1, 138.2, 134.5, 133.6, 129.6, 129.4, 128.8, 128.6, 127.76, 126.75, 127.1, 126.8, 114.9, 55.74, 55.73; m/z (EI) = 286 (M^+); IR (KBr) ν = 3053, 2993, 2956, 2919, 2845, 1607, 1249 cm^{-1}; UV-Vis λ_{max} /nm (ε/M.cm^{-1}): 234 (17687), 268 (24170), 309 (17560), 318 (17950), 384 (7612).

7.2.3 Photochemical Experiments

Examples of typical photochemical experiments are described in this section.

di-DPBQ: 3.3 mg of **DPBQ** was dissolved in spectral grade benzene (1.5 mL) and deoxygenated by a minimum of three freeze-pump-thaw cycles. The

sample was then irradiated in a Rayonet® photochemical reactor for 2 h. After irradiation, a white powder precipitated onto the side of the glass.

The solution was decanted and the white product was collected. EA Found: C, 86.61; H, 4.98; N, 8.15. Calc. for $C_{48}H_{32}N_4$ C, 86.72; H, 4.85; N, 8.43; ^{1}H-NMR (400 MHz, $CDCl_3$) δ_H (ppm) = 7.23 (m, 16 H), 7.14 (m, 8 H), 7.03 (m, 4 H), 5.05 (s, 4 H); ^{13}C-NMR (100 MHz, $CDCl_3$) δ_C (ppm) = 156.3, 148.7, 140.4, 138.8, 129.4, 128.1, 128.0, 126.9, 52.7 (Note: due to the limited solubility of this compound, we were unable to observe the signals for quaternary carbons) MALDI-TOF m/z = 665 (M+1); IR (KBr) ν = 3057, 2959, 2919, 2849, 1389, 1144 cm^{-1}; UV-Vis λ_{max} /nm (ε/M.cm^{-1}): 230 (47543), 270 (17967), 308 (23337), 328 (29242).

For the experiments in which a filter solution was employed, 3.3 mg **DPBQ** was dissolved in 0.75 ml of CH_3CN. The solution was transferred to an NMR tube and immersed in a test tube filled with a 2.0 M solution of KNO_3 in water. The sample was irradiated in the Rayonet® photochemical reactor for 150 min. The solvent was then removed *in vacuo*.

Irradiation of **BQ : BQ** (3.8 mg, 0.02 mmol) was dissolved in spectral grade CH_3CN (15.0 mL). A 6.0 mL aliquot was then immersed in a 2.0 M aqueous KNO_3 solution and irradiated in the Rayonet® photochemical reactor for 2.5 h. After irradiation, no white powder precipitated onto the side of the glass. The sample was dried *in vacuo* (41 %). ^{1}H-NMR (500 MHz, $CDCl_3$) δ_H (ppm) =

9.12 (s, 1 H), 8.9 (s, 2 H), 8.72 (s, 2 H), 8.46 (dd, J_1 = 3.3, J_2 = 5.7 Hz, 2 H), 8.15 (dd, J_1 = 3.3, J_2 = 6.5 Hz, 3 H), 7.93 (dd, J_1 = 3.3, J_2 = 5.8 Hz, 2 H), 7.62 (dd, J_1 = 3.2, J_2 = 6.6 Hz, 3 H), 7.26 ($CHCl_3$), 4.85 (s, 2 H); MALDI-TOF m/z = 394 (**di-BQ**+Na^+).

Irradiation of **PBQ : PBQ** (5.3 mg, 0.02 mmol) was dissolved in spectral grade CH_3CN (15.0 mL). A 6.0 mL aliquot was then immersed in a 2.0 M aqueous KNO_3 solution and irradiated in the Rayonet® photochemical reactor for 2.5 h. After irradiation, no white powder precipitated onto the side of the glass. The sample was dried *in vacuo* (13 %). ^{1}H-NMR (400 MHz, $CDCl_3$) δ_H (ppm) = 9.45-9.43 (m, 1 H), 9.35 (s, 2.1 H), 8.69 (s, 2 H), 8.65 (s, 3 H), 8.41-8.36 (m, 2 H), 8.21 (d, J = 7.05 Hz, 6 H), 8.10-8.05 (m, 8 H), 8.03-7.99 (m, 2 H), 7.99-7.95 (m, 2 H), 7.88-7.83 (m, 3 H), 7.77-7.73 (m, 4 H), 7.67-7.63 (m, 1 H), 7.58-7.44 (m, 1 H), 7.42-7.37 (m, 5 H), 5.42-5.39 (m, 1 H), 5.05-5.03 (s, 0.4 H), 5.03-5.01 (s, 0.3 H); MALDI-TOF m/z= 551 M(**di-PBQ**+K)$^+$, 258 M(**PBQ**)$^+$

Irradiation of **DMoBQ : DMoPBQ** (7.8 mg, 0.02 mmol) was dissolved in spectral grade CH_3CN (15.0 mL). A 6.0 mL aliquot was then immersed in a 2.0 M aqueous KNO_3 solution and irradiated in the Rayonet® photochemical reactor for 2.5 h. After irradiation, no white powder precipitated onto the side of the glass. The sample was dried *in vacuo* (13 %). ^{1}H-NMR (500 MHz, $CDCl_3$) δ_H (ppm) = 8.72 (s, 8 H), 8.47-8.43 (m, 3 H), 8.16-8.10 (m, 9 H), 8.08-8.03 (m, 4 H),

7.97 (d, J = 8.95 Hz, 8 H), 7.93-7.89 (m, 4 H), 7.83-7.78 (m, 4 H), 7.73-7.68 (m, 6 H), 7.64-7.60 (m, 6 H), 7.52-7.48 (m, 5 H), 6.99 (d, J = 8.9 Hz, 12 H), 6.97-6.95 (m, 6 H), 6.92 (d, J = 8.8 Hz, 18 H), 6.91-6.89 (m, 3 H), 5.48-5.46 (m, 1 H), 3.91 (s, 10 H), 3.90-3.86 (m, 40 H).

Irradiation of **MoPBQ : MoPBQ** (5.8 mg, 0.02 mmol) was dissolved in spectral grade CH_3CN (15.0 mL). A 6.0 mL aliquot was then immersed in a 2.0 M aqueous KNO_3 solution and irradiated in the Rayonet® photochemical reactor for 2.5 h. After irradiation, no white powder precipitated onto the side of the glass. The sample was dried *in vacuo* (8 %). ^{1}H-NMR (500 MHz, $CDCl_3$) δ_H (ppm) = 9.45-9.42 (m, 4 H), 9.37 (s, 11 H), 8.70 (s, 11 H), 8.67 (s, 11 H), 8.46-8.41 (m, 9 H), 8.31-8.28 (m, 9 H), 8.26 (d, J = 8.8 Hz, 22 H), 8.14-8.09 (m, 25 H), 7.92-7.87 (m, 6 H), 8.05-8.01 (m, 12 H), 7.58 (d, J = 3.6 Hz, 30 H), 7.12 (d, J = 8.9 Hz, 23 H), 7.10-7.08 (m, 7 H), 6.97-6.94 (m, 11 H), 5.64-5.63 (m, 1 H), 5.44-5.42 (m, 2 H), 3.86 (s, 12 H).

di-DPyBQ: DPyBQ (6.6 mg, 0.02 mmol) was dissolved in spectral grade CH_3CN (15.0 mL). A 6.0 mL aliquot was then immersed in a 2.0 M aqueous KNO_3 solution and irradiated in the Rayonet® photochemical reactor for 2.5 h. After irradiation, a white powder precipitated onto the side of the glass. The sample was dried *in vacuo* (40 %). ^{1}H-NMR (500 MHz, $CDCl_3$) δ_H (ppm) = 8.43 (d, J = 4.8 Hz, 2 H), 7.69-7.63 (m, 2 H), 7.45-7.37 (m, 2 H), 7.25 (dd, J_1 = 5.4, J_2

= 3.3 Hz, 2 H), 7.21-7.14 (m, 1H), 7.00 (dd, J_1 = 5.4, J_2 = 3.2 Hz, 2 H), 5.16 (s, 2 H); ^{13}C-NMR (125 MHz, $CDCl_3$) δ_C (ppm) = 157.3, 156.9, 149.1, 147.9, 140.0, 136.2, 128.0, 127.31, 124.3, 122.6, 109.7, 52.7; MALDI-TOF m/z = 669 (M+1)

7.2.4 Dissociation of photodimer:

Photodissociation of di-DPBQ: A 1x10^{-4} M solution of **di-DPBQ** in CH_3CN was irradiated at 328 nm in a quartz cuvette in the fluorimeter. Dissociation progress was followed by UV-Vis spectroscopy at 30 min intervals.

Thermal dissociation of di-DPBQ: **di-DPBQ** (6.6 mg, 0.01 mmol) was dissolved in 100 mL of DMSO in a 100 mL volumetric flask. 20 mL of this 1.00 x 10^{-5} M solution of **di-DPBQ** were transferred into four 25 mL glass vials. The open vials were then heated in oil baths at 60, 80, 100, 150 °C for a maximum of 4 h. The dissociation was followed by UV-Vis spectroscopy at 30 min intervals.

7.3 Experimental for chapter 4

7.3.1 Synthesis

Tetraphenylpyrazo[2,3-*g*]quinoxaline: Tetraaminobenzene tetrahydrochloride salt (0.144 g, 0.5 mmol), benzil (0.210 g, 1.0 mmol) and sodium acetate (0.780 g, 5.0 mmol) were dissolved in ethanol (20 mL). Upon addition of AcONa the resulting purple solution turned red. After 3 h at reflux the hot solution was poured over crushed ice and the aqueous orange suspension was extracted with dichloromethane (3 x 100 mL). The organic phases were

combined, dried over $MgSO_4$ and concentrated *in vacuo* yielding the crude target compound as a yellow powder (0.478 g). The powder was recrystallised from boiling ethanol yielding **TPPQ** (0.206 g. 0.424 mmol, 42 %) as yellow crystals. ^{1}H-NMR (500 MHz, $CDCl_3$) δ_H (ppm) = 9.04 (s, 2 H) 7.55 (d, J = 6.7 Hz, 8 H) 7.33 (m, 12 H)

2,3,7,8-tetrakis(3,4-bis(hexyloxy)phenyl)-pyrazo[2,3-*g*]quinoxaline

THPQ: Tetraaminobenzene tetrahydrochloride (0.150 g, 0.5 mmol), tetrahexyloxybenzil (0.487 g, 1.0 mmol) and sodium acetate (0.708 g, 5.0 mmol) were dissolved in 95% ethanol (50 mL). After 17 h at reflux, the hot reaction mixture was poured over crushed ice (200 g) and the brown suspension was filtered using a Buchner funnel. The brown powder collected was then purified by flash column chromatography (silica gel, toluene) yielding an orange powder which was recrystallised from methanol and dichloromethane (10 vol%) (8 %). ^{1}H-NMR (500 MHz, $CDCl_3$) δ_H (ppm) = 8.90 (s, 2 H), 7.22 (dd, J_1 = 2.5, J_1 = 8.8 Hz, 3.64 H), 6.87 (d, J = 8.4 Hz, 4.6 H), 4.03 (t, J_1 = 6.7, J_2 = 6.7 Hz, 8.1 H), 3.7 (t, J_1 = 6.7, J_2 = 6.7 Hz, 7.67 H), 1.80 (m, 20.7 H), 1.47 (m, 15.3 H), 1.35 (m, 25.8 H), 0.9 (t, 19.1 H); ^{13}C-NMR (125 MHz, $CDCl_3$) δ_C (ppm) = 194.05, 155.18 149.49, 126.39, 126.36, 69.43, 69.33, 31.78, 31.73, 29.25, 29.11, 25.92, 25.88, 25.82, 22.84, 22.80, 14.28, 14.26, 14.23.

7.3.2 Photoadduct formation

Irradiation of TPPQ: different solutions of **TPPQ** were irradiated in the Rayonet® photochemical reactor fitted with lamps centred at 350 nm for 150 min.

- (9.2 mg, 0.019 mmol) in spectral grade CH_3CN (100 mL)

- (5.0 mg, 0.010 mmol) in spectral-grade CH_3CN (100 mL)

- (9.3 mg, 0.019 mmol) in spectral-grade benzene (5 mL)

The solutions was concentrated *in vacuo.* ^{1}H-NMR (500 MHz, $CDCl_3$) δ_H (ppm) = 9.04 (s, 2 H), 7.61(dd, 8 H), 7.38-7.42(m, 12 H) ppm.

Anthracene-2,3,6,7-tetraphenylpyrazoquinoxaline (A-TPPQ): 5.00 mL of a 0.2 mM solution of **TPPQ** in CH_3CN was mixed with 5.00 mL of a 0.2 mM solution of **A** in CH_3CN. The resulting mixture was irradiated in the Rayonet photoreactor® for 150 min. ^{1}H NMR (500 MHz, $CDCl_3$) δ_H (ppm)= 9.05 (s, 14 H), 8.36-8.34 (m, 5 H), 8.33-8.32 (m, 2 H), 7.94-7.91 (m, 3 H), 7.85-7.82 (m, 4 H), 7.76-7.72 (m, 5 H), 7.66-7.62 (m, 51 H), 7.59-7.55 (m, 5 H), 7.45-7.39 (m, 80.8 H), 7.31 (dd, J_1 = 5.3, J_2 = 3.1 Hz, 8 H), 6.95-6.93 (m, 4 H), 6.84-6.82 (m, 4 H), 5.84-5.83 (m, 1 H), 5.82-5.81 (m, 1 H), 5.80-5.79 (m, 1 H), 5.57-5.54 (m, 2 H), 4.57-4.56 (m, 2 H); MALDI-TOF m/z= 488.4 (M(**TPPQ**)+2), 331 (M(**TPPA-A**)+2), 178 (M(**A**)+)

9',10'-Dimethylanthracene-2,3,6,7-tetraphenylpyrazoquinoxaline (DMA-TPPQ): 5.00 mL of a 0.2 mM solution of **TPPQ** in CH_3CN was mixed with 5.00 mL of a 0.2 mM solution of **DMA** in CH_3CN. The resulting mixture was irradiated in the Rayonet® photochemical reactor for 150 min The solution was irradiated in the Rayonet® photochemical reactor for 150 min. ^{1}H-NMR (500 MHz, $CDCl_3$) δ_H (ppm)= 9.05 (s, 6 H), 8.38-8.32 (m, 3 H), 8.12-8.08 (m, 1 H), 7.87-7.86 (m, 3 H), 7.86-7.82 (m, 1 H), 7.74-7.71 (m, 1 H), 7.64 (d, J = 7.0 Hz, 29 H), 7.57-7.53 (m, 2.4 H), 7.47-7.38 (m, 57 H), 7.30 (dd, J_1 = 5.45, J_2 = 3.2 Hz, 11

H), 6.92-6.90 (m, 1 H), 6.86-6.81 (m, 2 H), 6.71-6.68 (m, 1 H), 6.77-6.74 (m, 1 H), 4.99-4.97 (m, 1 H), 4.91-4.88 (m, 1 H), 4.72-4.68 (m, 1 H), 3.82-3.80 (m, 1 H), 3.77-3.74 (m, 1 H), 3.47-3.44 (m, 1 H), 3.33-3.31 (m, 1 H), 2.17 (s, 17 H); MALDI-TOF m/z= 698 (M(**TPPQ-DMA**)$^+$), 489 (M(**TPPQ**)+3), 206 (M(**DMA**)$^+$).

7.4 Experimental for chapter 5

The molecular weights of the copolymers were estimated by gel permeation chromatography (GPC) at 50 °C in DMF (0.01 M LiBr) using Waters Styragel HT columns (HT3, HT4, HT5), a Waters 1515 isocratic HPLC pump, a Waters 2414 differential refractometer and a Water 2487 dual λ absorbance detector set at 254 nm. Polystyrene standards were used for calibration.

BQP: was synthesised according to literature procedure.[81] **BQP** was obtained as yellow powder (quant.). ^{1}H-NMR (500 MHz, $CDCl_3$) δ_H (ppm)= 9.37 (s, 1 H), 8.74-8.66 (m, 2 H), 8.24-8.19 (m, 2 H), 8.12 (dd, J_1 = 6.1, J_2 = 3.4 Hz, 2.5 H), 7.59 (td, J_1 = 5.9, J_2 = 3.3 Hz, 2 H), 7.10-7.03 (m, 2 H).

Poly (*Co*-styrene-chloromethylstyrene) 1: Chloromethylstyrene (0.15 g, 0.96 mmol) and styrene (1.01 g, 9.60 mmol) were heated in an oil bath at 100 ºC for 18 h. The off-white solid was dissolved in dichloromethane and reprecipitated in a large excess of ethanol 5 times, yielding a solid after filtration (0.42 g). GPC determined a Mw = 38169 g/mol with a polydispersity of 1.74. The ratio of 1

chloromethylstyrene to 2 styrene units in the final pure polymer was determined by ^{1}H-NMR spectroscopy. ^{1}H-NMR (400 MHz, $CDCl_3$) δ_H (ppm) = 7.10 (br, 7 H), 6.57-6.46 (br, 8 H), 4.5 (br, 2 H) 2.2 (br, 2 H) 1.8 (br, 5 H) 1.42 (br, 5 H) 1.26 (s, 2 H).

Poly (*Co*-styrene-chloromethylstyrene) 2: chloromethylstyrene (2.00 mL, 13.15 mmol) and styrene (20.03 g, 192.31 mmol) were heated in an oil bath at 70 °C for 6 days. After 6 days, ^{1}H-NMR analysis only showed the starting materials in solution hence, AIBN (3.0 mg, mmol) was added to the reaction mixture. After 6 days, the reaction was cooled down as a thick off-white solid had precipitated. The off-white solid was dissolved in dichloromethane and reprecipitated in large volume of ethanol 5 times, yielding a solid after filtration (16.94 g). GPC determined a Mw= 426987 g/mol with a polydispersity of 1.58. The ratio of 1 chloromethylstyrene to 42 styrene units in the final pure polymer was determined by ^{1}H-NMR spectroscopy. ^{1}H-NMR (400 MHz, $CDCl_3$) δ_H (ppm) = 7.10 (br, 133 H), 6.58-6.46 (br, 79 H), 4.5-4.3(br, 2 H) 2.2 (br, 2 H) 2.05 (br, 33 H) 1.42 (br, 87 H) 1.26 (s, 3 H).

PS2BQ: A mixture of 4-(benzo[2,3-g]quinoxalyl)phenyl (7.0 mg, 0.03 mmol) and PS2 (0.108 g, 0.25 mmol) and K_2CO_3 (17.7 mg, 0.128 mmol) were dissolved DMF (3 mL) and heated under reflux. After 2 days, the reaction was quenched with water (5 mL). The resulting pale yellow milky solution was filtered to yield a white solid (84.7 mg, 84 %).

REFERENCE LIST

(1) Bouas-Laurent, H.; Durr, H. *Pure Appl. Chem.* **2001**, *73*, 639-665.

(2) Ikeda, T.; Mamiya, J.; Yu, Y. L. *Angew. Chem., Int. Ed.* **2007**, *46*, 506-528.

(3) Barrett, C. J.; Mamiya, J. I.; Yager, K. G.; Ikeda, T. *Soft Matter* **2007**, *3*, 1249-1261.

(4) Parthenopoulos, D. A.; Rentzepis, P. M. *Science* **1989**, *245*, 843-845.

(5) Irie, M. *Jpn. J. Appl. Phys. Part 1* **1989**, *28*, 215-219.

(6) Such, G.; Evans, R. A.; Yee, L. H.; Davis, T. P. *J. Macromol. Sci., Pol. Rev.* **2003**, *C43*, 547-579.

(7) Crano, J. C.; Flood, T.; Knowles, D.; Kumar, A.; VanGemert, B. *Pure Appl. Chem.* **1996**, *68*, 1395-1398.

(8) Irie, M. In *Molecular Switches*; Feringa, B. L., Ed.; Wiley-VCH: Weinheim, Germany, 2001, p 37.

(9) Jones, G.; Chow, V. L. *J. Org. Chem.* **1974**, *39*, 1447-1448.

(10) Kosar, J. *Light Sensitive Systems*; Wiley: New York, 1965.

(11) Creed, D.; Cozad, R. A.; Griffin, A. C.; Hoyle, C. E.; Jin, L. X.; Subramanian, P.; Varma, S. S.; Venkataram, K. In *Polymeric Materials for Microelectronic Applications* 1994; Vol. 579, p 13-26.

(12) Schreier, W. J.; Schrader, T. E.; Koller, F. O.; Gilch, P.; Crespo-Hernandez, C. E.; Swaminathan, V. N.; Carell, T.; Zinth, W.; Kohler, B. *Science* **2007**, *315*, 625-629.

(13) Cadet, J. V., P. *Bioorganic Photochemistry*; Wiley: New York, 1990.

(14) Fritzsche, J. *Bull. Acad. Imper. Sci. St.-Petersbourg* **1867**, *11*, 385.

(15) Benard, C. P.; Geng, Z.; Heuft, M. A.; VanCrey, K.; Fallis, A. G. *J. Org. Chem.* **2007**, *72*, 7229-7236.

(16) Kuckling, D.; Ivanova, I. G.; Adler, H. J. P.; Wolff, T. *Polymer* **2002**, *43*, 1813-1820.

(17) Ihmels, H.; Mohrschladt, C. J.; Schmitt, A.; Bressanini, M.; Leusser, D.; Stalke, D. *Eur. J. Org. Chem.* **2002**, 2624-2632.

(18) Bouas-Laurent, H.; Castellan, A.; Desvergne, J. P.; Lapouyade, R. *Chem. Soc. Rev.* **2000**, *29*, 43-55.

(19) Becker, H. D. *Chem. Rev.* **1993**, *93*, 145-172.

(20) Luther, R.; Weigert, F. *Z. Phys. Chem.* **1905**, *51*, 297-328.

(21) Luther, R.; Weigert, F. *Z. Phys. Chem.* **1905**, *53*, 385-427.

(22) Forster, T.; Kasper, K. *Z. Electrochem.* **1955**, *59*, 976-980.

(23) Bowen, E. J. *Advances in Photochemistry*; Interscience Publishers: New York, 1963; Vol. 1.

(24) Ferguson, J.; Mau, A. W. H. *Mol. Phys.* **1974**, *27*, 377-387.

(25) Anderson, B. F.; Ferguson, J.; Morita, M.; Robertson, G. B. *J. Am. Chem. Soc.* **1979**, *101*, 1832-1840.

(26) Cohen, M. D.; Ludmer, A.; Yakhot, V. *Chem. Phys. Lett.* **1976**, *38*, 398-400.

(27) Bouas-Laurent, H.; Castellan, A.; Desvergne, J. P.; Lapouyade, R. *Chem. Soc. Rev.* **2001**, *30*, 248-263.

(28) Kuckling, D.; Adler, H. J. P.; Arndt, K. F. *Poly(N-isopropylacrylamide) copolymers: Hydrogel formation via photocrosslinking*; American Chemical Society: Washington, D.C., 2003; Vol. 833.

(29) Zheng, Y. J.; Mieie, M.; Mello, S. V.; Mabrouki, M.; Andreopoulos, F. M.; Konka, V.; Pham, S. M.; Leblanc, R. M. *Macromolecules* **2002**, *35*, 5228-5234.

(30) Tomlinso.Wj; Chandros.Ea; Lamola, A. A.; Pryde, C. A.; Fork, R. L. *Appl. Opt.* **1972**, *11*, 533-&.

(31) Tomlinso.Wj *Appl. Opt.* **1972**, *11*, 823-&.

(32) Trinh, X. A.; Fukuda, J.; Adachi, Y.; Nakanishi, H.; Norisuye, T.; Tran-Cong-Miyata, Q. *Macromolecules* **2007**, *40*, 5566-5574.

(33) Ali, A. H.; Srinivasan, K. S. V. *J. Appl. Polym. Sci.* **1998**, *67*, 441-448.

(34) Zhao, D. L.; Ren, B. Y.; Liu, S. S.; Liu, X. X.; Tong, Z. *Chem. Commun.* **2006**, 779-781.

(35) Nakanishi, H.; Satoh, M.; Norisuye, T.; Tran-Cong-Miyata, Q. *Macromolecules* **2006**, *39*, 9456-9466.

(36) Coursan, M.; Desvergne, J. P.; Deffieux, A. *Macromol. Chem. Phys.* **1996**, *197*, 1599-1608.

(37) Matsui, J.; Ochi, Y.; Tamaki, K. *Chem. Lett.* **2006**, *35*, 80-81.

(38) Liu, R. H.; Winnik, M. A.; Di Stefano, F.; Vanketessan, J. *J. Polym. Sci., Part A: Polym. Chem.* **2001**, *39*, 1495-1504.

(39) Bailey, D.; Williams, V. E. *J. Org. Chem.* **2006**, *71*, 5778-5780.

(40) Bailey, D.; Williams, V. E. *Tet. Lett.* **2004**, *45*, 2511-2513.

(41) Bailey, D.; Murphy, J. N.; Williams, V. E. *Can. J. Chem.* **2006**, *84*, 659-666.

(42) Bradsher, C. K.; Beavers, I. E.; Jones, J. H. *J. Org. Chem.* **1957**, *22*, 1740-1741.

(43) Warrener, R. N.; Golic, M.; Butler, D. N. *Tet. Lett.* **1998**, *39*, 4717-4720.

(44) Jouvenot, D.; Glazer, E. C.; Tor, Y. *Org. Lett.* **2006**, *8*, 1987-1990.

(45) Berni, E.; Dolain, C.; Kauffmann, B.; Léger, J. M.; Zhan, C.; Huc, I. *J. Org. Chem.* **2008**, *73*, 2687-2694.

(46) Maga, J. A.; Sizer, C. E. *J. Agric. Food. Chem.* **1973**, *21*, 22-30.

(47) Barlin, G. B. *The Pyrazines*; J. Wiley: New York, 1982.

(48) Taber, D. F.; DeMatteo, P. W.; Taluskie, K. V. *J. Org. Chem.* **2007**, *72*, 1492-1494.

(49) Naskar, J. P.; Chowdhury, S.; Drew, M. B. G.; Datta, D. *New J. Chem.* **2002**, *26*, 170-175.

(50) T. Eicher, S. H., A. Speicher *The Chemistry of Heterocycles*; 2nd ed.; Wliey-VCH GmbH & Co. KGaA: Weinhiem, 2003.

(51) Buchi, G.; Galindo, J. *J. Org. Chem.* **1991**, *56*, 2605-2606.

(52) Bailey, D.; Williams, V. E. *Chem. Commun.* **2005**, 2569-2571.

(53) Goldstein, H.; Streuli, M. *Helv. Chim. Acta* **1937**, *20*, 650-653.

(54) Liao, Y.; Bohne, C. *J. Phys. Chem.* **1996**, *100*, 734-743.

(55) M. Monalti, A. C., L. Prodi, M. T. Gandolphi *Handbook of Photochemistry*; 3rd, rev. and expanded ed.; Francis and Taylor, 2006.

(56) Parker, C. A. *Photoluminescence in Solution*; Elsevier Amsterdam-London-New York, 1968.

(57) Blanchard, P. M.; Gilbert, A.; Mitchell, G. R. *J. Mater. Chem.* **1993**, *3*, 1015-1018.

(58) Tatistcheff, H. B.; Hancock, L. F.; Wrighton, M. S. *J. Phys. Chem.* **1995**, *99*, 7689-7693.

(59) Floyd, M. B.; Du, M. T.; Fabio, P. F.; Jacob, L. A.; Johnson, B. D. *J. Org. Chem.* **1985**, *50*, 5022-5027.

(60) Venuti, M. C. *Synthesis* **1982**, 61-63.

(61) Paul, S.; Gupta, M.; Gupta, R.; Loupy, A. *Synthesis* **2002**, 75-78.

(62) Demeester, J. W. G.; Vanderplas, H. C.; Middelhoven, W. J. *J. Heterocycl. Chem.* **1987**, *24*, 441-451.

(63) Cornil, J.; Beljonne, D.; dosSantos, D. A.; Bredas, J. L. *Synthetic Metals* **1996**, *76*, 101-104.

(64) Cornil, J.; Dossantos, D. A.; Beljonne, D.; Bredas, J. L. *J. Phys. Chem.* **1995**, *99*, 5604-5611.

(65) Oelkrug, D.; Tompert, A.; Gierschner, J.; Egelhaaf, H. J.; Hanack, M.; Hohloch, M.; Steinhuber, E. *Journal of Physical Chemistry B* **1998**, *102*, 1902-1907.

(66) Yeomans, B. D.; Kelso, L. S.; Tregloan, P. A.; Keene, F. R. *Eur. J. Inorg. Chem.* **2001**, 239-246.

(67) Holliday, B. J.; Mirkin, C. A. *Angew. Chem., Int. Ed.* **2001**, *40*, 2022-2043.

(68) Wang, J. H.; Fang, Y. Q.; Bourget-Merie, L.; Poison, M. I. J.; Hanan, G. S.; Juris, A.; Loiseau, F.; Campagna, S. *Chem. Eur. J.* **2006**, *12*, 8539-8548.

(69) Polson, M. I. J.; Howell, S. L.; Flood, A. H.; Burrell, A. K.; Blackman, A. G.; Gordon, K. C. *Polyhedron* **2004**, *23*, 1427-1439.

(70) Bridgewater, J. S.; Vogler, L. M.; Molnar, S. M.; Brewer, K. J. *Inorg. Chim. Acta* **1993**, *208*, 179-188.

(71) Molnar, S. M.; Nallas, G.; Bridgewater, J. S.; Brewer, K. J. *J. Am. Chem. Soc.* **1994**, *116*, 5206-5210.

(72) Job, P. *Ann. Chim. Fr.* **1928**, *9*, 113-203.

(73) Bouas-Laurent, H.; Castellan, A. *J. Chem. Soc. Chem. Commun* **1970**, 1648-&.

(74) Kobayashi, T.; Kobayashi, S. *Eur. J. Org. Chem.* **2002**, 2066-2073.

(75) Cohen, Y.; Meyer, A. Y.; Rabinovitz, M. *J. Am. Chem. Soc.* **1986**, *108*, 7039-7044.

(76) Aldred, M. P.; Contoret, A. E. A.; Farrar, S. R.; Kelly, S. M.; Mathieson, D.; O'Neill, M.; Tsoi, W. C.; Vlachos, P. *Adv. Mat.* **2005**, *17*, 1368-1372.

(77) Marvel, C. S.; Porter, P. K. *Org. Synth.* **1929**, *9*, 58-59.

(78) Chacko, A.; Mathew, B. *Asian J. Chem.* **2007**, *19*, 2502-2516.

(79) Overberger, C. G.; Arnold, L. H.; Taylor, J. J. *J. Am. Chem. Soc.* **1951**, *73*, 5541-5545.

(80) Lee, Y. S.; Byoun, Y. S. *Bull. Korean Chem. Soc.* **2002**, *23*, 1833-1835.

(81) von Nussbaum, F.; Miller, B.; Wild, S.; Hilger, C. S.; Schumann, S.; Zorbas, H.; Beck, W.; Steglich, W. *J. Med. Chem.* **1999**, *42*, 3478-3485.

(82) Brotin, T.; Utermohlen, R.; Fages, F.; Bouaslaurent, H.; Desvergne, J. P. *J. Chem. Soc. Chem. Commun.* **1991**, 416-418.

(83) Pozzo, J. L.; Clavier, G. M.; Desvergne, J. P. *J. Mater. Chem.* **1998**, *8*, 2575-2577.

(84) Wenz, G. *Makromolekulare Chemie-Rapid Communications* **1985**, *6*, 577-584.

(85) Schaefer, J. P.; Bertram, J. L. *J. Am. Chem. Soc.* **1967**, *89*, 4121-4124.

(86) Gunn, V. E.; Anselme, J. P. *J. Org. Chem.* **1977**, *42*, 754-755.

(87) Katritzky, A. R.; Chapman, A. V.; Dowlatshahi, H. M. *Acta Chim. Acad. Sci. Hung.* **1981**, *107*, 315-319.

(88) Gazit, A.; App, H.; McMahon, G.; Chen, J.; Levitzki, A.; Bohmer, F. D. *J. Med. Chem.* **1996**, *39*, 2170-2177.

(89) Ohta, A.; Takahashi, H.; Miyata, N.; Hirono, H.; Nishio, T.; Uchino, E.; Yamada, K.; Aoyagi, Y.; Suwabe, Y.; Fujitake, M.; Suzuki, T.; Okamoto, K. *Biol. Pharm. Bull.* **1997**, *20*, 1076-1081.

(90) Pflugrath, J. W. *Acta Cryst.* **1999**, *55*, 1718-1725.

(91) Altomare, A.; Cascarano, G.; Giacovazzo, C.; Guagliardi, A.; Burla, M.; Polidori, G.; Camalli, M. *J. Appl. Cryst.* **1994**, *27*, 435-436.

(92) Betteridge, P. W.; Carruthers, J. R.; Cooper, R. I.; Prout, K.; Watkin, D. J. *J. Appl. Cryst.* **2003**, *36*, 1487-1488.

(93) *International Tables for X-ray Crystallography*; Kynoch Press: Birmingham, U.K. , 1975; Vol. IV.

APPENDIX 1: CRYSTALLOGRAPHIC DATA FOR di-DPBQ

Crystals of **di-DPBQ** were obtained by slowly evaporating a solution of this compound in chloroform and acetonitrile (1:1). Under these conditions, **di-DPBQ** crystallizes in the monoclinic system P $2_1/n$. Analysis of the structure shows the presence of head-to-tail dimers of **DPBQ** with a bridge-head carbon to carbon distance of 1.605 Å.

Crystallographic data for **di-DPBQ** is summarised in Table **A-1**. A pale yellow crystal of **di-DPBQ** having dimensions 0.34 x 0.23 x 0.23 mm^3 was mounted on a glass fibres using epoxy adhesive. The data range 9.4 ° ≤ 2θ ≤ 144.4 ° was recorded at room temperature on a Rigaku RAXIS RAPID image plate area detector with Cu Kα radiation. The data was corrected by integration for the effects of absorption using a numerical absorption correction (transmission range: 0.8704 – 1.000). Data reduction included corrections for Lorentz and polarization effects. Final unit-cell dimensions were determined based on 597 well-centred reflections with range 9.4 ° ≤ 2θ ≤ 144.4 °.

The coordinates and anisotropic displacement parameters for all non-hydrogen atoms were refined. Hydrogen atoms were placed in calculated positions (d C-H 0.95 Å) and refined with coordinate shifts linked with those of the respective carbon atoms. Isotropic thermal parameters for the hydrogen

atoms were initially assigned proportionately to the equivalent isotropic thermal parameters of their respective carbon. Subsequently, the isotropic thermal parameters for the C-H hydrogen atoms were constrained to have identical shifts during refinement. Selected bond lengths and angles for **di-DPBQ** are found in Table **A-2**.

The software package *Crystal Clear* (d*trek, Rigaku) was used for all absorption corrections, data reduction and processing.[f,90], All structures were solved using Sir 92,[91] expanded using Fourier techniques and refined using *CRYSTALS*.[92] Complex scattering factors for neutral atoms were used in the calculation of structure factors.[93] Diagrams were made using Mercury 1.4.2 and Material Studio 1.1.

[f] Rigaku Corporation©, 1999. CrystalClear Software User's Guide, Molecular Structure Corporation© 2000.

Table A-1 Summary of crystallographic data

	di-DPBQ
Empirical formula	$C_{48}H_{32}N_4$
Formula weight	664.79
Crystal system	Monoclinic
Space group	P 1 2_1/n 1
a, Å	8.6132(9)
b, Å	18.4915(17)
c, Å	10.9618(16)
α, °	90
□, °	96.550(6)
γ, °	90
V, Å^3	1734.5(4)
Z	2
T, K	293
λ, Å	1.5418
ρ_{calcd}, g·cm^{-3}	0.16
μ, mm^{-1}	0.580
R[a], (I > 2.5σ(I))	0.0436
R_w[a], (I > 2.5σ(I))	0.0645
Goodness of fit	1.4097

[a]Function minimized $\Sigma w(|F_o| - |F_c|)^2$ where $w^{-1} = [\sigma^2(F_o) + (0.020*F_o)^2]$, $R = \Sigma||F_o| - |F_c|| / \Sigma|F_o|$, $R_w = [\Sigma w(|F_o| - |F_c|)^2 / \Sigma w|F_o|^2]^{1/2}$.

Table A-2. Selected Bond Lengths (Å) and Angles (°) for **di-DPBQ** [a]

C(1) – C(2)	1.5168(19)	C(2) – C(9*)	1.605(2)
C(2) – C(3)	1.518(2)	C(8) – C(9)	1.516(2)
C(9) – C(10)	1.5095(19)		
C(2) – C(1) – C(10)	117.38(12)	C(1) – C(2) – C(9*)	111.67(12)
C(1) – C(2) – C(3)	107.02(12)	C(9*) – C(2) – C(3)	112.12(11)
C(2) – C(3) – C(4)	123.06(15)	C(2) – C(3) – C(8)	117.13(14)
N(2) – C(1) – C(2)	120.72(13)	C(3) – C(8) – C(9)	117.81(14)
C(7) – C(8) – C(9)	122.74(15)	C(8) – C(9) – C(2*)	111.95(11)
C(8) – C(9) – C(10)	107.63(12)	C(2*) – C(9) – C(10)	111.23(12)
C(9) – C(10) – C(1)	117.84(13)	C(9) – C(10) – N(1)	120.35(13)

[a] Symmetry transformations: *, -x+1, -y+1, -z+1

Table A-3 Fractional atomic coordinates and equivalent isotropic thermal parameters [U(iso) ($Å^2$)] for **di-DPBQ**.

Atom	X	Y	Z	[U(iso) ($Å^2$)]
N(1)	0.48296(14)	0.34968(6)	0.35530(11)	0.0466
N(2)	0.20574(14)	0.43059(6)	0.32918(11)	0.0463
C(1)	0.32400(17)	0.44634(8)	0.41392(14)	0.0443
C(2)	0.31328(17)	0.50948(8)	0.50088(13)	0.0463
C(3)	0.36389(18)	0.48176(8)	0.62963(14)	0.0484
C(4)	0.2846(2)	0.49799(10)	0.72951(15)	0.06
C(5)	0.3396(3)	0.47138(11)	0.84533(17)	0.0713
C(6)	0.4724(3)	0.42996(11)	0.86168(17)	0.0694
C(7)	0.5530(2)	0.41379(9)	0.76254(16)	0.0583
C(8)	0.49958(18)	0.43905(8)	0.64614(14)	0.0478
C(9)	0.58271(18)	0.42330(8)	0.53439(14)	0.0468
C(10)	0.45989(17)	0.40407(8)	0.43001(14)	0.0451
C(11)	0.36580(17)	0.33411(8)	0.26561(14)	0.0453
C(12)	0.22449(17)	0.37278(8)	0.25626(13)	0.0449
C(13)	0.39976(18)	0.27493(8)	0.18031(15)	0.0501
C(14)	0.4881(2)	0.21621(10)	0.2260(2)	0.0669
C(15)	0.5233(3)	0.16116(11)	0.1467(2)	0.0837
C(16)	0.4738(3)	0.16526(12)	0.0230(2)	0.0858
C(17)	0.3869(3)	0.22321(13)	-0.0225(2)	0.0796

C(18)	0.3498(2)	0.27806(10)	0.05457(16)	0.0627
C(19)	0.08309(17)	0.35184(8)	0.17286(14)	0.0474
C(20)	0.0063(2)	0.40208(10)	0.09361(16)	0.0623
C(21)	-0.1259(2)	0.38283(12)	0.01701(19)	0.0773
C(22)	-0.1866(2)	0.31346(12)	0.02260(19)	0.0759
C(23)	-0.1120(2)	0.26390(11)	0.10057(17)	0.0666
C(24)	0.02266(19)	0.28243(9)	0.17523(15)	0.0547
H(21)	0.20731(17)	0.52452(8)	0.49635(13)	0.0533(16)
H(41)	0.1932(2)	0.52712(10)	0.71896(15)	0.0705(16)
H(51)	0.2847(3)	0.48205(11)	0.91354(17)	0.0846(16)
H(61)	0.5092(3)	0.41225(11)	0.94109(17)	0.0811(16)
H(71)	0.6453(2)	0.38530(9)	0.77443(16)	0.0670(16)
H(91)	0.64916(18)	0.38269(8)	0.55171(14)	0.0537(16)
H(141)	0.5245(2)	0.21346(10)	0.3110(2)	0.0788(16)
H(151)	0.5820(3)	0.12044(11)	0.1783(2)	0.1000(16)
H(161)	0.4998(3)	0.12794(12)	-0.0306(2)	0.1039(16)
H(171)	0.3520(3)	0.22573(13)	-0.1078(2)	0.0955(16)
H(181)	0.2898(2)	0.31816(10)	0.02193(16)	0.0742(16)
H(201)	0.0449(2)	0.45015(10)	0.09202(16)	0.0714(16)
H(211)	-0.1752(2)	0.41702(12)	-0.03941(19)	0.0880(16)
H(221)	-0.2797(2)	0.30058(12)	-0.02776(19)	0.0873(16)
H(231)	-0.1528(2)	0.21631(11)	0.10381(17)	0.0779(16)
H(241)	0.07421(19)	0.24724(9)	0.22851(15)	0.0637(16)

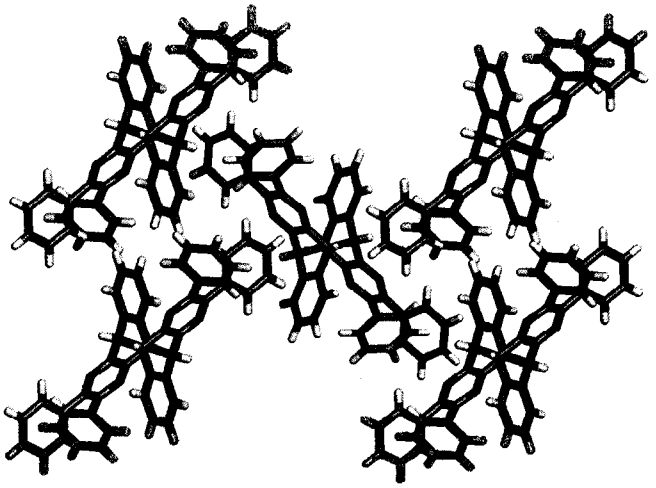

Figure A-1: Crystal structure of **di-DPBQ** showing 1 x 1 x 1 unit cell. View along the *a* axis.

APENDIX 2: LIQUID CRYSTAL CHARACTERISATION OF THPQ

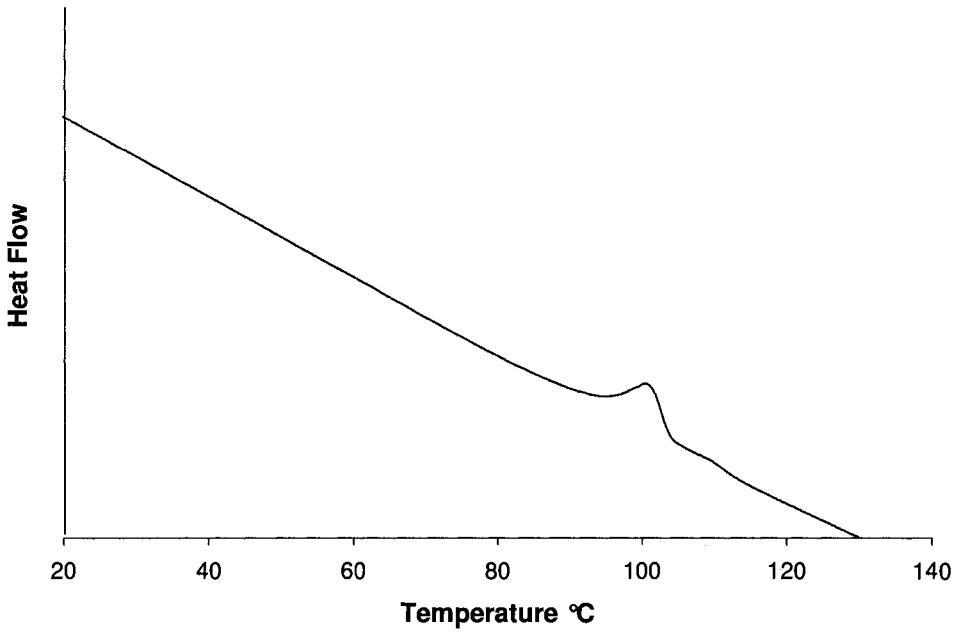

Figure A-7.1: Metling transition of **THPQ** determined by DSC.

Table A-4: X-Ray Diffraction Data of **THPQ**.

temperature (°C)	Miller index (hkl)	d-spacing (Å)	Lattice Constant (Å)
	(100)	23.5	
	(110)	13.7	
90	(200)	11.5	27.1
	alkyl halo	4.5	
	π–π stacking	3.5	